Fatigue assessment in finite element analysis

A post-processor to FEA output for hot spot stress calculation

E.P. Swierstra


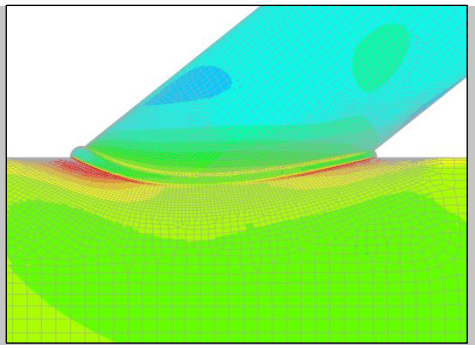


DIANA FEA
a TNO Company

TU Delft

Fatigue assessment in finite element analysis

Master of Science thesis

Delft University of Technology
Faculty of Civil Engineering and Geosciences
Department of Structural Engineering

Author: E.P. Swierstra

Committee:

Prof. Dr. M.V. Veljkovic	TU Delft
Dr. Ir. M.A.N. Hendriks	TU Delft
Dr. M. Pavlovic	TU Delft
Ir. C.M. Frissen	Diana FEA

July 7, 2017

Preface

This thesis is submitted for the degree of Master of Science at Delft University of Technology. It gives insight into the work that I performed over a nine month period. During my studies, my interests have been in both computational mechanics and the design of steel structures. In this thesis I have combined these fields of engineering and attempted to form a bridge between the practical experimental and the theoretical computational sides.
In my opinion, knowledge on both fields is equally important in engineering practice. I believe the civil engineering industry will benefit from continuously developing a link between theory and practice. Through this work, I gained expertise on both of these aspects. I developed an invaluable level of understanding of the finite element method, as well as significant insight into the limitations arising from structural experiments performed in the labs.

My work has been conducted at the finite element software company DIANA FEA. Throughout this period I continuously aimed to contribute to the development of the software, while my colleagues at DIANA FEA guided me to deliver a product that meets academic standards. Firstly, I would like to show my gratitude to Dr. Gerd-Jan Schreppers for giving me the opportunity to conduct my MSc thesis at DIANA FEA. I enjoyed my time with DIANA FEA immensely and have learnt a great deal from this experience, particularly about what goes into developing finite element software. I hope that I can take my new-found expertise into my future career. I would especially like to thank my supervisor Ir. Chantal Frissen. Your experience with finite element analysis has been invaluable to my work. But also, while my head was running with many ideas, you were able to see the bigger picture, narrow the scope down and break up the workload systematically.

Many thanks also go to my graduation committee from TU Delft. To both Prof. Dr. Milan Veljkovic and Dr. Marko Pavlovic from the Department of Steel and Composite Structures, your knowledge and enthusiasm on the topic of fatigue have been inspirational. To Dr. Ir. Max Hendriks from the Department of Structural Mechanics, your ability to provide a clear and pragmatic approach to any issue I was facing contributed greatly to the quality of this work.

Of course, special thanks go to Rebecca for always being there for me; waiting with a cold 'stubby' when I came home late at night (again). And finally I need to thank my loving parents for their everlasting support. You made all my years in university happen.

Abstract

For the fatigue assessment of welded structures, several design methods are described by the design codes of IIW [9], Eurocode3 [6][12] and DNV [3]. The relation between the stress range and cycles to failures were derived from experiments: the SN-curves. With the increased accessibility of finite element software to engineers, a more flexible approach emerged: the so-called hot spot stress method. Particularly suitable for welded structures, it assesses the influence of the geometric discontinuity on the stress distribution. A stress extrapolation procedure is required to overcome the high stresses computed by FEA at the notch.

Normal stresses at the surface, perpendicular to the weld, are to be used. For curved welds and surfaces, e.g. in case of tubular joints, these stresses are complex to determine from FEA output. A method that automates the hot spot stress calculation as a post-processor to FEA output would facilitate the process. Such an automated subroutine would further enable a study on the finite element modelling aspects, including the use of shell and solid elements and the inclusion of the weld profile, in relation to conducted fatigue experiments.

This report describes the development of a subroutine as post-processor for FEA output to calculate the hot spot stresses. Read out points for stress extrapolation are located independently of the finite element mesh. In addition, for each weld node the local coordinate system is to be determined and subsequently the corresponding stress transformation is to be performed. Equivalent stresses at the read out points are determined by means of interpolation from a triangle-shaped plane formed by three element nodes.

Cut-out specimens of an orthotropic bridge deck were tested against fatigue and strain gauges were used to measure the strains. This report shows that FEA stresses corresponded well with the measurements. Inclusion of the weld profile is important; ignoring the weld underestimates the stress levels by 10%. Use of shell elements resulted in 4% lower nominal stresses than solid elements, however in the weld region only the solid element model accurately reproduced the stress distribution. An alternative method for the fatigue classification described in EC3 [12] is proposed, which represents better the observed stress levels for the crack initiation point at the weld root.

Finally, this report considers stress concentration factors of tubular joints as recommended by CIDECT design guide [2]. The FEA results are compared to the SCFs from parametric formulae. Good correspondence was found between the FEA and CIDECT results. A validation analysis of the boundary and loading conditions was performed, from comparing the joint model with the entire truss structure for shell elements. A correction function is derived to cover the small observed differences. Additionally, strain gauge measurements from experiments on large scale tubular joints in a marine environment are compared to the FEA results. Good correspondence was found between the measured and numerically computed strains. For solid element models, the weld leg size is found to be important for the hot spot stresses; each millimetre shift of the weld toe affected the stress levels by 3%. A characteristic SN-curve was derived from the experiments. Fatigue assessment by means of the FEA hot spot stress in combination with the corresponding DNV SN-curve was found to be more conservative.

Table of contents

Nomenclature

List of symbols

β	Chord/brace diameter ratio (hollow section joint parameter)
d	Diameter
FAT	Fatigue strength at $2 \cdot 10^6$ cycles
γ	Diameter/thickness ratio (hollow section joint parameter)
N	Normal force
M	Bending moment
t	Thickness
τ	Chord/brace thickness ratio (hollow section joint parameter)

List of abbreviations

DNV	Det Norske Veritas
DOF	Degrees of freedom
EC3	Eurocode3
FEA	Finite element analysis
FEM	Finite element method
GUI	Graphical user interface
HAZ	Heat affected zone
IIW	International Institute of Welding
HSS	Hot spot stress
LSE	Linear surface extrapolation
PWT	Post weld treatment
RWS	Rijkswaterstaat
TIG	Tungsten inert gas
TTWT	Through thickness at the weld toe
VBA	Visual Basic for Applications

1 Introduction

1.1 Background

First research on fatigue failure is dated back to the mid-19th century. The Industrial Revolution in Europe led to significant amounts of heavy duty equipment failing under cyclic loading as a result of fatigue cracks. A tragic train disaster in 1842 claimed many lives after the locomotive's axle broke. Its importance becoming obvious, some researchers started developing prediction methods on fatigue. It laid the groundwork for the approaches still adopted these days. From World War II onwards the importance of the subject was finally fully realised. This is partly due to the emergence of large offshore facilities for oil and gas extraction, and tragically also accidents involving the Comet Jet airliners in the 1950s.

Recently, Rijkswaterstaat (RWS) discovered fatigue cracks appearing in the Merwede Bridge deck plate during a routine inspection. RWS was forced to ban all heavy traffic until repairs were carried out. Situated on the A27 highway, it is part of a main transport route from/to the Port of Rotterdam. The transportation industry estimated the economic damage of the closure to be at least half a million euros a day [22]. Perhaps the situation surrounding the Merwede Bridge was simply a high-profile incident that drew much media attention. However, it emphasised how difficult it still is to predict fatigue failure.

Fatigue is the phenomenon where cracks grow under a repetitive stress cycle. Once the cracks have grown until insufficient base material is left, static failure of the structure occurs. Usually, cracks initiate in an area containing geometrical or metallurgical discontinuities. The most common example of this are welds.

Fatigue strength can be assessed by two main methods. The first method is the most common and will form the basis for this report. It links the number of cycles to the stress range, plotted on a logarithmic scale as a straight line, the so-called SN-curve. From experiments the design SN-curve is obtained. The second method contains the fracture mechanics approach, where crack growth is assessed by the stress intensity at the crack tip.

Design codes like DNV [3], IIW [9] and EC3 [6] cover the fatigue assessments extensively. For a wide range of connections, many fatigue experiments were performed. As a result, each connection type is assigned a reference classification, based on which the fatigue life is to be calculated. Each fatigue classification contains a corresponding SN-curve. Any geometrical discontinuities are included in the classification and the nominal stress range is the input value for the calculation. A wide range of connection types are covered and the method of calculation is relatively straightforward. However, in case of more complex structures or loading conditions significant limitations arise from this approach. Therefore the so-called 'hot spot stress' method was adopted for welded connections. Each weld type is described by a SN-curve, which takes into account the local notches and metallurgical discontinuities, but not any stress increases as result of the geometry. Stress concentrations as a result of the geometrical discontinuity are derived by either parametric formulae or finite element analysis. Until recently, highly detailed structural finite element analysis was limited by the engineer's access to computers with sufficient computational capacity. Currently most engineers have this access, allowing them to perform fatigue assessments on the most complex structures.

This report aims to give better understanding on the implementation and validity of the hot spot stress method in combination with finite element analysis.

1.2 Fatigue methodologies

This section aims to introduce two methodologies for fatigue assessments that are considered common practice. They form the basis for this research, therefore a short theoretical background will provide better understanding of the adopted methodologies and assumptions described throughout this report.

1.2.1 Stress-cycle (SN) curve

The performance of a material under repetitive loading is characterised by a stress-cycle or SN-curve. It is also known as Wöhler's curve. The curve is commonly plotted on a logarithmic scale, where it can be presented as a straight line.

SN-curves are derived from experiments, where specimens are exposed to a repetitive loading cycle. The stress ranges are measured while the amount of cycles until failure is counted. Plotting these results gives a graph as presented in Figure 1-1.

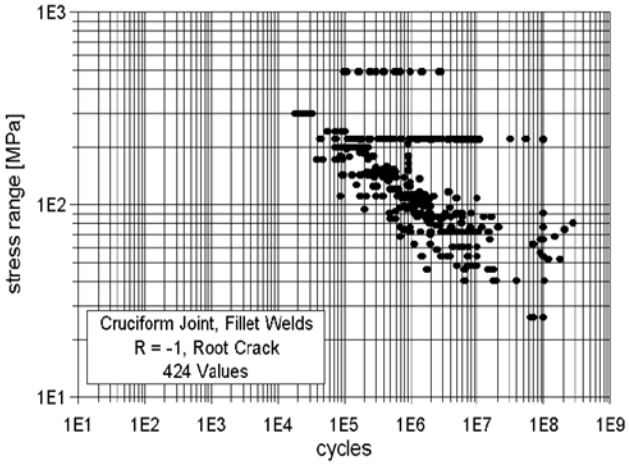

Figure 1-1 Example of fatigue experiment data [9]

The large scattering of results shows how complex predicting the fatigue lifetime can be. The fatigue strength depends on many effects of mechanical, microstructural and environmental factors. A curve is fitted to the test data and is evaluated statistically. A Gaussian log-normal distribution is to be assumed. The test results should be evaluated to produce characteristic values in order to obtain a sufficient confidence level. The characteristic values represent a 75% two-sided confidence level of 95% survival probability [9], see Figure 1-2. This characteristic curve represents the SN curve and forms the basis for the fatigue assessment.

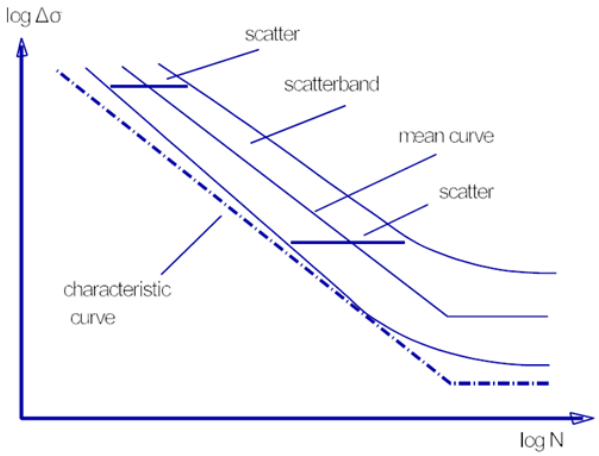

Figure 1-2 Statistical evaluation SN-curve [9]

1.2.2 Hot spot stress

The hot spot stress method describes the stresses as a result of geometric discontinuities. The hot spot stresses are also referred to as structural or geometric stresses. These stresses will form the design stresses for a fatigue assessment. The design codes provide a wide range of weld types with corresponding SN-curves applicable to the hot spot stress method. Its range of application is limited to cracks occurring at the weld toe. Cracks initiating from the weld root are not covered by the hot spot stress method.

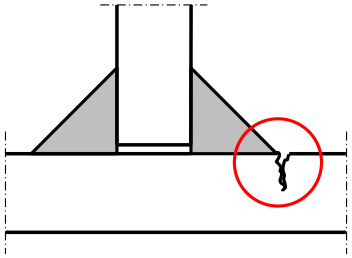

Figure 1-3 Fatigue crack at weld toe

The hot spot stress can be calculated using stress concentration factors from parametric formulae described in the design codes. Alternatively, finite element analysis is used to obtain the hot spot stresses.

Stresses computed at the weld by FEA include both the so-called geometric and notch effects. Geometric effects result from geometrical discontinuities that lead to stress concentrations. At the weld toe corner, i.e. the notch, as a result of singularities high peak stresses occur here. This effect has a purely computational origin; it does not represent the actual mechanical behaviour at the weld toe. It is to be realised that high notch stresses do occur at the actual weld toe. This is, however, a result from the change in composition from the welding process and other local effects. Besides its actual composition being extremely hard to predict, current computational methods are unable to represent these conditions. Therefore the local notch effects are included in the weld's corresponding SN-curve. The computed peak stress at the notch is disregarded by extrapolating the stresses from points further away, see Figure 1-4. This gives the hot spot stress, which represents the geometric effects only.

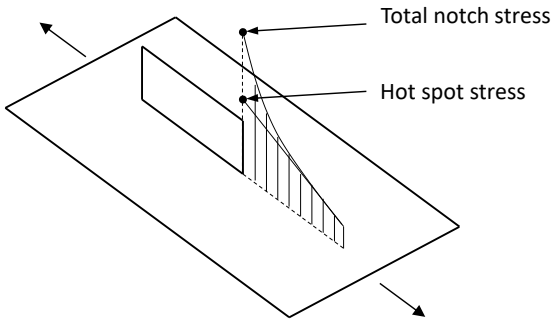

Figure 1-4 Total notch vs hot spot stress

Three main methods for calculation the hot spot stress are discussed here (Figure 1-5). The first method involves extrapolation of the normal stresses at the surface. The second method extrapolates the stress through the thickness of the plate. The third method, called the Dong method, is based on nodal equilibrium and combines features from both methods [4]. The most common approach is the extrapolation of the normal stresses at the surface, which will be the main focus of this research.

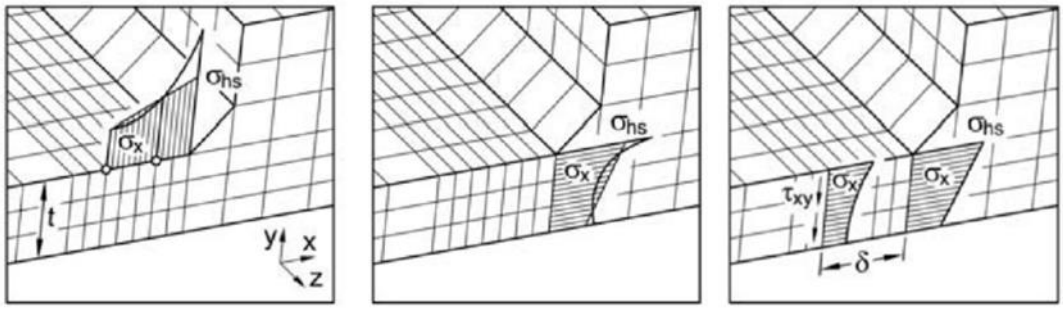

Figure 1-5 Hot spot stress: surface stress (left), through thickness (middle) and Dong (right)

In order to obtain the hot spot stress from the computed stress, stresses are extrapolated from read out points at the plate surface, see Figure 1-6. The location of these read out points are specified by the design codes.

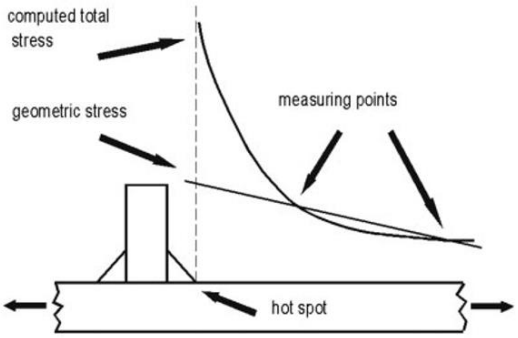

Figure 1-6 Stress extrapolation

1.3 Problem definition

The structural hot spot stresses required for fatigue assessment can be obtained using most commercial finite element software packages. However, these packages' functionality is often considered too limited for performing fatigue failure assessments. Engineers usually have to perform additional calculations from the FEA output in order to obtain the required stress values. For complex structures this can be cumbersome and also prone to error for engineers with limited knowledge on computational mechanics.

Finite element software company DIANA FEA would like to extend their functionality by implementing a fatigue assessment subroutine. This subroutine would function as a post-processor to the finite element analysis output. Its purpose is to calculate the hot spot stresses at a user-defined weld, followed by a fatigue life prediction according to the applicable SN-curve.

It is well known that care has to be taken when setting up a finite element model, for any type of analysis. Aspects like element type, element size and boundary conditions need to be well considered in order to obtain reliable results. Particular to fatigue analysis, an accurate representation of the weld profile is important when analysing a local area. This also leads to the aspect of mesh-size; a fine mesh gives more flexibility of analysing the stress distribution locally. Use of both shell and solid elements are discussed in the design codes, however different behaviour at the plate intersections for these element types can be identified. Taking all aspects into account, the variation in obtained stress magnitudes can be significant. The best way to validate each adopted modelling approach is by comparing the results to conducted fatigue experiments, from which extensive strain gauge measurements are available.

The goals of this thesis are therefore described by the following two research questions:

How can the hot spot stress calculations be automated in a subroutine as a post-processor to finite element analysis output?

To what extend is the outcome of a hot spot stress analysis influenced by finite element modelling aspects, including the use of shell and solid elements and the inclusion of a weld profile, in relation to conducted fatigue experiments?

1.4 Scope and limitations

The scope of this research is described in this section. Also the limitations of this research are discussed.

1.4.1 Scope of research

Fatigue assessment recommendations are covered by a wide range of design codes. Even though the described recommendations are all based on the same concepts, several differences in approaches can be recognised. Looking from the finite element software user's perspective, the distinction on which design code the fatigue analysis will be based on is of relevance. The applicable design codes will be reviewed. A study is made on how the different recommendations can be represented in the subroutine.

In addition to the design codes, a literature study is performed on further research that is not covered by these codes (yet). Its aim is to provide an understanding of the challenges that still need to be overcome. Also several fatigue experiments are well documented and are used for both validation and further research.

The basis of this research is formed by the development of a fatigue subroutine, which is applied as a post-processor to DIANA FEA output. It will provide a reliable, automated hot spot stress calculation. Validation and further research studies are performed with use of this subroutine. From conducted experiments the strain gauge measurements are a reliable method to validate the computed stresses/strains from FEA and the subroutine. Additionally, characteristic SN-curves can be obtained from these experiments and compared to the calculated fatigue life from the hot spot stress method.

Validation of the subroutine and further research is done through three case studies. Welded joints from two main types of structures are considered, i.e. steel bridge decks and circular hollow section (CHS) joints.

For the steel bridge deck structure, conducted experiments on cut-out specimens of a orthotropic deck plate are used as reference. The focus of research will be on the implementation of the subroutine on this type of bridge decks. In addition, the improved fatigue life by performing automatic rather than hand welding is assessed.

Two different CHS joint case studies are performed. The research focus will be on comparing the use of shell and solid elements in the finite element model. Additionally, the influence of the weld profile in the FEA model is assessed. The first case will consider a structure based on the design recommendations of CIDECT. Hot spot stresses are calculated through stress concentration factors from parametric formulae and compared to FEA results. For the second case, reference is made to conducted experiments on a large diameter CHS joint in a marine environment under corrosive conditions.

1.4.2 Limitations

This research only focusses on the fatigue assessment of welded components in steel structures. The discussed methods are valid for steel grades with a yield strength up to 960 MPa. Aluminium structures or different components (e.g. bolts or prestressing cables) can be considered for future implementation in the subroutine, but are not applicable to this research.

The fatigue assessments are stress based. For low cycle fatigue, a strain based approach is to be adopted. Only high cycle fatigue is therefore considered. Also, the effects of shear stresses are to be sufficiently small that a uniaxial stress state can be assumed. Significant research is still being done on the fatigue behaviour in multiaxial stress states. This will therefore be outside of this scope.

The hot spot stress method is applicable to cracks initiating at the weld toe only. This will be the main focus of this report. However, for the bridge deck experiments, fatigue cracks initiated in the weld root. Even though the hot spot stress is not applicable in this case, an extrapolation method in conjunction with FEA can be proposed according to a fatigue classification from EC3.

1.5 Outline

The literature review is presented in Section 2. It provides insight in both the applicable design codes for fatigue, as well as a discussion on relevant research and publications on this topic. The concept of the developed subroutine is discussed in Section 3. It addresses the general workflow but also describes certain procedures in more depth.

Three case studies are considered in this research. The first case study, which focusses on bridge deck stiffener experiments conducted at TU Delft, is presented in Section 4. The study on the design recommendation on tubular joints by CIDECT is presented in Section 5. The case study considering the marine tubular joint fatigue experiments is presented in Section 6. Finally, some complexities that were experienced during the FEA modelling of tubular joints are discussed in Section 7.

The findings and conclusions from this research are discussed in Section 8. This section will also provide recommendations for further studies.

2 Literature review

This section provides an overview of the considered literature for this study. It includes the considered design codes containing fatigue assessment recommendations. Also, a selection of research publications that have provided more insight on this topic is discussed.

2.1 Design codes

Internationally well-recognised institutions that address fatigue include International Institute of Welding (IIW) [9], International Organization for Standardization (ISO), American Petroleum Institute (API), Eurocode3 (EC3) [6] and Det Norske Veritas (DNV) [3], to name just a few. This research will be limited to IIW, EC3 and DNV, which represent the most common codes in the Dutch industries. In addition, CIDECT recommendations on the design of tubular joints [2] are considered. Its recommendations are mostly based on IIW, but are extended for the particular application of tubular joints.

2.1.1 SN-Curve classification

Both IIW and Eurocode classify the weld types identical, both in category 100 and 90. Eurocode3 provides an additional category 112 for flush butt welds. The reduction factor from size effects is described in IIW for the hot spot stress method, using 25 mm as reference thickness. EC3, however, provides guidance on this for the nominal stress method classifications, but not for the hot spot stress method. This aspect cannot be neglected; therefore size effects are to be considered according to IIW recommendations. The size reduction factor is given as:

$$f(t) = \left(\frac{t_{ref}}{t_{eff}}\right)^n$$

DNV uses for all welded connections the D-Curve, which is equivalent to IIW FAT category 90, unless the principal direction is smaller than 30 degrees from the weld. In this case the C2-curve is applicable, which is equivalent to category 100 in IIW. The size reduction factor is also applicable for DNV, with a reference thickness of 25 mm as in IIW. DNV, however, applies a single thickness correction exponent of 0.2 to all welds related to the D-Curve. Even though this exponent is also 0.2 in IIW for most applications, this exponent could vary for certain joint categories.

Since DNV is applicable to the offshore industry, it provides also guidance for a marine environment. Corrosion has a deteriorating effect on fatigue life. Each fatigue classification contains a specific SN-curve for applications in air, in seawater with kathodic protection, and seawater without kathodic protection (i.e. free corrosion). IIW and EC3 classifications are only applicable to structures in air.

2.1.2 Extrapolation method

Both IIW and DNV describe extrapolation methods dependent on the mesh-size. The smallest element size that DNV considers equals the plate thickness. A linear extrapolation with read out points at 0.5t and 1.5t from the weld toe is used, with t being the plate thickness. For larger elements a second order polynomial is fitted for the stress results, then using the same read out points for linear extrapolation.

IIW describes a wide range of extrapolation methods, depending on mesh-size, thickness dependence and choice of element (solid or shell). Compared to the equivalent DNV case, using an element size equalling the plate thickness is considered a coarse mesh. As for DNV the read out points are at 0.5t and 1.5t from the weld toe. The read out points for a fine mesh, using an element size smaller than 0.4t, are at 0.4t and 1.0t from the weld toe.

Additionally, for thick walled structures with fine mesh IIW recommends quadratic extrapolation. The IIW extrapolation read out points for each case are presented in Figure 2-1.

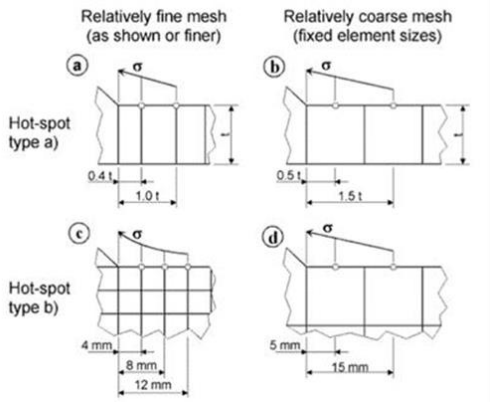

Type of model and weld toe		Relatively coase models		Relatively fine models	
		Type a	Type b	Type a	Type b
Element size	Shells	t x t max t x w/2*)	10 x 10 mm	≤0.4 t x t or ≤0.4 t x w/2	≤ 4 x 4 mm
	Solids	t x t max t x w	10 x 10 mm	≤0.4 t x t or ≤0.4 t x w/2	≤ 4 x 4 mm
Extra-polation points	Shells	0.5 t and 1.5 t mid-side points**)	5 and 15 mm mid-side points	0.4 t and 1.0 t nodal points	4, 8 and 12 mm nodal points
	Solids	0.5 and 1.5 t surface center	5 and 15 mm surface center	0.4 t and 1.0 t nodal points	4, 8 and 12 mm nodal points
*) w = longitudinal attachment thickness + 2 weld leg lengths **) surface center at transverse welds, if the weld below the plate is not modelled (see left part of fig. 2.2-11)					

Figure 2-1 IIW extrapolation guide for hot spot stress [9]

EC3 does not describe any hot spot stress extrapolation method. IIW recommendations should be followed in this regards.

2.1.3 Tubular joints

Special SN-curves are applicable for tubular joints, which are also subjected to the size effect reduction factor. Eurocode and IIW do not get into much detail on tubular joints. CIDECT design guide is required to address this limitation. CIDECT defines the SN-curves as a function of the plate thickness. The CIDECT SN-curve applicable to a reference plate thickness of 16 mm is equivalent to fatigue classification 114 MPa. From the SN-curve definition a thickness effect exponent of 0.38 is calculated. The T-curve described by DNV for tubular joints (reference thickness 32 mm) is equivalent to fatigue classification 90 MPa. Relating the CIDECT SN-curve definition to the DNV reference thickness of 32 mm, the equivalent CIDECT fatigue classification becomes 88 MPa.

2.1.4 Steel bridges

The Dutch Annex of the EC3 on the design of steel bridges [12] provides at the time of writing the most recent fatigue classifications on orthotropic steel decks. For fatigue cracks through the main deck plate, the hot spot stress method is recommended. For cracks through the weld, initiating either from the toe or weld, a different calculation method is recommended. It is based on the local nominal stress in the weld, calculated from the local normal force and bending moment in the stiffener determined from FEA, see Figure 2-2. Distinction is made between hand and automatic welded connections, providing fatigue classification 90 MPa and 100 MPa respectively.

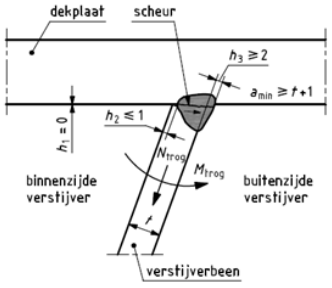

Figure 2-2 Fatigue classification deck-stiffener crack through weld [12]

The basis of this classification is that the geometrical discontinuity at the connection is to be disregarded. When using the stresses from the FEA results, a stress value is to be chosen that represents the reference stress upon which the classification is defined.

2.1.5 Summary

The design code review is summarised in Table 2.1. Only the general applications from this report are presented. This regards SN-curves in air, for thin walled structures. For the extrapolation method only a fine mesh will be applied. Equivalent IIW fatigue classifications at 2 million cycles (FAT) are presented.

Table 2.1 - Summary of design code review for hot spot stress method

	IIW	EC3	DNV	DNV tubular joints	CIDECT tubular joints
Extrapolation points	0.4t x 1.0t	N/A	0.5t x 1.5t	$0.1\sqrt{rt}$ 2)	0.4t x 1.0t 3)
SN-curve FAT class	90/100 1)	90/100 1)	90	90	114
Reference thickness	25	N/A	25	32	16
Correction exponent	0.2/0.3 1)	N/A	0.2	0.25	0.38 4)

1) Distinction is made between the weld types
2) Single read out point recommended for tubular structures
3) Minimum values presented; CIDECT describes boundaries for the extrapolation region
4) Derived from set of SN-curves for each individual thickness

2.2 FEA for fatigue

For fatigue assessments using finite element analysis, the focus is primarily on the hot spot stress method using surface extrapolation. Different methodologies are developed, however. This section provides an overview of these methods, based on comparative studies available in literature.

2.2.1 Structural stress approaches

As discussed in Section 1.2.2 and presented in Figure 1-5, alternative methods are developed for determining the hot spot stresses. A study by Poutiainen et al. [15] compared the three methods. It assessed the limits and accuracy of the methods. The recommendations from the design codes are based on the linear surface extrapolation (LSE). A second method is linearisation through the thickness at the weld toe (TTWT). A third alternative method was developed by Dong [4], which combines features of surface and through thickness extrapolation. Dong developed a mesh-insensitive structural stress definition, which maps a complex stress state in a joint to a simple structural stress state based on nodal force equilibrium.

Radaj [16] demonstrated that linearisation through thickness is a successful approach to determine the hot spot stress. The nonlinear stress distribution is integrated through the thickness, from which a linear distribution is generated (which produces equivalent membrane and bending forces). A common problem with this method is when the FEA post-processor applies nodal averaging close to the weld toe. One needs to make sure only the elements in front of the weld toe are considered, otherwise lower stresses are found in the output.

The Dong method uses a reference plane at a distance from the weld toe where the stress distribution is known a priori. In addition to this structural stress distribution, the shear stress distribution at this distance is integrated to produce a force. As a result of the bending

moment from this eccentrically applied force, a bending stress component can be added to the structural stress distribution at the weld toe. The basis of this method is satisfying equilibrium conditions between the crack plane and the reference plane.

Poutiainen et al. found that for shell element structures, all structural stress methods work adequately well, but care needs to be taken for each method. LSE is the most mesh-sensitive, for TTWT and Dong the mesh-size is of a lesser issue. Care needs to be taken with the nodal averaging feature from FEA software. Dong method requires shear stresses in addition to normal stresses. Additionally, a mesh-size variation resulting in distorted elements as shown in Figure 2-3 was required to obtain good results. This meshing technique is usually to be avoided in good finite element practice. For solid element models, the method for 2D and 3D elements is similar. For TTWT and Dong it is important to take the issue of nodal averaging into account. For Dong method, also the distance and sign of the shear stress is important to consider correctly.

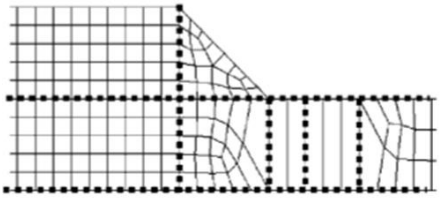

Figure 2-3 Mesh variation for Dong method of analysed 2D cover plate [15]

2.2.2 Effective notch stress

In addition to the hot spot stress method, IIW described the method of the effective notch stress. A reference notch radius of 1 mm (for thick-walled structures) is applied to the weld notch in the finite element model. The stresses computed from FEA can be used directly in the SN-curve of FAT 225. The main advantage of this method is its flexibility to be applied to all possible weld geometries.

A study by Sonsino et al. [20] assessed this concept for four applications from different industries: offshore tubular K-nodes [21], ship deck sandwich panels, automobile door and a trailing link from an automotive chassis. The considered experiment for the tubular K-node is the same as used for the case study considered in this report (Section 6; EU Report [23]).

During the studies, it was found that for each application the fatigue analysis based on the effective notch stress was always on the safe side of design. Some limitations were summarised by Schijve [18] with regards to extending the concept in view of design considerations. Mainly, there is still a lot of ongoing debate on the notch radius size to be adopted. Also, a fully rational solution for the stress gradient at the surface in view of size effects is not yet available.

Considering the development of this concept, it would have great potential to be implemented in a similar subroutine as for the hot spot stress approach. However, it will not be further considered at this stage.

2.2.3 Bending behaviour shell and solid elements

For hot spot stress calculation, stress distributions close to the notch region between two plates are to be considered. As part of this research, the different behaviour between shell and solid elements for complex structures are considered. Differences can be expected, due to the different nature of the connection / intersection between two plates for these element types.

Osawa et al. [13] did research on web-stiffened cruciform welded joints for ship structures from shell finite element analyses. Of particular focus of their research was the influence from transversal bending of the main plate for a T-shape cantilever beam, see Figure 2-4.

Consider the deformation of the flange plate at the intersection, induced by a transverse bending condition. As a result from the transversal stretching, the Poisson's effect causes longitudinal shrinkage. This can be interpreted as longitudinal compressive strains. The transverse bending of the flange is negligible over the entire web thickness for the solid elements; the interface itself restricts this. However, the size of this interface is reduced to a line for the shell elements, which therefore influences the longitudinal stress differently. Osawa et al. examined this behaviour. Based on the outcome of the research, the following correction was proposed for stress from shell element models:

$$\sigma_{sx,SOLID} = \sigma_{sx,SHELL} - 0.09\left(\frac{t_{web}}{t_{flange}}\right)\sigma_{sy,B}$$

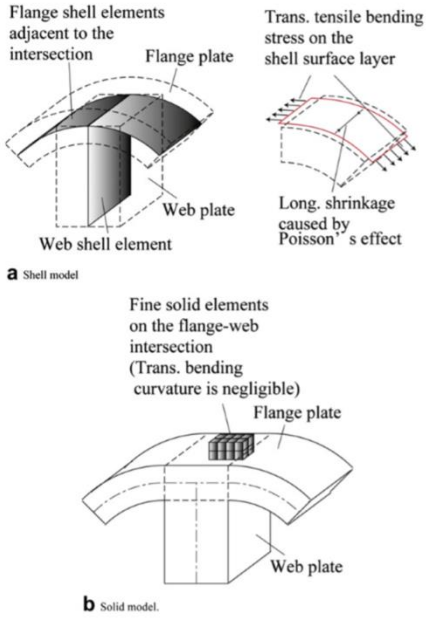

Figure 2-4 Deformation of shell and solid elements [13]

Comparing the corrected shell FE results with solid FE results, good correspondence was found from the study. The proposed correction factor 0.09, however, is only valid for a limited range of wall thicknesses (i.e. 10 to 20 mm). Also, straight plate connections were considered only. E.g. for tubular joints, the curved shape would result in a behaviour difficult to describe by a single correction equation. A quantitative assessment of this correction factor will therefore be outside the scope of this research.

2.3 Circular hollow sections

A short overview of the considered literature for the fatigue analysis on circular hollow sections is provided in this section.

2.3.1 CIDECT K-joint design recommendations

The parametric formulae in CIDECT [2] for calculating the stress concentration factors (SCF) in circular hollow section (CHS) joints are mostly based on research by Romeijn [17] and Karamanos et al. [11]. From a large amount of parametric studies on FEA models, partly validated by experiments, the design equations were developed.

A few considerations when comparing FEA results to the calculated SCFs from CIDECT are of importance. Romeijn developed a method of applying compensating moments to the boundaries, in order to eliminate the effect of the boundary conditions. This allowed for deriving SCFs independently of chord bending stresses. For K-joints, not much information is provided on the derivation of these compensating moments. In addition, the stress direction in the brace is considered to be parallel to the brace axis. This is merely a simplification; it is contradicting the standard hot spot stress approach of considering the stresses perpendicular to the weld toe.

2.3.2 Marine tubular joint experiments

The experiments on the tubular joint reported in [23] provided a follow-up study by Sonsino on the validation of the effective notch stress concept [21]. For this particular application, he found good agreement between the hot spot, notch stress and crack propagation concepts. Hot spot stress calculations were, however, only performed on shell element models considering the Von Mises stresses. Also, the shell plate intersection was considered the hot spot location. Osawa et al. [13], for example, discusses the importance of considering the surface intersection, rather than the shell elements themselves, as the hot spot. It can be said that the hot spot method discussed by Sonsino [21] is subjected to several simplifications. For this reason a more accurate finite element analysis of the experimental results is performed in this report.

2.3.3 Weld quality experiments

Several aspects influencing the quality of the weld are not included in the hot spot stress method for tubular joints. From experiments it was found, however, that these aspects have a positive influence on the fatigue life. The hot spot stress method provides a conservative approach in this regards. This subsection discusses some of the findings from experiments, and to what extent they are part of the hot spot stress method.

The experiments conducted by the European Coal and Steel Community reported in [23] considered the positive effect on the fatigue life of using high strength steel and post-weld treatment (PWT). Also the effect of the marine environment was assessed. The standard welded joints consisted of fine grain structural steel StE 355. Furthermore, four welded joints made of high-strength steel StE 690 with post-weld treatment were tested. The welds of two joints were improved by shot-peening, whereas the other two joints were improved by profile reinforcement and subsequent TIG-dressing. In addition, the joints were either tested in air, in seawater with kathodic protection and in seawater under free corrosion. An overview of the test data is presented in Appendix E.

From the experiments it was found that shot-peening for the StE 690 joints did not significantly improve the fatigue life with regards to the standard StE 355 joints. However, the PWT of profile reinforcement and TIG-dressing improved the fatigue life by factor 2.4 and 3.7 for each joint. From these results it can be said that neither high-strength steel nor shot-peening improves the fatigue life significantly. Profile reinforcement with TIG-dressing provides sufficient improvement that considering the standard hot spot SN-curve leads to significant conservatism.

Marine environments are adequately considered in certain design codes, including DNV. The use of kathodic protection, compared to free corrosion, reduces the crack initiation period. Crack propagation from this stage, however, no significant difference was observed.

Experiment carried out by Schumacher & Nussbaumer [19] focussed on large scale tubular joints typical to bridges. All specimens were made of steel grade S355 J2. The studied parameters were the use of a backing ring for the butt weld, PWT by needle peening and the

size effect. Size effect is already considered for the hot spot stress method, but PWT and use of a backing ring are not.

Backing rings provide a surface for the initial weld pass. It facilitates a better penetration for the butt weld. Even though it improves the quality of the weld, it was found that it had no influence on the fatigue life. On the other hand, significant benefits were found from the needle peening. At least three times as many cycles were required for the first crack to appear, compared to the other tests. For these joints, experiments were not continued until full fatigue failure, so a total improved fatigue life factor could not be derived.

From both experiments [23] and [19], significant benefits from PWT were found, which are neglected in fatigue design. However, each PWT method contributes differently to the fatigue life. E.g. shot peening from [23] and needle peening from [19] are similar methods, but the benefits appear different from each other. It shows that each method needs to be sufficiently tested individually. Existing approaches are continuously further developed and PWT can already be considered in design to a certain extent. IIW Recommendations on Methods for Improving the Fatigue Strength of Welded Joints [8] covers the conventional PWT methods for simple welded plate connections already. Further research by Ummenhofer [24] expanded the database for welded joints for plate thicknesses exceeding the range of applicability of [8]. However, for tubular joints the considered design codes in this research do not cover PWT improvements yet.

3 Fatigue assessment subroutine

This section describes the workflow of the developed subroutine. It describes what user input would be required and discusses the calculation procedures. A final workflow summary of the subroutine is provided. For a selection of screenshots of the user interface, reference is made to Appendix F.

3.1 Introduction

The hot spot stress method is a widely adopted method in combination with finite element analysis. Critical fatigue locations are easily identified by areas of high stress concentrations in complex structures. Even though sufficient information is provided by most design codes, obtaining the correct design stress value for the fatigue assessment from the FEA output proves to be difficult.

For welded structures, normal tensile stresses at the surface perpendicular to the weld are required. However, FEA output provides the stresses in either the global coordinate system or local element coordinate system. The stresses need to be transformed to the orientation of the local weld/surface coordinate system. In case of e.g. a tubular joint as shown in Figure 3-1, the weld follows a curved line. Unless the critical location is known beforehand, for each spot around the weld two main calculations are to be performed; the local weld/surface axis directions and the corresponding stress transformation. This process is cumbersome and prone to error if calculated by hand, hence the benefit for automating this process in a subroutine.

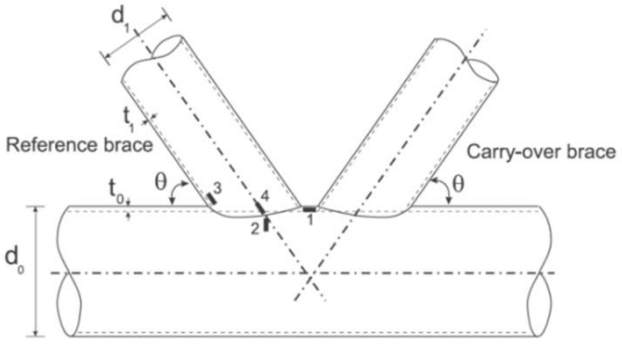

Figure 3-1 Tubular joint weld

The subroutine will function as a post-processor of the FEA data. For this research it is developed as a separate procedure from the DIANA FEA software, for the most part using VBA in Microsoft Excel. Python scripting is used for exporting the relevant FEA data into CSV files, which in turn form the input files for the VBA subroutine. Work flow procedures described in this section are based on this subroutine written in VBA. However, the subroutine is to be fully implemented in the DIANA FEA software in the future. The adopted workflow has taken this into account, where possible.

3.2 User input

To calculate the hot spot stresses for welded structures, user input is required first. The user is to define the following:

- Weld geometry in the finite element model
- Applicable design code and corresponding SN-curve
- Stress extrapolation method

Two types of welds can be identified in finite element models, i.e. edge and face weld (see Figure 3-2). The edge weld usually represents, but is not limited to, a butt welded connection using shell elements. The stresses in the edge are calculated in two directions; the two adjoining surfaces. The face weld represents the weld geometry itself. Stresses are calculated at each edge of the weld. At each edge the stresses are calculated at one surface direction only. The user is to define the relevant connecting surface, so the correct direction is chosen (see Figure 3-3).

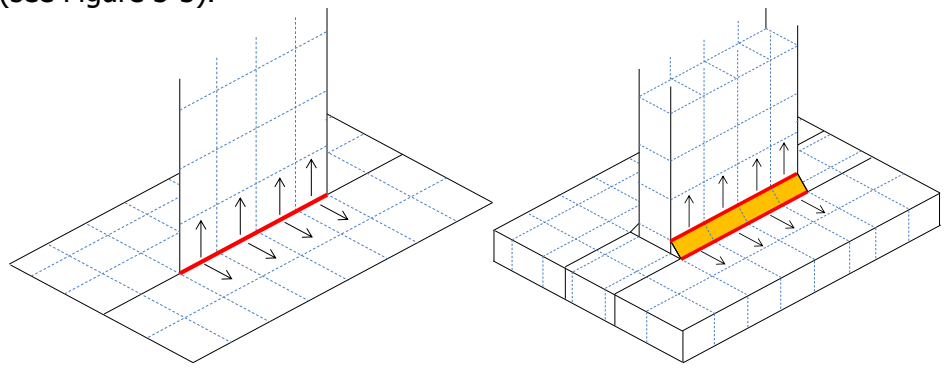

Figure 3-2 Edge weld (left) and face weld (right)

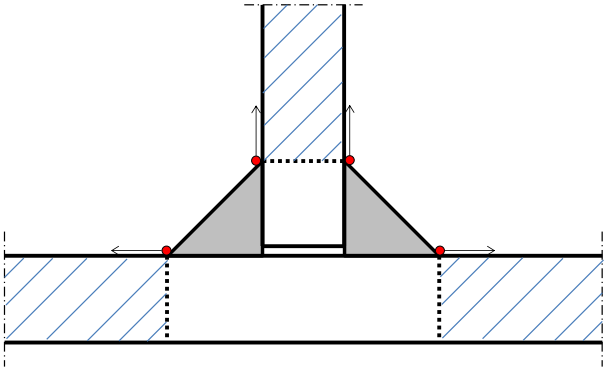

Figure 3-3 Considered hot spot locations

The SN-curves for four design codes are implemented: IIW, CIDECT, EC3 and DNV. It accounts for the (slightly) different SN-curves definitions that are adopted in each code. In addition DNV includes SN-curves for fatigue in a marine environment.

In addition, the user is to select the extrapolation method, through which the hot spot stress is calculated. The standard method is linear extrapolation, which requires two read out points. Default distances would be according to the applicable design code's recommendations as discussed in Section 2.1. An alternative method uses quadratic extrapolation, which requires three read out points. This is sometimes recommended for highly nonlinear stress distributions. This method will not receive further attention in this report.

3.3 Hot spot stress calculation

The procedure of the hot spot stress method is as follows:

- Define local weld coordinate system
- Determine coordinates of read out points for stress extrapolation
- Perform stress transformation to obtain equivalent surface stress at the nodes
- Interpolate equivalent stresses from nodes to read out points
- Extrapolate stresses to weld toe for the hot spot stress
- Assuming constant amplitude, calculate fatigue life according to applicable SN-curve

3.3.1 Local weld coordinate system

From the finite element mesh, a line of element nodes are defined as the weld toe. These nodes are from here referred to as 'weld nodes'. For each weld node, a hot spot stress calculation is performed. This calculation consists of the following steps:

- Determine normal vector to the parent shape faces (see Figure 3-4)

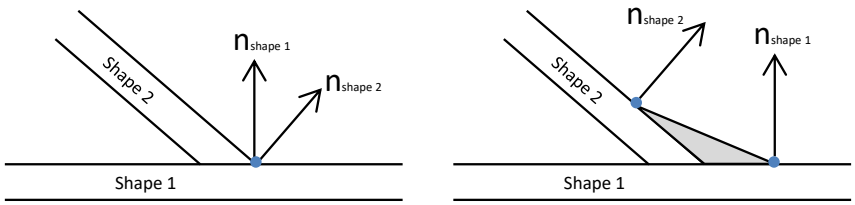

Figure 3-4 Face normal for edge (left) and face (right) welds

- Determine the tangent vector, i.e. longitudinal weld direction. This is approximated by the relative position of the nodes on either side of the considered node (see Figure 3-5).

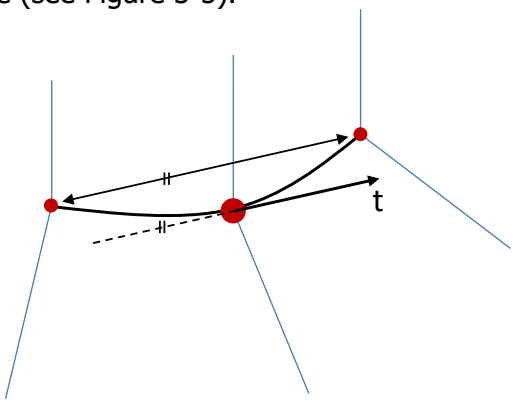

Figure 3-5 Tangent vector relative to connecting nodes

- Use cross-product of normal and tangent vectors to calculate surface vector
- Transformation (rotation) matrix consists of these n-t-s vectors. Each weld node is assigned its respective transformation matrix, see Figure 3-6.

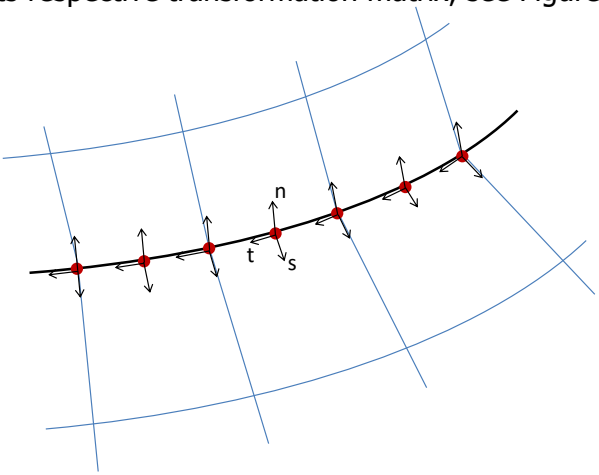

Figure 3-6 Local n-t-s coordinate system at weld nodes

- Determine location of the read out points for stress extrapolation, see Figure 3-7. These positions are either according to the applicable design code or defined by the user. The points are computed in the direction of the surface vector.

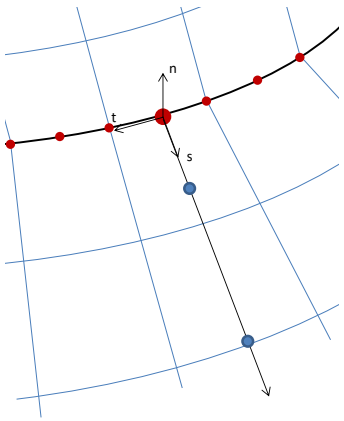

Figure 3-7 Stress read out points

3.3.2 Stresses at read out points

At predefined distances from the weld the stresses are obtained and subsequently extrapolated to the weld. These read out points are located in the direction of the surface vector. These points are positioned independently from the position of the mesh elements. Finite element analysis calculates the stresses in the integration points of the element. The stresses in the element nodes are calculated by extrapolating from the integration points. The stresses in the nodes are presented by default in DIANA FEA output. The stresses in the read out points do therefore not follow directly from the FEA output. Therefore a method is adopted to find the representative stress from the FEA output in the read out points. Three methods are considered and are briefly discussed below:

- Extrapolate stresses from integration points
- Virtual element
- Probe curve (DIANA FEA feature)
- Interpolate stresses from element nodes

Extrapolation from integration points

Stresses are calculated in the integration points with finite element analysis. At these locations the stresses are considered the most representative. Therefore it can be expected that extrapolating from these points would give the most accurate stress value in the read out points. However, exact location in terms of x-y-z coordinates of the integration points cannot be obtained from DIANA FEA output[1]. For future implementation in the DIANA software, when this data is available during the analysis itself, this method would be advantageous. For the current subroutine, where CSV data files are exported from DIANA FEA output, this method is considered too impractical.

Virtual element

The read out point is located on the surface of a specific element. From the finite element analysis, the displacements of each node on this element are extracted. A new finite element model is created, consisting of only this element (the virtual element). The nodal displacements are applied to each element node. The shape is re-meshed, ensuring an element node coincides exactly with the read out point. Subsequent finite element analysis directly gives the stresses at the required location. This method can be accurate, but is only practical if building a new finite element model for each read out point is automated.

[1] From tabulated files the coordinates and stresses of the integration points are available. However, the work is performed from DIANA's GUI, where this data is unavailable.

Probe curve
DIANA FEA contains a feature in the post-processor which will give results at predefined coordinates, independent of the finite element mesh. If the read out points are known, the required stresses can be calculated by using this feature. However, the coordinates of the read out points are to be calculated first, which is done outside of the DIANA FEA software. It is therefore preferred to calculate the stresses in the environment where the coordinates are calculated, to avoid having to import/export data back and forth. The probe curve feature was used, however, to validate the stresses from the chosen method described below. The same results were found from both methods.

Interpolation from element nodes
Stresses in the element nodes are presented in DIANA FEA output. When selecting three nodes at the surface, a triangle shaped plane can be formed around the required read out points, see Figure 3-8. From the known stresses at each node, the stresses can be interpolated to the read out point. The nodal stresses are calculated from FEA by extrapolation from the integration points. Some loss in accuracy can be expected when performing an interpolation calculation from extrapolated values. Particularly if badly shaped elements are present around the node, a peak stress at one of the elements is observed (see Figure 3-9). It is assumed that the stress at a node is represented by the average nodal stress among the elements. Even though this would not be entirely accurate, it is found sufficiently representative when a fine mesh is applied. Because the nodal stresses follow directly from the DIANA FEA output, its ease of use makes this the preferred method above the other discussed methods.

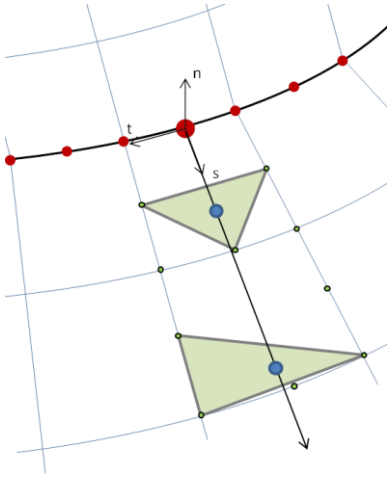

Figure 3-8 Stress extrapolation from nodes to read out point

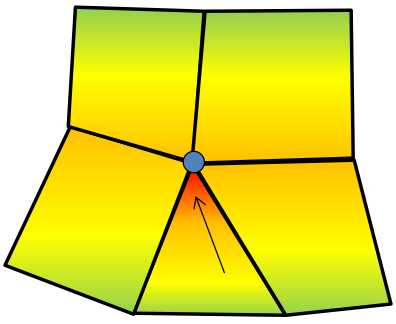
Figure 3-9 Inconsistent stresses around node

For curved surfaces, the read out points are positioned with a slight offset from the surface when the surface vector is followed, as shown in Figure 3-10. The read out point is therefore projected onto the surface in the direction of the weld node's normal vector. Subsequently,

the stresses are interpolated from the element nodes to this intersection point. For shell elements, depending on the integration scheme, the correct layer representing the outer surface is to be selected.

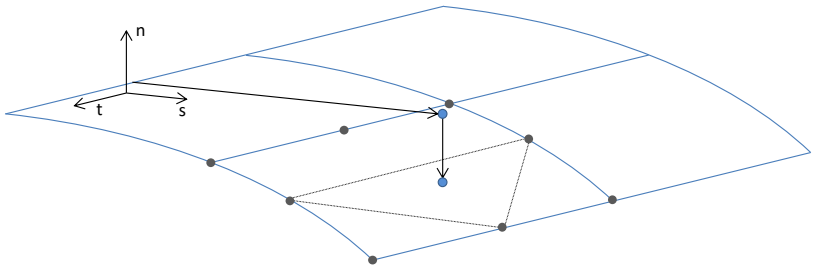

Figure 3-10 Reference point projection on surface

A couple of criteria are to be met to select the three nodes that form the most optimal plane. First a shortlist of the 10 closest nodes to the reference point is made. A cut-off distance is specified, if no nodes are found within this distance the iteration is aborted. It means the stresses from those nodes cannot represent reliable values at the read out point.

The shortlist is sorted on relevance. For solid elements, nodes away from the surface can also be included in this shortlist. Therefore both the absolute distance and the relative surface offset are considered. It is decided that the nodes are sorted on the sum of the absolute distance and three times the offset. This relation was found empirically to give the most reliable results.

Now the nodes are sorted on relevance, iterated is through all possible triangle combinations, starting with the first three nodes on the list. A reliable plane for interpolation is found when the following criteria are met:

- Nodes are not on one line
- Plane not orthogonal to surface (see Figure 3-11)
- Read out point is within the triangle shape (see Figure 3-12)

Nodes not on one line
If the three nodes are positioned on one line, no plane can be formed. The surface area of the triangle formed by the three nodes is calculated. If the area is smaller than a predefined tolerance (close to zero) the nodes are considered on one line.

Plane not orthogonal to surface
The intersection point with the surface is projected in the normal direction from the required reference point. If the node combination forms a plane orthogonal to the surface vector, this intersection point would occur towards infinity. If the cross-product of the plane equation and the surface vector is close to zero, the plane is considered orthogonal to the surface.

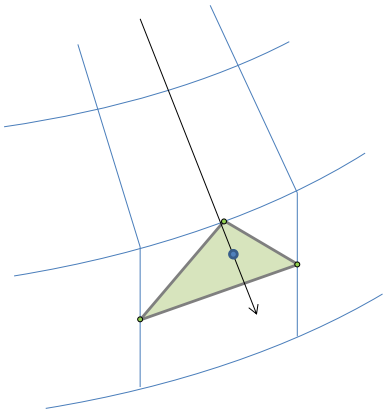

Figure 3-11 Plane orthogonal to surface vector

Read out point within triangle shaped plane
Generally it was found that results were better if the stresses were interpolated rather than extrapolated to the read out points. Even though it would not necessarily be considered an error, the algorithm disregards for this reason the node combination if it does not encompass the read out point.

Three triangles can be formed from the read out point in addition with two of the three considered nodes. This criterion is checked by comparing the sum of these surfaces with the triangle surface of the three nodes. If the surface sum equals the base surface, the reference point lays within the triangle shape.

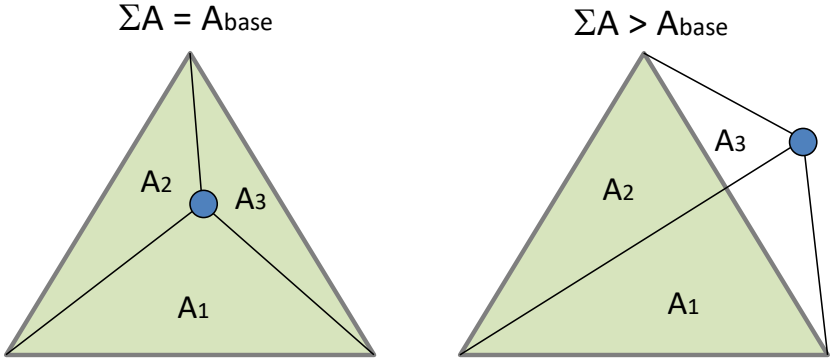

Figure 3-12 Reference point inside and outside triangle shape

3.3.3 Stress transformation

The representative stresses at each read out point are transformed to the orientation of the local n-t-s coordinate system. With the transformation matrix defined as:

$$\boldsymbol{R} = \begin{bmatrix} n_x & t_x & s_x \\ n_y & t_y & s_y \\ n_z & t_z & s_z \end{bmatrix}$$

The transformation becomes:

$$\overline{\boldsymbol{\sigma}} = \boldsymbol{R}^T \boldsymbol{\sigma} \boldsymbol{R} = \begin{bmatrix} n_x & n_y & n_z \\ t_x & t_y & t_z \\ s_x & s_y & s_z \end{bmatrix}^T \begin{bmatrix} \sigma_{xx} & \sigma_{xy} & \sigma_{zx} \\ \sigma_{xy} & \sigma_{yy} & \sigma_{yz} \\ \sigma_{zx} & \sigma_{yz} & \sigma_{zz} \end{bmatrix} \begin{bmatrix} n_x & t_x & s_x \\ n_y & t_y & s_y \\ n_z & t_z & s_z \end{bmatrix}$$

Giving:
- σ_{ss} = Normal stress at surface
- σ_{ts} = Shear stress at longitudinal weld direction

3.4 Workflow summary

As a final overview, a summary of the subroutine's workflow is depicted below.

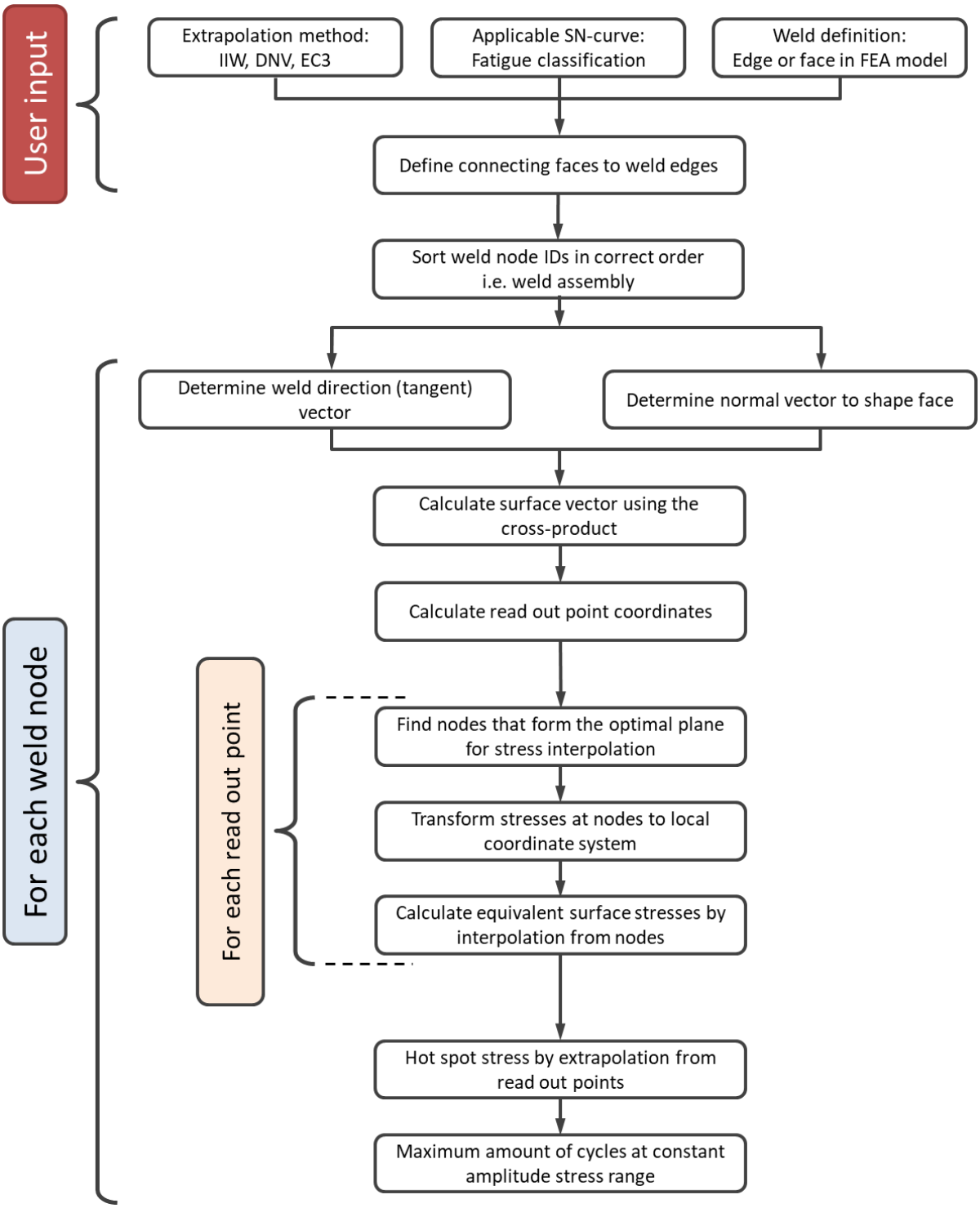

4 Experiments on orthotropic deck plate

This section presents a case study on small-scale specimens from an orthotropic deck plate. Fatigue experiments were conducted from which the results are compared to the FEA and subroutine results.

4.1 Introduction

As part of a research on fatigue in orthotropic deck plates for steel bridges [14], fatigue experiments were performed on cut-out specimens of the deck as shown in Figure 4-1. This resulted in a simple stiffener to deck plate connection, where the fatigue behaviour in the weld could be well assessed.

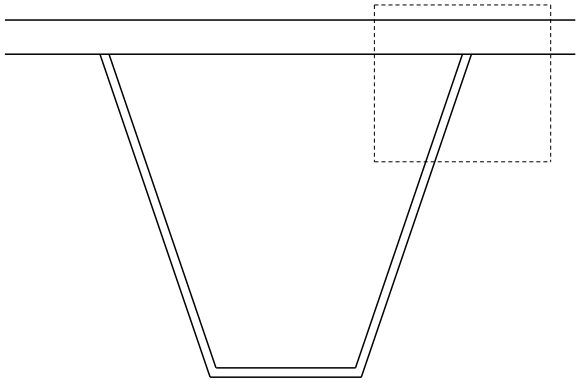

Figure 4-1 Deck plate cut-out

Specimens consist of both automatic and hand welded connections. The quality of the weld influences the fatigue life significantly. Therefore a separate fatigue assessment is performed for the two weld types.

The purpose of this case study is to validate the finite element model with the measurements from the experiments. Furthermore, a comparison is made between the use of shell and solid elements, in which the influence of the weld profile is also assessed. Finally, a fatigue assessment is performed according to the Dutch Annex of Eurocode 3 on the design of steel bridges [12] and compared to the experiments.

Based on the findings from this case study, a recommendation can be written on how to implement the hot spot stress subroutine in combination with FEA software on an entire orthotropic bridge deck.

Fatigue failure of all tests occurred through the weld, with crack initiation in the weld root. Emphasis of this case study will therefore be on this location. Note that the hot spot stress method is only applicable to cracks initiating at the weld toe, which is not the case here. For this specific application, however, similar steps can be taken in order to implement the fatigue assessment into the subroutine.

4.2 State of the art

As discussed in the previous section, the test specimens consist of cut-outs from an entire orthotropic deck plate. The load is applied perpendicular to the stiffener, and evenly distributed along the entire width. The main plate is clamped on either side. The dimensions and schematics are presented in Figure 4-2. The profiles of the automatic and hand welds are presented in the photos of Figure 4-3.

The following material properties are applicable:

Young's Modulus: $E = 210000\ MPa$
Poisson's ratio: $\nu = 0.27$

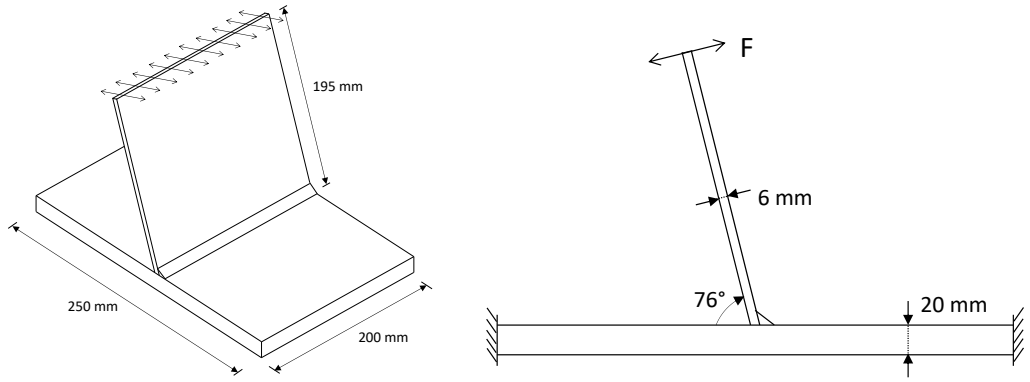

Figure 4-2 Test set-up

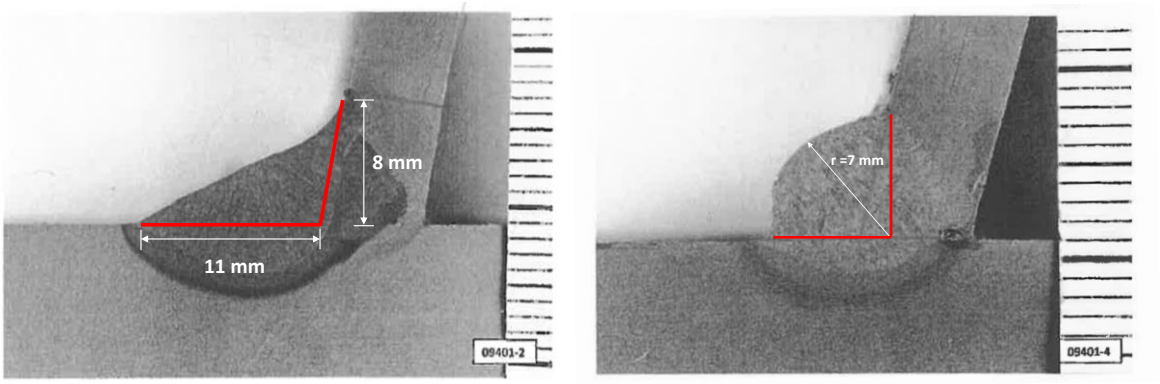

Figure 4-3 Weld profiles: automatic weld (left), hand weld (right)

Strain gauges were placed at various spots on both plates, though main emphasis was on the inside of the stiffener. This can be seen from the strain gauge arrangement shown in Figure 4-4, where most gauges are placed on the web close to the weld root.

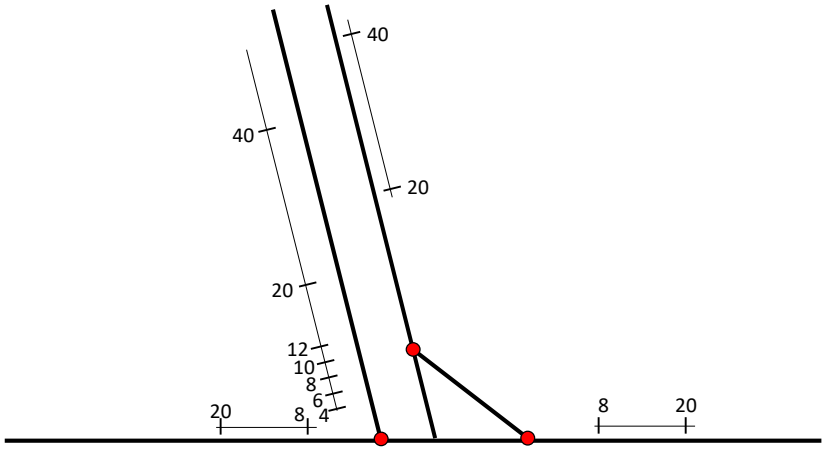

Figure 4-4 Strain gauge arrangement

For calculating the stresses from the measured strains, the classic bending beam theory is not applicable. The Poisson effect is resisted in lateral direction, which results in higher stresses compared to beams. The constitutive relation for bending in plates gives:

$$\sigma_x = \frac{E}{(1-\nu^2)}\varepsilon_x$$

4.3 Finite element analysis

Finite element analyses are performed of the experiment set-up by using both shell and solid elements. For the shell element model, regular quadratic curved shell elements are used. Quadratic structural solid elements are used for the solid element model.

During the experiments both forces and displacements were measured. It is chosen to perform a displacement controlled analysis, since the displacements were well monitored during the experiments. Displacements are prescribed on the line edge for both the shell and solid element models.

According to the test set-up, both translations and rotations are constrained at each plate end. Solid elements do not have rotational degrees of freedom. Therefore only for the shell model the rotations are constrained. Since the analysis is displacement controlled, displacement in the direction perpendicular to the stiffener is constrained on the top edge. This is required for DIANA FEA input using prescribed displacements. For the base case, a distributed displacement of 5.21 mm is applied to the top edge, corresponding to test #7.

The models are subdivided in order to create a finer mesh around the area of interest. The finite element model (solid elements) with its boundary conditions is shown in Figure 4-5.

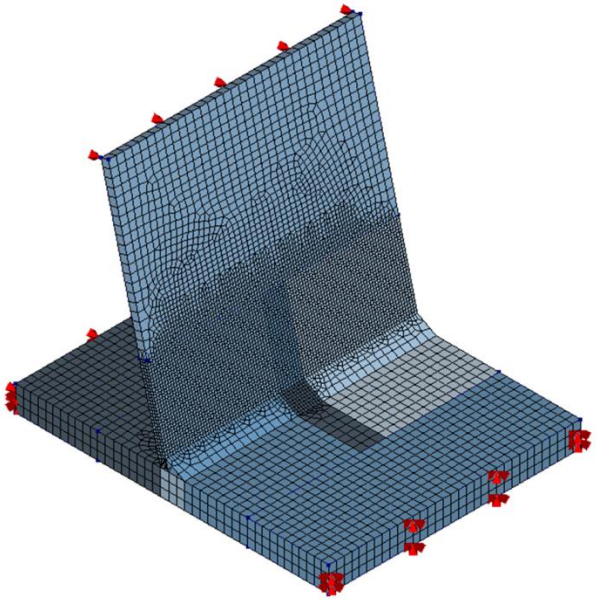

Figure 4-5 Solid element model (automatic weld example)

4.3.1 Shell element model

Regular quadratic curved shell elements are used for this finite element analysis. Through the thickness a 3-point Simpson integration scheme is applied. This integration scheme is sufficient for a linear elastic analysis, to which this study is limited. For nonlinear analyses, a higher order integration scheme would be required.

For analysing the hot spot stresses using shell elements, the location of the hot spot is to be defined at the intersection of the plate surfaces rather than the shell intersection. In particular for the stresses on the inside of the stiffener, the presence of the weld is of high importance for the local stiffness and stress distribution. Using only shell elements, a thorough approach is required to represent the correct geometry. A visual representation of the weld using shell elements with corresponding hot spot locations is presented in Figure 4-6. The thickness of the shell element representing the weld should equal the throat thickness. Note that the surface of the main deck plate and weld intersects behind the shell elements intersection. This is a downside of using shell elements for this application. For best results, the hot spot is shifted towards the plate intersection. No further attention is given to the stresses in the main deck plate, however. This analysis will focus on the stresses in the stiffener only.

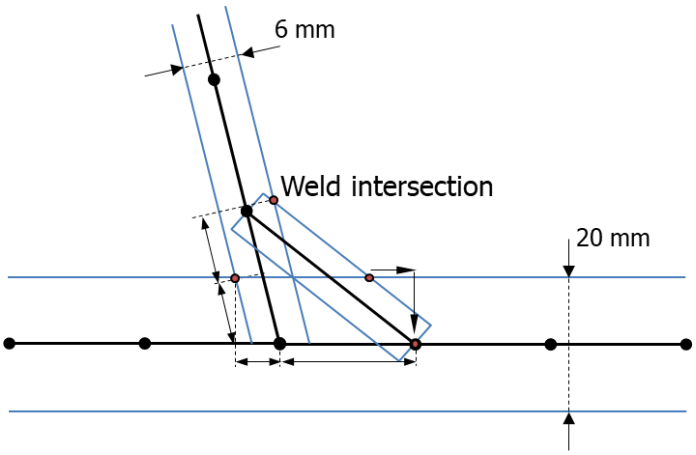

Figure 4-6 Weld profile using shell elements

Referring to Figure 4-3, only the automatic weld profile can be represented accurately using shell elements. The circle shaped hand weld profile would be impractical. The results presented in this section are therefore only applicable to the automatic weld specimen.

4.3.2 Solid element model

Quadratic structural solid elements are used for this model.

For the hand welds, the geometry is of a more circular nature as can be seen in Figure 4-3. When using shell elements this geometry is impractical to represent, for solid elements this distinction between hand and automatic welds can easily be realised. The weld profiles in the finite element model are shown in Figure 4-7.

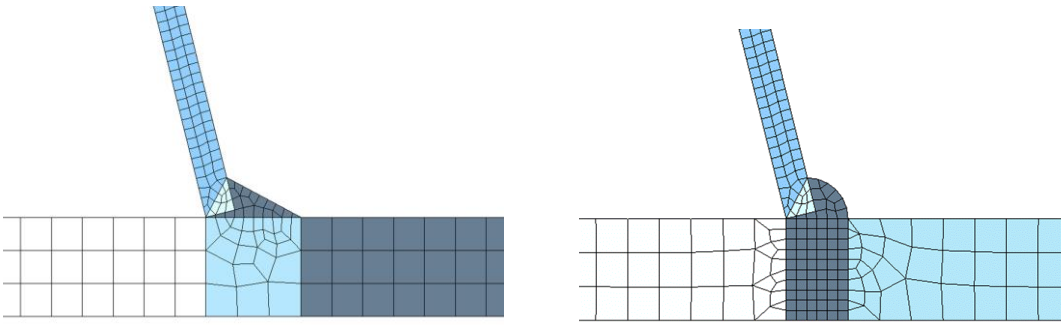

Figure 4-7 Finite element weld profiles: automatic weld (left), hand weld (right)

4.4 Mesh refinement

A mesh refinement study is performed to find the optimal element size for both the shell and solid element models. As mentioned before, only considered are the stresses on the inside of the stiffener. The stresses for the remainder of this case study are presented with regards to the orientation shown in Figure 4-8. The blue line shows the general shape of the found stress distribution. The red line indicates the considered surface.

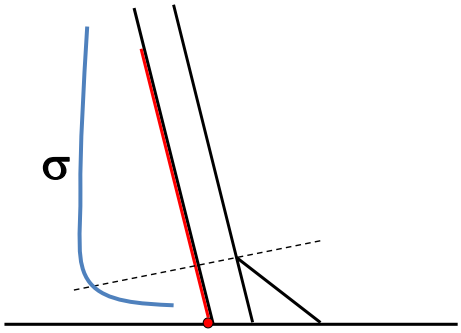

Figure 4-8 Orientation considered stresses

4.4.1 Shell elements

Contrary to solid elements, computation time is not that much of an issue with shell elements. However, the behaviour at the plate intersections can be influenced by the mesh-size and needs to be assessed.

The hot spot for this analysis is the weld root, located at the plate surface intersection. All distances are relative to this intersection, in the direction of the surface of the stiffener. The mesh-size is selected relative to the stiffener plate thickness (i.e. 6 mm), ranging from one time the thickness to a sixth of the thickness. The results are presented in Figure 4-9.

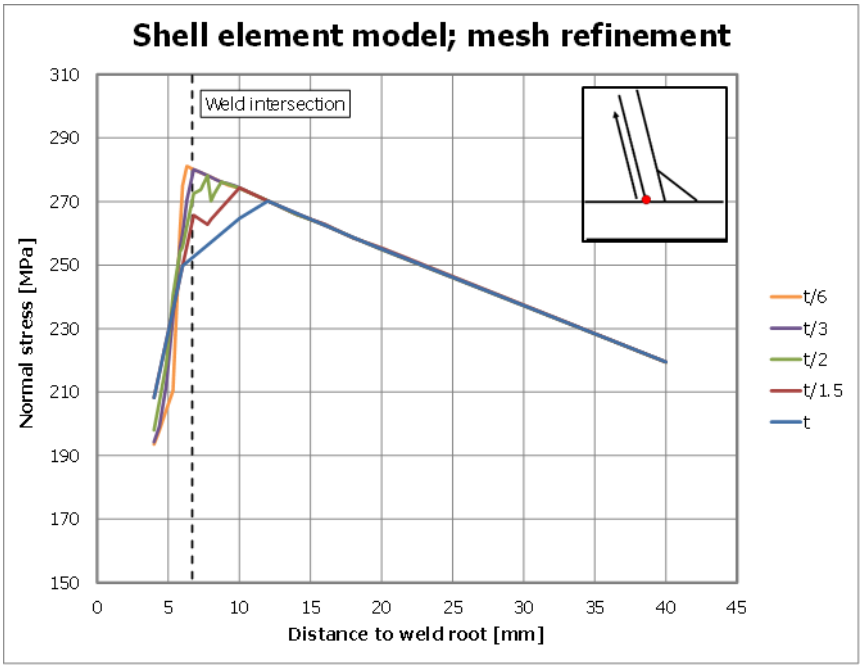

Figure 4-9 Shell elements; mesh refinement

It can be observed that the behaviour close to the intersection of the weld and web plates is influenced significantly by the mesh-size. For the larger mesh-sizes, some level of distortion is seen. Also, the location of the peak stress shifts towards the intersection for decreasing mesh-sizes. It is found that the peak occurs at the closest element edge to the weld intersection, hence its mesh-size dependence. However, the stresses are only influenced by the mesh-size close to the weld. Away from the weld, the stresses for a coarse mesh give the same results. The linear stress path further away from the weld allows for a reliable extrapolation to the weld root.

For a reliable representation of the stresses close to the weld, it is recommended to adopt a minimum mesh-size of t/3. However, when using read out points for extrapolation further away from the weld, a larger mesh-size equalling the plate thickness would be sufficient. A maximum mesh-size equalling the distance from the weld intersection to the first read out point should be adhered, to avoid using a pre-peak stress value.

4.4.2 Solid elements

A mesh refinement study is performed to find the optimal solid element size. Since computation time is of significance for the solid element model, it is preferred to adopt an element size that is as large as possible. The results are presented in Figure 4-10.

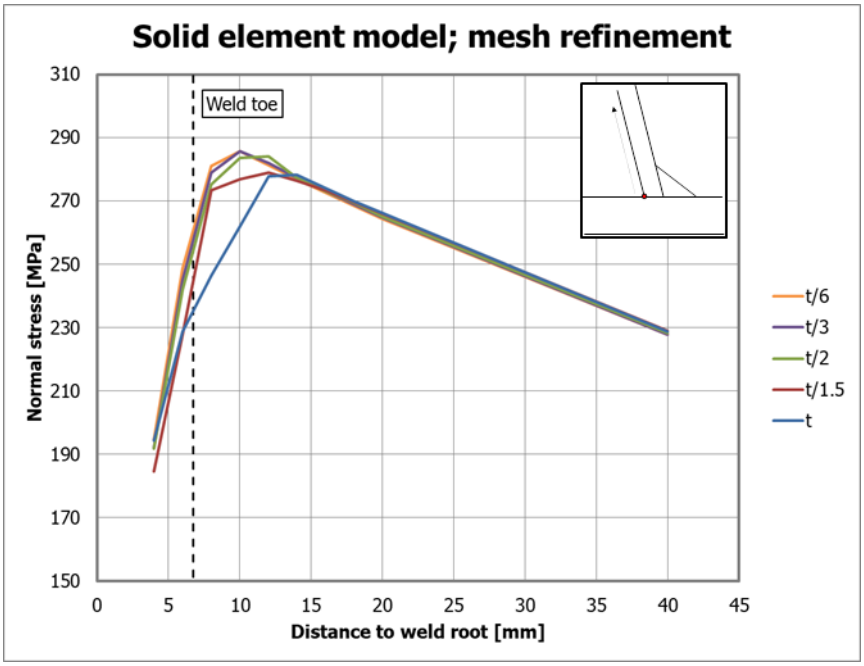

Figure 4-10 Solid elements; mesh refinement

From the curves it can easily be observed that the general outline of the curve differs if the mesh-size is larger than t/1.5 (equals 4 mm). However, looking a bit further in detail shows that the peak stress level (at x = 10 mm) and the post-peak slope converges at a mesh-size of t/3 (equals 2 mm). These two criteria are actually of high importance for the stress extrapolation to the hot spot at the weld root. For example, a slightly steeper slope can amplify the hot spot stress when extrapolated.

As discussed for the mesh refinement study of the shell element model, when using read out points for extrapolation further away from the weld, a larger mesh-size equalling the plate thickness would be sufficient.

A further mesh refinement study was performed to analyse the stresses in the weld region. It was found that an element size of 0.2 mm had to be adopted to obtain a smooth solution. With regards to the fatigue assessment, this region is of less significance however. Only the peak stress and the region beyond the weld are to be used. The results are presented in Figure 4-11. The region within the first millimetre weld root is to be disregarded, because of the singularity in notches where highly fine meshes are adopted.

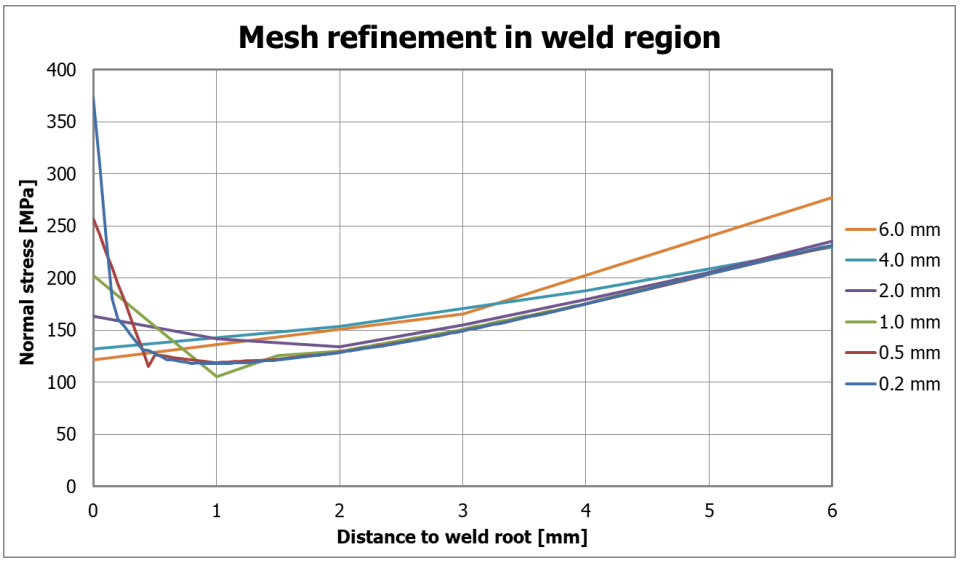

Figure 4-11 Weld region mesh refinement

4.5 Relation FEA results to experiments

The FEA results are compared to the outcome of the experiments. First, the computed stresses are validated by the stresses calculated from the strain gauge measurements. Next, a comparison between the different finite element models is made.

4.5.1 Validation

Data is collected for a set of 18 experiments, with particular emphasis on the stresses at the inside surface of the stiffener. Comparison is made between the stresses that follow from finite element analysis and the strain gauge measurements. Reference is made to Appendix A for the stresses of each experiment. A typical graph for test #7 is presented in Figure 4-12. The presented measurements are taken at approximately 5000 cycles, which can be considered the start of each experiment. The solid element model is used for the comparison of results. Corresponding to the observations from the mesh refinement study, a highly fine mesh is adopted in the weld region, whereas further away the mesh is slightly coarser. Additionally, a simple analytical calculation is included. It assumes the stiffener to be a cantilever beam clamped at the weld. The stress at each location is calculated as follows:

$$\sigma = \frac{M}{W} = \frac{F \cdot (L - x)}{\frac{1}{6} b t^2}$$

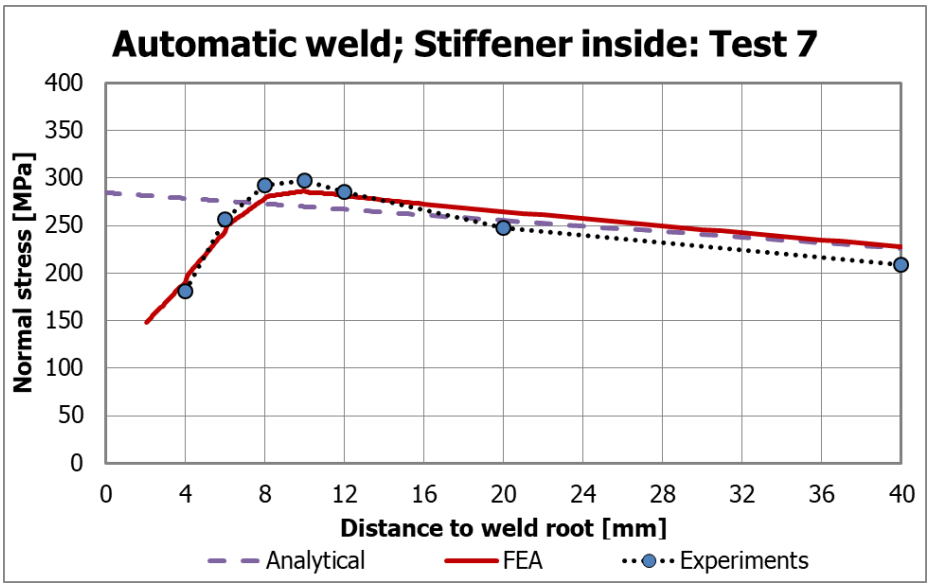

Figure 4-12 FEA vs. experimental results

For the analytical solution, the reaction forces from the solid element model FEA at the imposed displacement are used for the calculation. The analytical solution corresponds well with the numerical solution further away from the weld. In addition, the general shape of the curve in the weld region of the finite element analysis corresponds well with the stresses from the experiments.

However, the experimental results show lower stresses further away from the weld. E.g. for test #7 at 40 mm from the weld root, the stress is 10% lower. The peak stress on the other hand, which is located approximately half the plate thickness from the weld toe, is higher than the stress calculated from FEA. Also a change in slope is observed, between 10 and 20 mm from the weld root. As a result the stress magnitude drops with respect to the stresses from FEA. The lower stresses measured from the gauges at 20 and 40 mm are consistently lower for each conducted experiment. Influence from the weld geometry can be neglected at these locations.

The effect the welding process has on the local geometry and material properties is complex. The general stress distribution is well modelled by a simple solid element weld profile. However, some parametric studies are performed to assess the measurements with more detail. It will give a better understanding on how the quality of the weld can be reproduced in FEA, which can form the basis for further research. The parametric studies presented in Section 4.6 focus on the weld size, level of protrusion and the influence of a different Young's modulus of the filler material.

4.5.2 Finite element model comparison

Stresses for both the shell and solid element models including the weld profile are computed using the fatigue subroutine. Additionally, an analysis is performed using solid elements without the presence of the weld profile. The results are presented in Figure 4-13. The highly fine mesh to accurately compute the stresses close to the weld root is not adopted for this comparison.

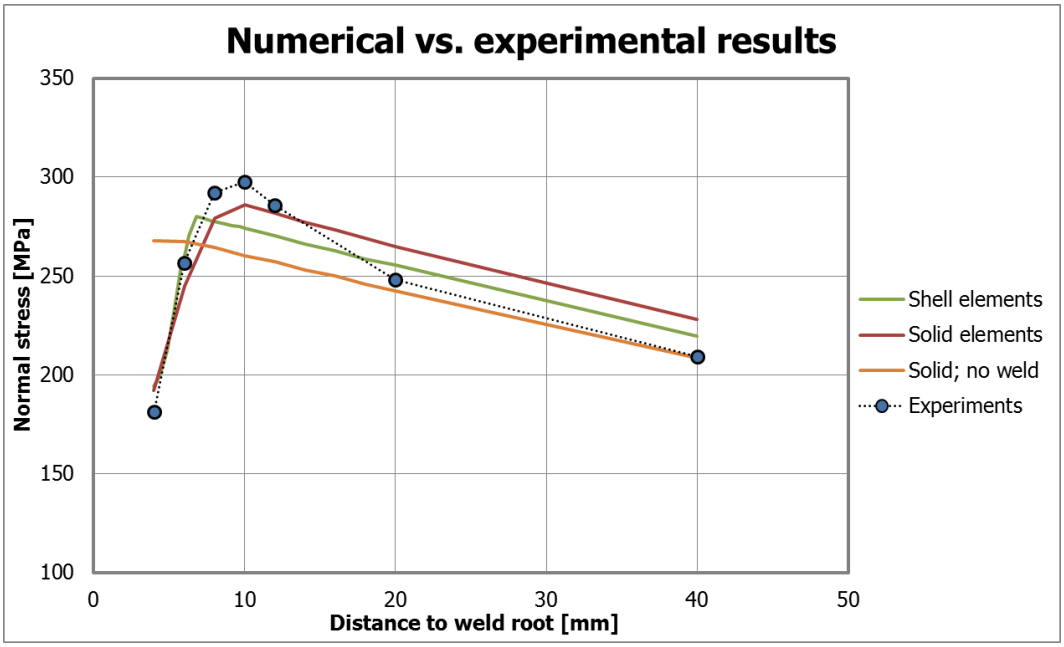

Figure 4-13 Comparison of results

The importance of including the weld profile becomes clear from the figure; ignoring its influence would significantly underestimate the stresses. Though not presented, a similar observation was made for the shell element model without the weld profile. When carefully selecting the mesh-size for the shell elements, decent correspondence with the experiments can be found. However, both increasing and decreasing the mesh-size could give different results. Overall it can be concluded that the solid element model represents the stresses in the weld more accurately.

For fatigue cracks through the weld of a bridge deck stiffener, a recommended fatigue classification is available in the Dutch Annex of Eurocode 3 on the design of steel bridges [12]. The fatigue class is based on the local nominal stress in the weld. Influence of the weld profile is ignored for this stress value. Despite the experiments showing a reduced stress at the crack initiation point, the larger local nominal stress is used as the reference stress. This stress can easily be obtained from the FEA output, since the stresses in the stiffener increase linearly towards the weld. The influence of the weld needs to be avoided, therefore extrapolation from read out points relatively far from the weld region is required (e.g. 20 and 40 mm from the weld root).

The dashed lines in Figure 4-14 represent the recommended stress extrapolation for the stresses at the weld root. Stresses using solid elements are approx. 4% higher than shell elements. An overview of the hot spot stresses for the various described models is presented in Table 4.1.

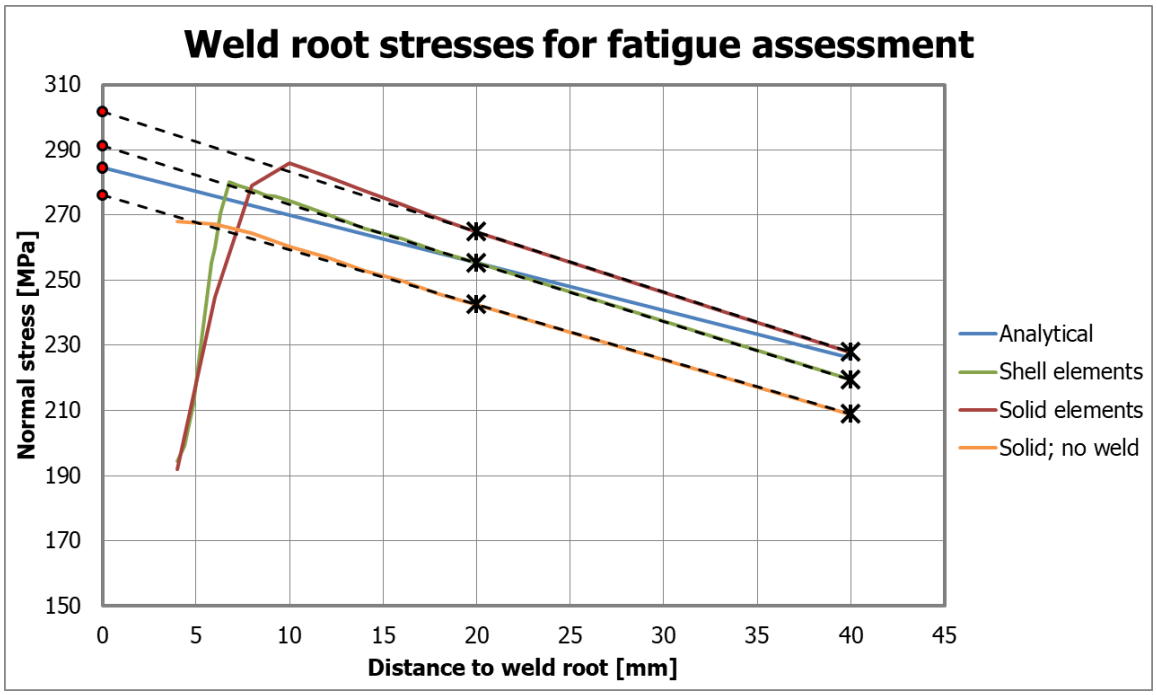

Figure 4-14 FEA model comparison and extrapolation

Table 4.1 - Fatigue design stresses in weld root for test #7

Model type	*Fatigue design stress [MPa]*
Shell elements	291
Solid elements	302
Solid elements, without weld profile	276
Analytical	285

4.6 Parametric study weld profile

The influence on the local stresses of several weld profile properties are presented in the following subsections. Only the solid element model is considered for this study.

4.6.1 Weld size on deck plate

The position of the weld toe on the deck plate is shifted horizontally, see Figure 4-15.

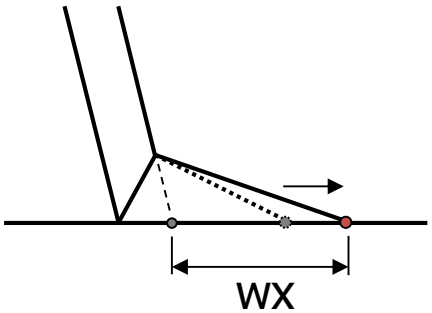

Figure 4-15 Increased weld size in horizontal direction

For the base case, which represents the actual weld profile, the horizontal distance parameter wx is 13 mm. For several distances, the stresses in the stiffener are compared. The results are presented in Figure 4-16. It can be observed that a shift of the weld toe only marginally influences the stress distribution in the stiffener. Only for a reduced size (wx = 8 mm) the peak stress is approx. 1% lower with regards to the base case. A larger

influence on the stresses in the deck plate is expected, however. This is outside of the scope for this research.

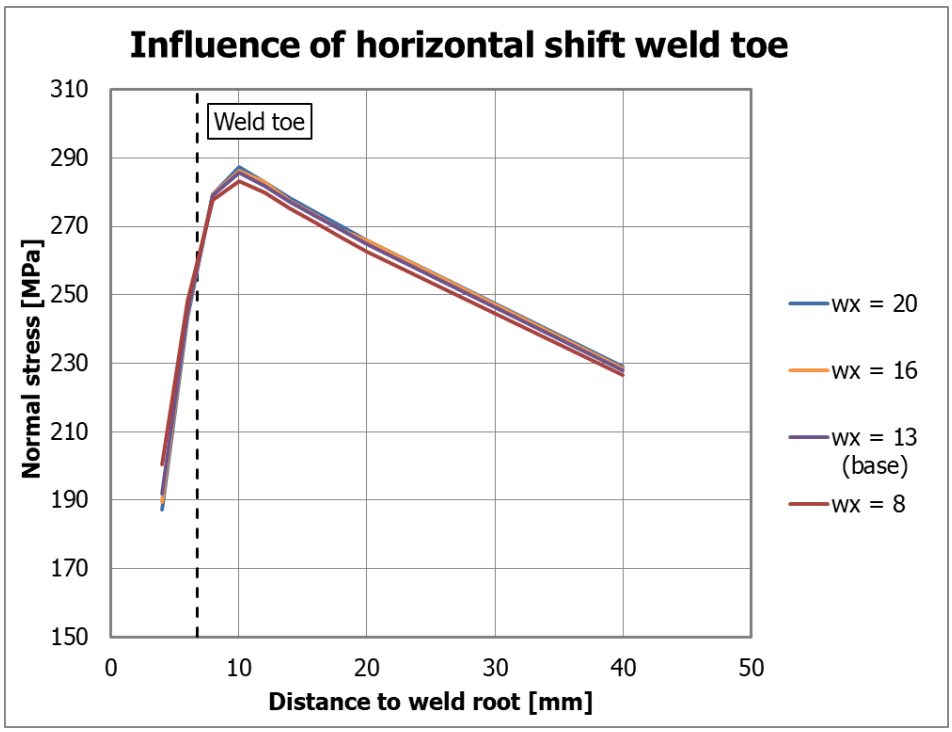

Figure 4-16 Position weld toe on deck plate influence

4.6.2 Weld size on stiffener

The position of the weld toe on the stiffener is shifted vertically, see Figure 4-17.

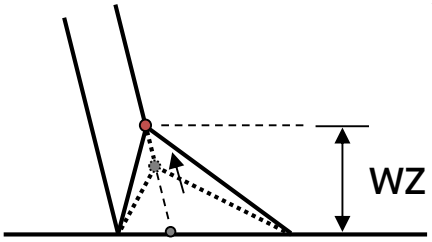

Figure 4-17 Increased weld size in vertical direction

For the base case, which represents the actual weld profile, the vertical distance parameter wz is 8 mm. For several distances, the stresses in the stiffener are compared. The results are presented in Figure 4-18. It is observed that the position of the stress peak shifts linearly along with the position of the weld toe; for each case the peak is positioned approximately half the plate thickness from the weld toe. In addition, the local stiffness increases with an increase of the weld size. The stresses around the weld are found to be lower in the weld region for a larger weld, but from the weld toe onwards the stresses are increased. Generally it can be seen that stresses are about 3% larger if the weld toe is moved vertically by 2 mm.

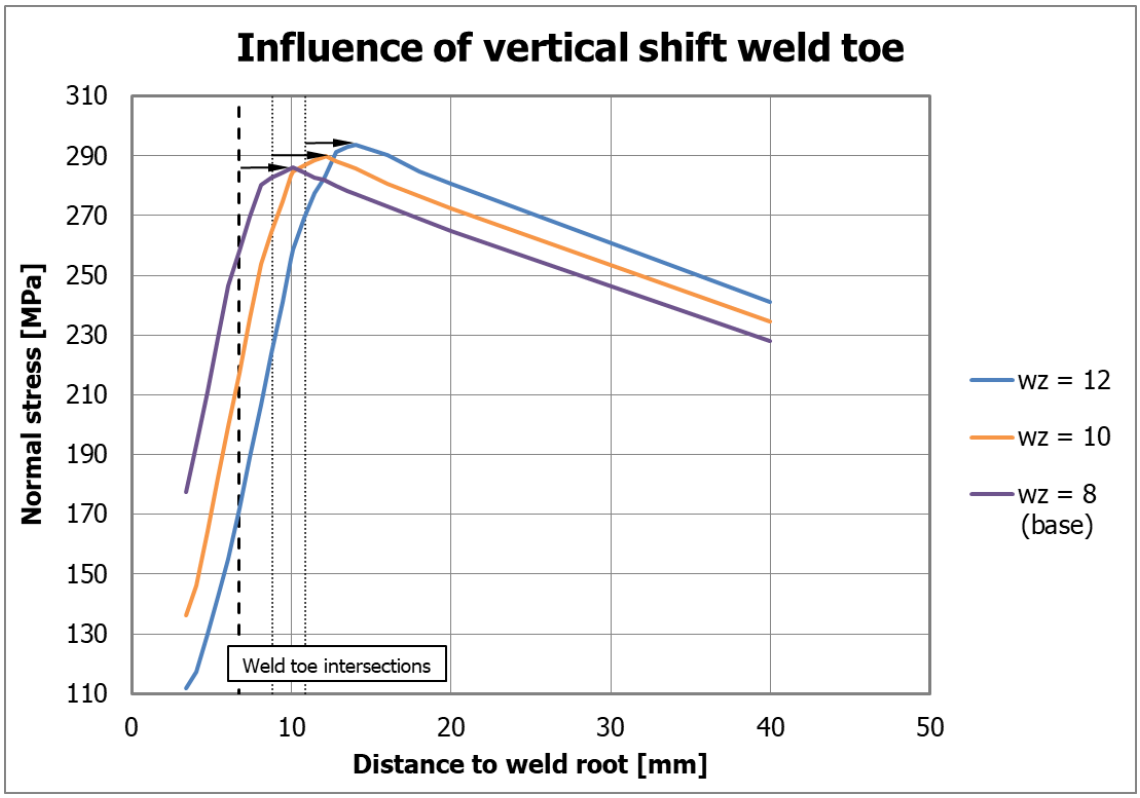

Figure 4-18 Position weld toe on stiffener influence

4.6.3 Level of weld root protrusion

As can be seen from Figure 4-3, both the hand and automatic welds are not fully protruded at the weld root, resulting in an undercut. The finite element model on the other hand neglects this undercut; full interaction is assumed between the entire interface between the weld, stiffener and deck plate. In reality, there is no such interaction at the undercut. The undercut should be limited to 1 mm according to EC3 [6]. This requirement is quite stringent and was not met for many of these specimens, particularly for the hand welded connections. Observed undercut sizes were around 2-3 mm.

In the finite element model, a gap with a height of 1 mm at the weld root is used to represent the undercut, see Figure 4-19. The level of protrusion is measured from the weld toe to root, with 100% protrusion representing zero undercut.

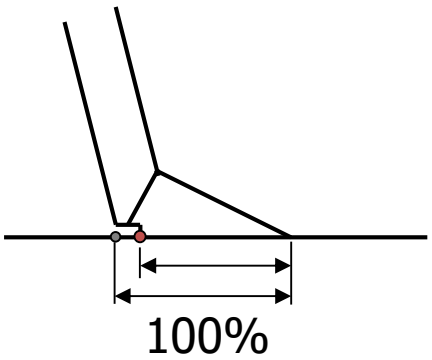

Figure 4-19 Reduced level of weld protrusion at the root

The results are presented in Figure 4-20. It is found that by a reduced level of protrusion, the stresses around the weld decrease. A small change in slope between 10 and 16 mm from the weld root is found as well (see Figure 4-21 for slope references). For 85% protrusion,

the curve's slope decreases by 20% at 16 mm from the root. For 100% protrusion, the decrease of the curve's slope is only 10%. Comparing this with the experiments, a more significant decrease was observed. E.g. for test #7, the slope decreased by 60%.

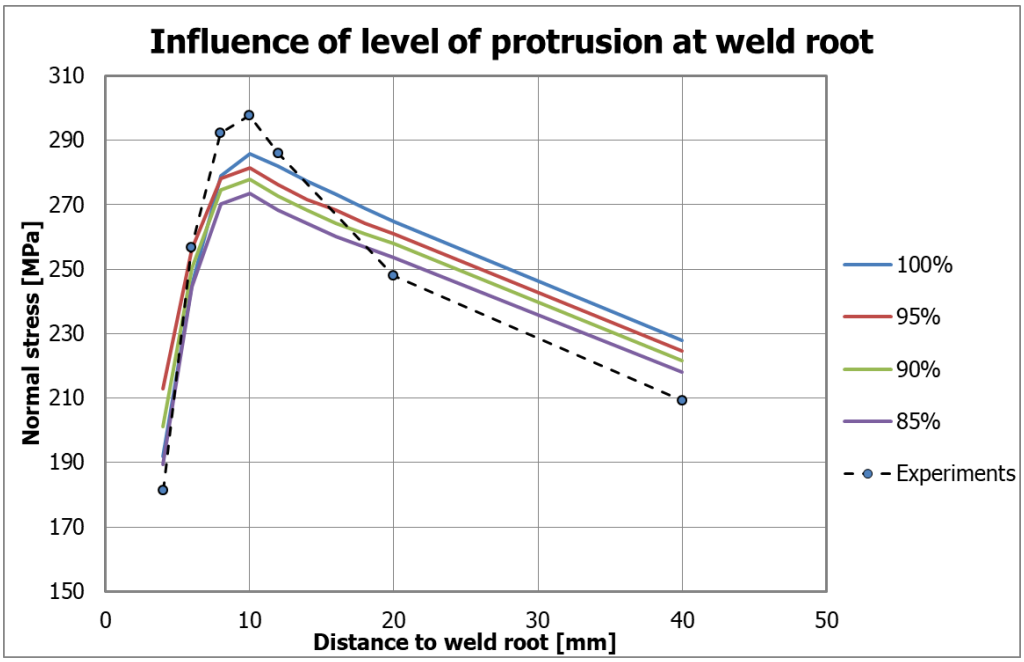

Figure 4-20 Influence of level of protrusion for stresses in the stiffener

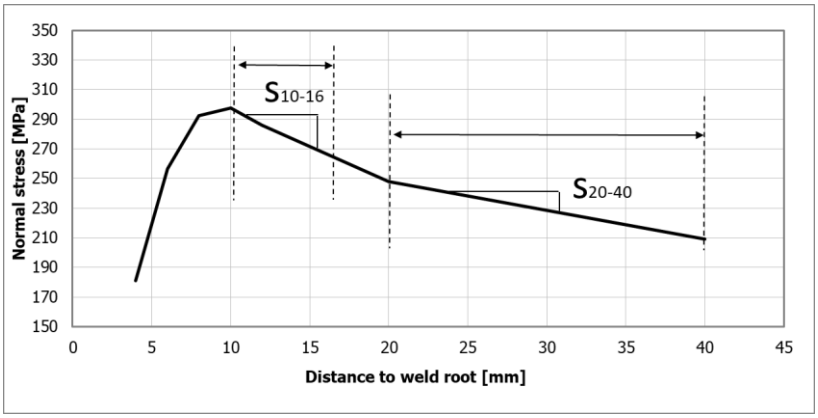

Figure 4-21 Stress curve slopes

Generally, lower stresses result in an improved fatigue life. The general stresses at the stiffener plate surface are lower. However, of more interest is the relative stress level at the root for each case. For each analysed case, the Von Mises stresses at the root are compared in Figure 4-22. In absolute sense, the stress values at the notch have no meaning. However, there is an obvious increase in stress level in case of the presence of an undercut (46% for zero to one mm). For an increasing undercut, the stress level increase is less pronounced (12% for one to three mm). From this can be concluded that meeting the EC3 requirement for a maximum undercut of one mm is beneficial. However, relatively the best improvement is gained by avoiding the presence of an undercut altogether.

It is to be noted that the quality of the weld at the root cannot be assessed by this study. The presented Von Mises stresses in Figure 4-22 are merely intended to provide a sensitivity analysis. The undercut size of each individual specimen in combination with its amount of cycles to failure is required to assess the influence on the fatigue life.

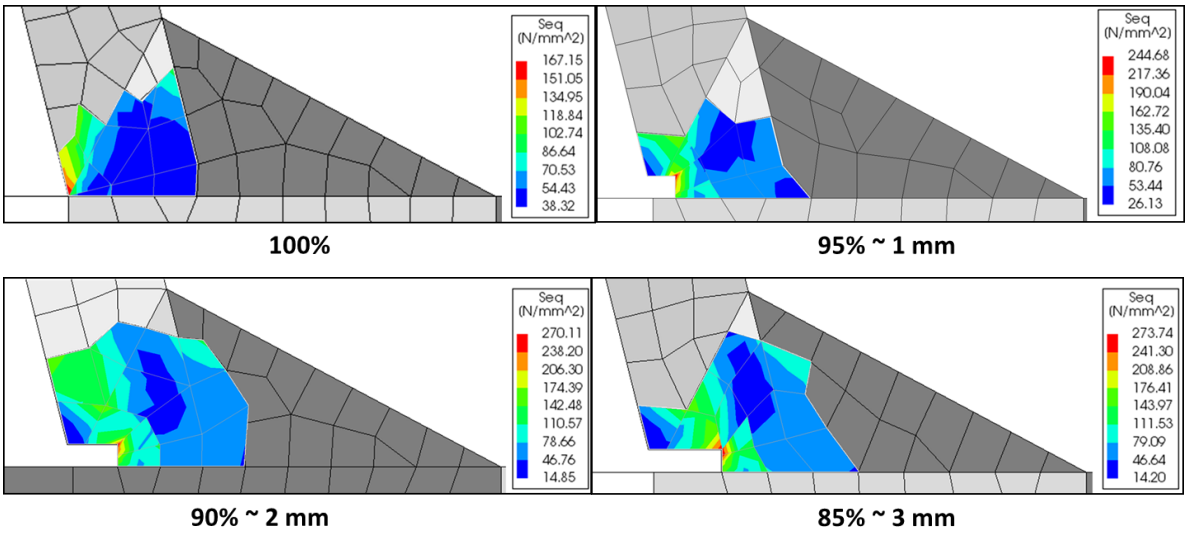

Figure 4-22 Relative Von Mises stresses for levels of weld protrusion

4.6.4 Filler material and HAZ Young's Modulus

From the experiments a pronounced stress peak was observed with regards to the FEA results. From the previous parametric studies, no geometrical parameters were found that could explain this behaviour. During the welding process, the material undergoes significant metallurgical changes. The actual material properties of the weld and heat affected zone (HAZ) cannot be reproduced. However, for numerical calibration purposes an affected Young's Modulus is studied as shown in Figure 4-23. It is known that the Young's Modulus in this area is slightly higher than the base material. First, an equivalent Young's Modulus for the weld and HAZ of 250 GPa is analysed. It was found, however, that the effect on the stresses at the considered surface was marginal (as is shown in Figure 4-25). Therefore, the situation is considered where the Young's Modulus is reduced rather than increased by the welding process. It is stressed that this does not represent the actual material properties at the weld, this option is merely studied for numerical calibration purposes.

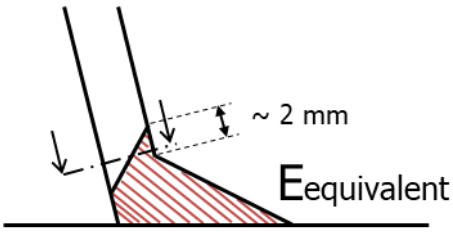

Figure 4-23 Reduced Young's Modulus weld and HAZ

Assuming a reduced equivalent Young's Modulus for the material in the HAZ, the highlighted cross-section is simplified to a composite of two materials. The stiffer material is on the weld root side of the plate, where the stresses are considered. The neutral axis shifts towards the stiffer material, but also experiences larger stresses as shown in Figure 4-24.

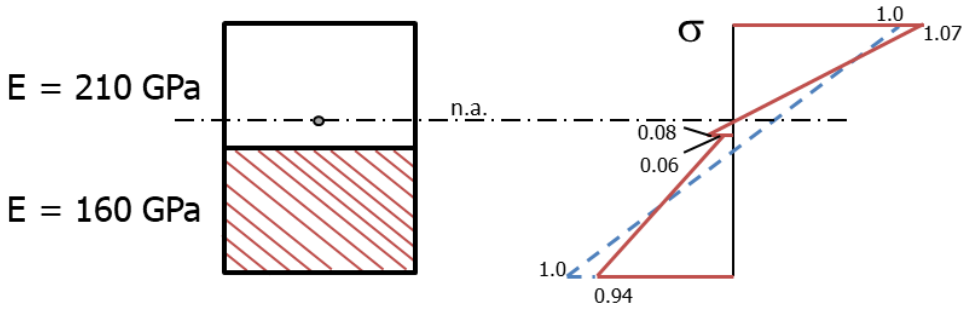

Figure 4-24 Composite cross-section in pure bending

The red dashed line represents the stress distribution in case of a homogeneous cross-section, to which the composite stresses are compared to. The maximum stress at the outer fibre of the normal steel is 7% higher, in case of this simplified composite cross-section. From a mechanics point of view, the observed stress peaks could therefore be explained by the change in material properties by the welding process.

A simplified FEA model is developed based on this concept. The changed Young's Modulus geometry is modelled according to Figure 4-23. The results are presented in Figure 4-25. Even though not pronounced, an increased stress peak according to the experimental results is visible for the reduced Young's Modulus. As mentioned before, a reduced Young's Modulus does not represent the actual weld material properties. Even though a decent curve fit is obtained with the experiments, this possibility should be disregarded as an explanation for the observed stress behaviour at the weld.

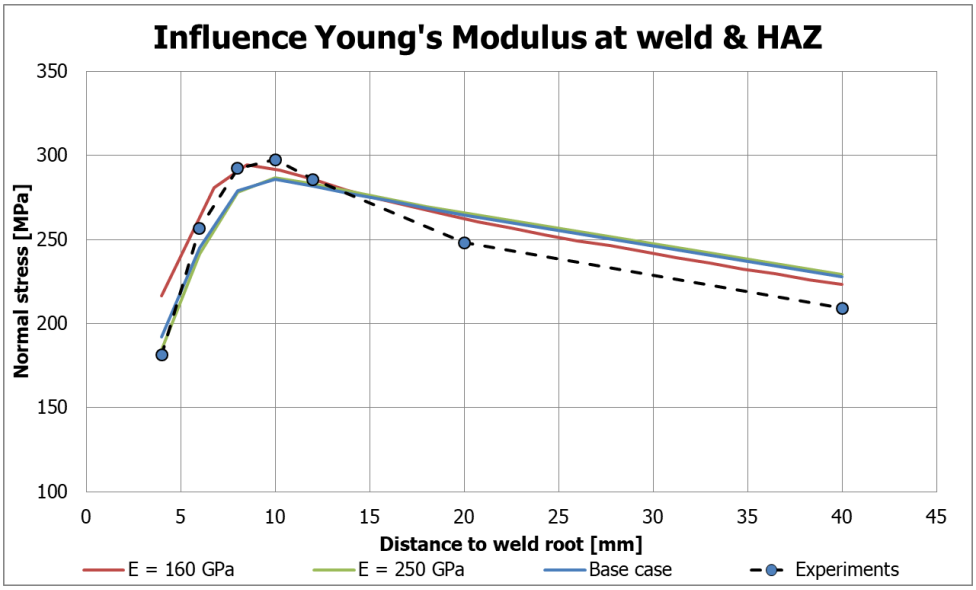

Figure 4-25 Influence of reduced Young's Modulus for weld and HAZ

4.7 Fatigue assessment

The fatigue classification for cracks through the weld in bridge deck stiffeners is given in the Dutch Annex of Eurocode 3 on the design of steel bridges [12]. The classification for hand welds is 90 MPa and for automatic welds is 100 MPa. The design stress is described as the nominal local stress, which in this simple test case can be described as a clamped cantilever beam as presented in Figure 4-26.

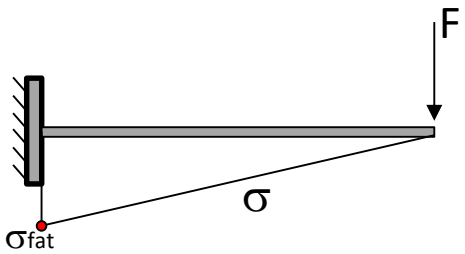

Figure 4-26 Simple stiffener fatigue stress

The recommended stress extrapolation method described in Section 4.5.2 is based on this concept. It can also directly be applied to more complex finite element analysis where e.g. the entire bridge deck is modelled. Since the fatigue classification does not take the influence of the weld into account, it is important that the stress is linearly extrapolated from read out points at a considerable distance from the weld region.

For each type of welds (i.e. automatic and hand) nine experiments were performed. For nine samples, the characteristic SN-curve is obtained by reducing the mean curve by 2.825 times the standard deviation. An example of the statistical calculation for obtaining this value is presented in Appendix B. The cycles to failure from the numerical results are calculated according to stress extrapolation described in Section 4.5.2 and the corresponding fatigue classification of EC3 [12].

The cycles to failure are plotted in Figure 4-27 for the automatic welding and in Figure 4-28 for hand welding. The cycles to failure are plotted against the imposed deformation of the stiffener plate, which is equal for both numerical and experimental results for each test. This is contrary to the convention of plotting the cycles to failure against the stresses ranges. The reason for plotting the cycles against the displacement is that no representative stresses could be derived from the measurements. No reliable comparison between the experimental and numerical results could therefore be made based on applied stress ranges.

It is easily observed that the calculated cycles to failure comply with the characteristic SN-curve obtained from the experiments. Particularly for automatic welding the safety margin is rather large. Based on this data, an improved fatigue classification can be recommended.

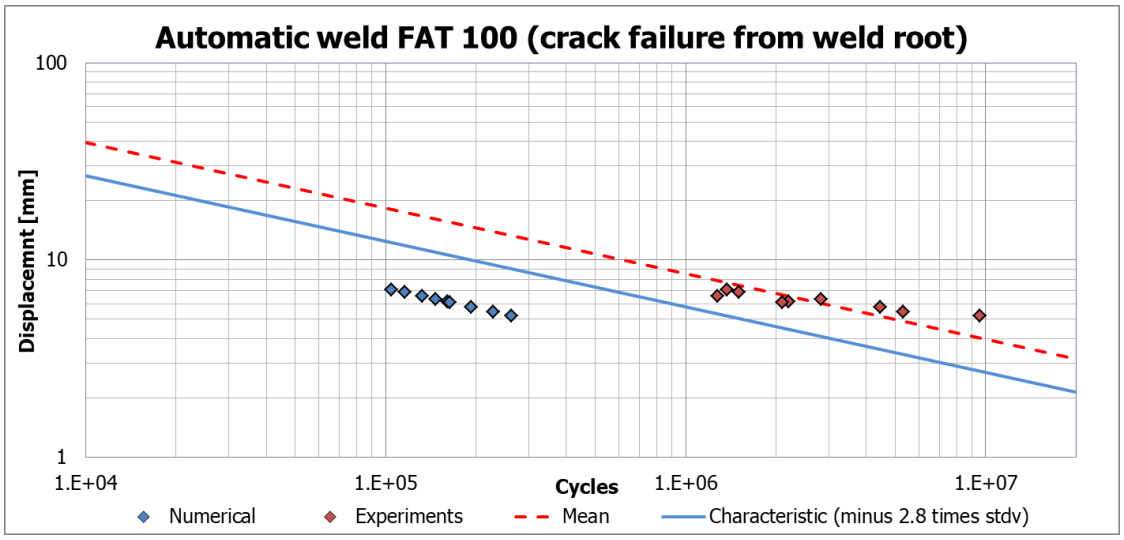

Figure 4-27 Cycles to failure for automatic weld

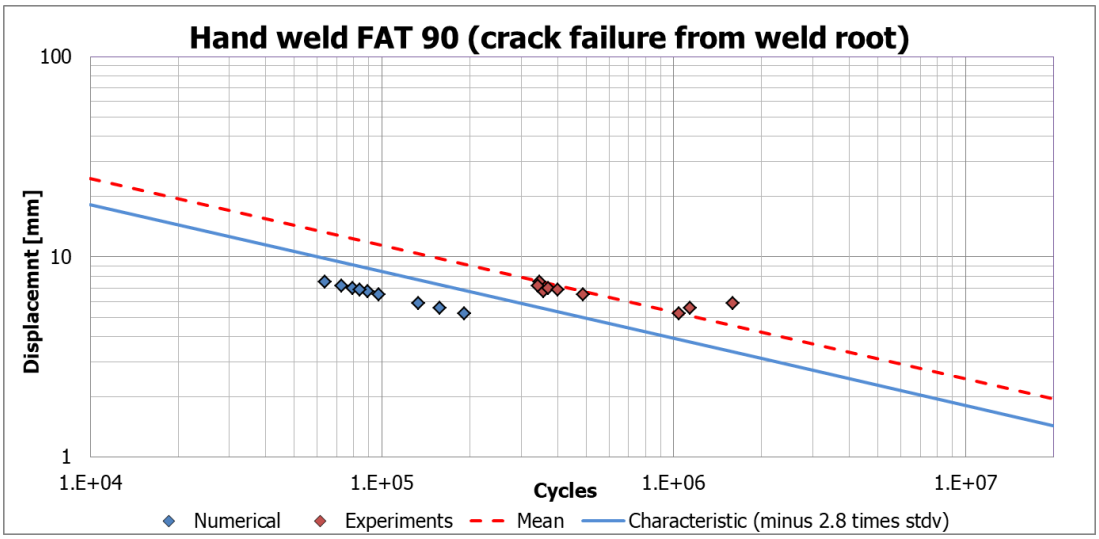

Figure 4-28 Cycles to failure for hand weld

4.8 Conclusions & recommendations

This case study has provided good insight into the fatigue behaviour of stiffeners welded to bridge deck plates. The stress distribution in the weld region is assessed by finite element analysis and validated by strain gauge measurements from experiments. Further parametric studies are performed to provide better understanding of the stress behaviour in the weld region.

4.8.1 Fatigue classification EC3

Despite the stress values used for the fatigue calculation according to EC3 not being representative to the actual stresses at the root, the calculation is relatively simple and can easily be implemented in the subroutine. A few recommendations on the implementation were made. A mesh-size equalling the plate thickness is sufficient. Extrapolation read out points are to be chosen further away from the weld. This is to overcome the influence of the weld profile, which is not considered in the fatigue classification. For this case, points at 20 mm and 40 mm from the weld root were chosen. Using solid elements instead of shell elements resulted in 4% larger stresses.

It was found that automatic welding improved fatigue life significantly compared to hand welding. EC3 takes this into account by recommending a higher fatigue class to automatic welded connections (i.e. FAT 100). As can be seen in Figure 4-27, there is still a significant margin for increasing this classification. Based on the available data from these experiments, a fatigue classification of 150 MPa could be achieved. Even though more test data and research would be required in order to actually increase this classification, it highlights the potential of automatic welding for fatigue problems.

The fatigue classification in EC3 considers the largest stress to occur at the weld root, which is where the cracks initiated in the experiments as well. However, both FEA and experiments showed the largest stress values occurring outside of the weld region. Within the weld region, the stress levels reduce with the lowest stress occurring close to the weld root (at 1 mm from the root, see Figure 4-11). The simplified model adopted in the fatigue classification therefore does not represent the actual observed stresses at the crack initiation point. A new fatigue classification could be proposed based on the reduced stresses in the weld. Since the computed stresses in the weld correspond well with the measurements, FEA would be suitable for this calculation method. For example, a downward extrapolation towards the root could be considered, see Figure 4-29. The first read out point in the weld

region and should not be too close to the weld root. The second read out point is located where the stress peak occurs, which is approximated to be half a thickness from the weld toe intersection. The first point could then be at 2/3 thickness from the second point.

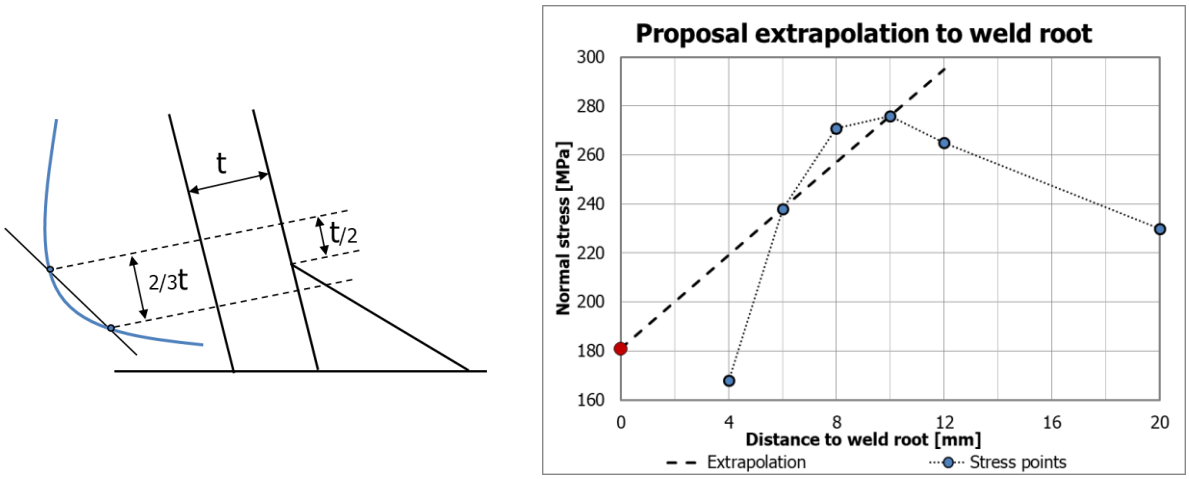

Figure 4-29 Proposal fatigue classification

The proposed extrapolation could be used for both the FEA and experimental stresses. A new SN-curve can now be derived for both welding types. The mean and characteristic curves are derived in the same manner described in Appendix B. Fatigue classifications 100 MPa for automatic welding and 55 MPa for hand welding are subsequently obtained. No thickness effect correction is considered for this classification. The proposed SN-curves for both weld types are presented in Figure 4-30 and Figure 4-31.

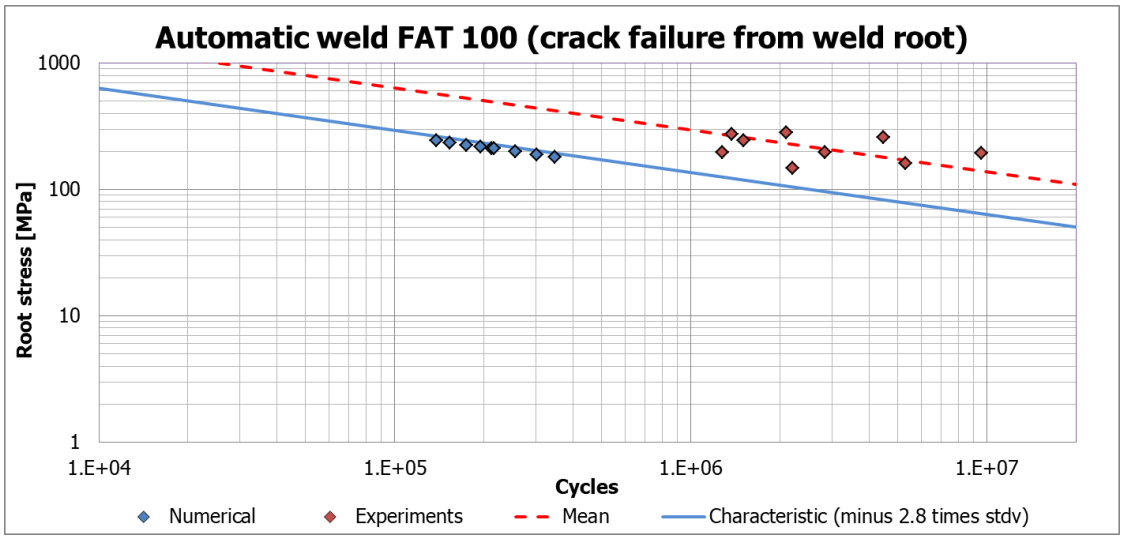

Figure 4-30 Proposed SN-curve for automatic welding

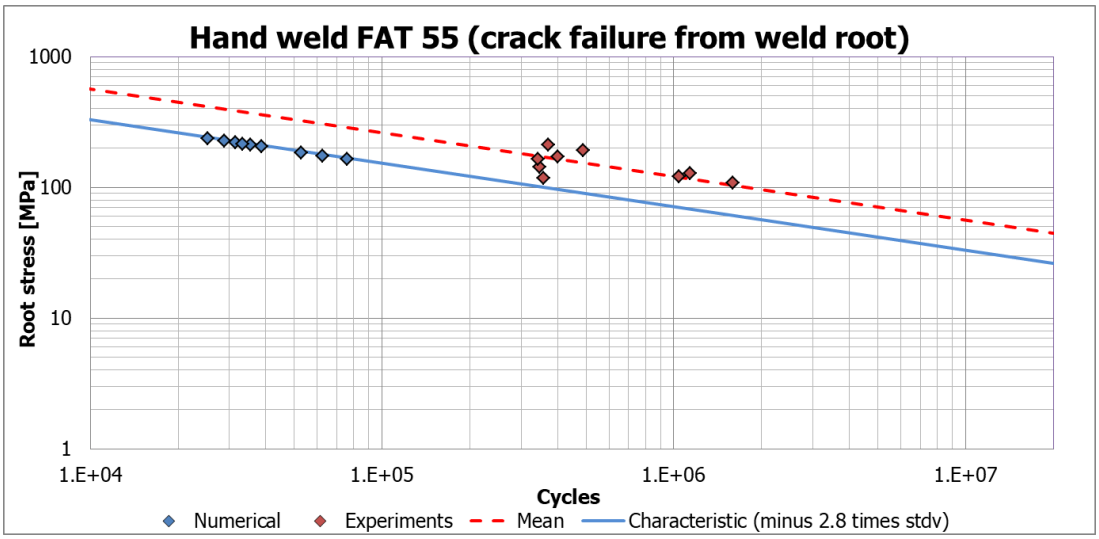

Figure 4-31 Proposed SN-curve for hand welding

4.8.2 Parametric studies

Regarding the influence of the size of the weld, particularly the height of the weld resulted in the largest stress increase. A height increase of 2 mm was found to increase the stresses by 3%, also at locations further away from the weld. This effect can be considered minor.

A not fully protruded weld resulted at a stress decrease. By increasing the undercut, the stresses in the weld region would reduce. However, of most concern are the stresses at the weld root itself. The Von Mises stresses at the tip were compared, showing an increasing stress level for larger undercuts. An undercut of 1 mm (maximum allowed according to EC3) results in approximately a 50% stress level increase compared to the fully protruded weld.

Finally, the effects from an affected Young's Modulus by the welding process were assessed. A simplified model of a two material composite was considered, with a different Young's Modulus for the weld and HAZ. First, an increased Young's Modulus was considered, which is according to the actual change in material properties. However, for numerical calibration purposes a reduced Young's Modulus was considered. A good curve fit was obtained with the experiments. The inhomogeneous cross-section resulted in a different stress distribution, with a shift of the neutral axis and larger stresses in the stiffer material. The finite element model showed a pronounced stress peak as observed in the experiments. However, this representation of the material properties at the weld does not represent the actual properties. It was merely considered for numerical calibration; therefore the findings should be disregarded as explanation for the stress distribution observed in the experiments.

From the considered parameters in this study, none explained the observed pronounced stress peak at the weld. A final possibility that could explain this stress distribution would be the effect of residual stresses in the weld. This aspect is not further studied here.

4.9 Further studies

Many aspects influencing the fatigue life of the welds of orthotropic deck plates were found in this case studies. Not only did it validate the models for finite element analysis, it also brought to light areas of further research.

The studies were performed on small scale specimen. The recommendation for implementing the subroutine would also be applicable for full scale bridge decks. No such analysis was performed during this study. If experimental data is available for this bridge deck, the FEA

model could be further validated. In addition, only separate shell and solid element models were considered. The possibility of sub-modelling the weld region with solid elements, while the rest of the model consists of shell elements, is to be considered. Particularly for full scale deck models, this could lead to a significant reduction in computation time.

More research is required on the improved fatigue life of automatic welding. From these experiments, it shows that there is a large potential for improving the fatigue classification from EC3. In addition, the influence of the undercut size is also to be research during experiments. The undercut size of each specimen is to be measured and related to the specimens fatigue life.

No explanation was found for the observed stress distribution at the weld region from the experiments. Further research would be required for explaining the stress peak. It is suggested to focus on the influence of residual stresses.

5 CIDECT design guide for tubular joints

A case study is performed on tubular joints. Stress concentration factors (SCF) are calculated according to CIDECT [2] parametric formulae. A comparison with finite element analysis is made.

5.1 Introduction

For a wide range of applications, circular hollow sections (CHS) are used. Offshore jackets or bridge spans commonly consist of this type. In these applications the structures are exposed to cyclic loading, making fatigue particularly in the CHS (or tubular) joints a major issue. A different methodology is to be considered for assessing these joints. Secondary bending moments and the non-uniform stress distribution are taken into account here. CIDECT has developed design recommendations for tubular joints, from which special loading conditions and corresponding stress concentration factors can be derived. The SCFs are determined through parametric formulae. These parametric formulae were developed based on numerical analyses from several researchers. A validation study is performed on a K-joint as shown in Figure 5-1. Several finite element modelling aspects are compared to the design recommendations from CIDECT Design Guide 8 [2].

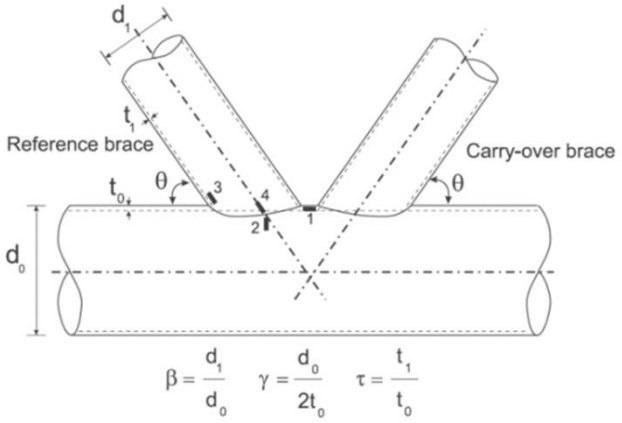

Figure 5-1 CHS K-joint

5.2 Structure of analysis

Considered is a truss bridge structure from an example for the Fatigue MSc course of TU Delft, see Figure 5-2. This example is similar to the example presented in Section 7.1 of CIDECT DG8 [2]. This section describes the geometry of the structures, the recommended weld profile and the boundary conditions for the finite element model.

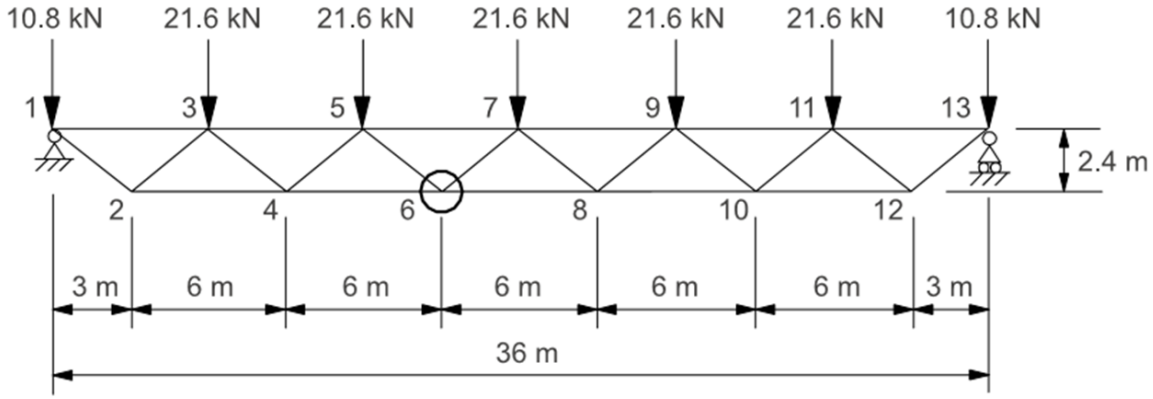

Figure 5-2 Uniplanar truss subjected to constant amplitude loading

5.2.1 Geometry

The member properties are presented in Table 5.1.

Table 5.1 - Member properties

Member	*Outer diameter [mm]*	*Wall thickness [mm]*	*Area [mm^2]*	*Section modulus [mm^3]*
Chord	193.7	8	4667	208100
Brace	101.6	8	2352	51100

Chord symbols are denoted with the index '0'. Brace symbols are denoted with the index '1'. The angle between the brace and chord members is 38.66 degrees. The parameters for the SCF calculation are as follows:

$$\beta = \frac{d_1}{d_0} = 0.525$$
$$\gamma = \frac{d_0}{2t_0} = 12.1$$
$$\tau = \frac{t_1}{t_0} = 1$$

The parameters are within the validity range of the detail classes as defined in Table D.3 [2].

5.2.2 Weld profile

CIDECT Design Guide 6 [1] provides a recommendation for the weld between the chord and the brace as shown in Figure 5-3. For the geometrical parameters of this case, a butt weld is required. Applicable for the crown detail X1, detail Y3 for the saddle and detail Z2 for the heel.

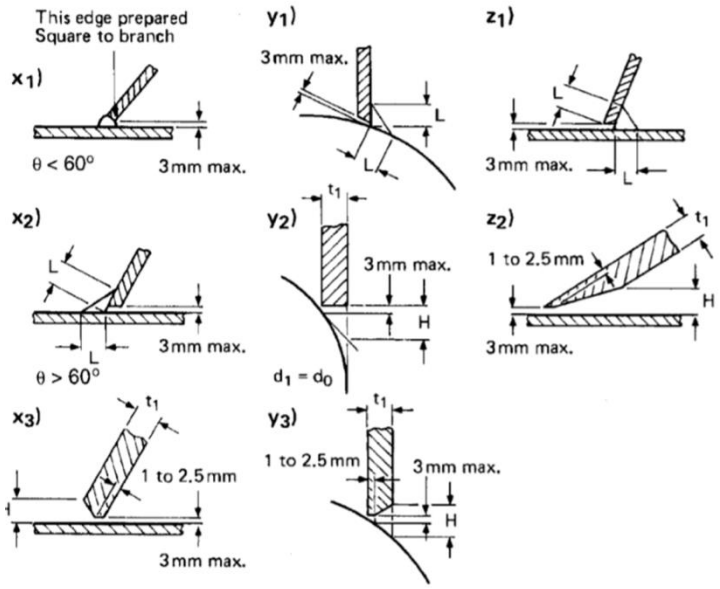

Figure 5-3 Fillet weld and butt weld recommendations [1]

5.2.3 Boundary conditions

In the FEA model, the tubular joint is modelled as part of the truss structure. Boundary conditions are applied at the chord ends. Ovalisation should not be constrained. In addition, rotation at each end and horizontal deformation of the chord should be allowed. Constraints at each at end are therefore applied as shown in Figure 5-4. Both shell and solid element

models are represented by these boundary conditions. The dashed centre line represents the shell model.

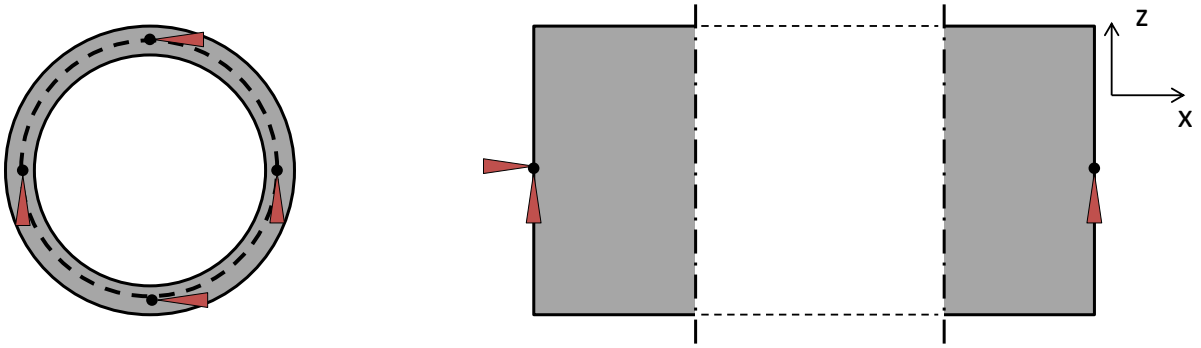

Figure 5-4 Boundary conditions at chord ends

5.2.4 Loads

A rigid truss model is assumed for the structure. The CIDECT recommendation derives two loading conditions from the truss forces, namely balanced axial loading and chord loading (Figure 5-5). The SCFs are calculated separately for each condition. The obtained loads from the example are presented in Table 5.2. In addition to Figure 5-5, (small) bending moments are present in the members for loading condition 1. For the finite element analysis, a third loading condition is added, which simply combines the forces from both load cases.

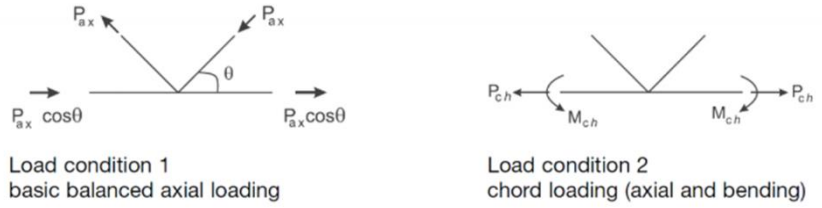

Figure 5-5 Loading conditions

Table 5.2 - CHS load cases

Loading condition 1	**Loading condition 2**
Brace member	
$N_{br,ax} = 17.2\ kN$	$N_{br,ax} = 0\ kN$
$M_{br,ax} = 0\ kNm$	$M_{br,ax} = 0\ kNm$
Chord member	
$N_{ch,ax} = cos\theta N_{br,ax} = 13.4\ kN$	$N_{ch,ax} = 228.5\ kN$
$M_{ch,ax} = 0.015\ kNm$	$M_{ch,ax} = 0.759\ kNm$

5.3 CIDECT hot spot stresses

The stress concentration factors are calculated according to CIDECT DG8 - Table D3 [2]. The SCFs are applied to the nominal stresses to obtain the hot spot stresses, which are presented in Table 5.3. As specified by Karamanos et al. [11], the average brace axial stress is to be taken as the nominal reference stress for balanced axial loading, in both chord and brace.

Table 5.3 - CHS CIDECT hot spot stresses

Loading condition 1		Loading condition 2		Combined
Brace member				
$SCF_{br,ax} = 2.444$	$\sigma_{br,ax} = 7.3\ MPa$	N/A	$\sigma_{br,ch} = 0\ MPa$	
$\sigma_{hs,br} = 17.9\ MPa$		N/A		$\sigma_{hs,br} = 21.2\ MPa$
Chord member				
$SCF_{ch,ax} = 5.965$	$\sigma_{br,ax} = 7.3\ MPa$	$SCF_{ch,ch} = 2.256$	$\sigma_{ch,ch} = 45.3\ MPa$	
$\sigma_{hs,ch} = 43.6\ MPa$		$\sigma_{hs,ch} = 102.2\ MPa$		$\sigma_{hs,ch} = 145.8\ MPa$

5.4 Finite element analysis

Both shell and solid element models are used and compared. Also methods of modelling the weld profile for both element types are considered.

Because of symmetry only one half of the joint is to be modelled, see Figure 5-6. Both rotation around the x-axis and displacements in the y-direction are to be constrained. Solid elements do not have rotational degrees of freedom; lateral displacements (y-direction) are therefore to be constrained over the entire thickness.

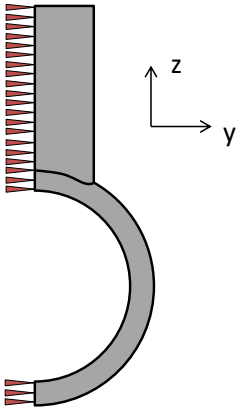

Figure 5-6 Symmetry tubular joint

5.4.1 Load cases

The internal forces and bending moments are calculated from a beam analysis of the truss structure. These internal forces provide the input loads for the joint. The loads for each loading condition are presented in Table 5.4 and correspond to the CIDECT load cases in Table 5.2. Figure 5-7 shows the load definition and their positive directions.

Table 5.4 - Load definition

Load name		LC1	LC2	LC3
N_{ch1}	[kN]	-13.4	228.5*)	215
N_{ch2}	[kN]	13.4	228.5*)	242
N_{br1}	[kN]	17.2	0	17.2
N_{br2}	[kN]	-17.2	0	-17.2
M_{ch1}	[Nm]	-15.0	759*)	746
M_{ch2}	[Nm]	-15.0	759*)	744
M_{br1}	[Nm]	41.8	0	41.8
M_{br2}	[Nm]	69.6	0	69.6

*) Average values from each end are used for this load case

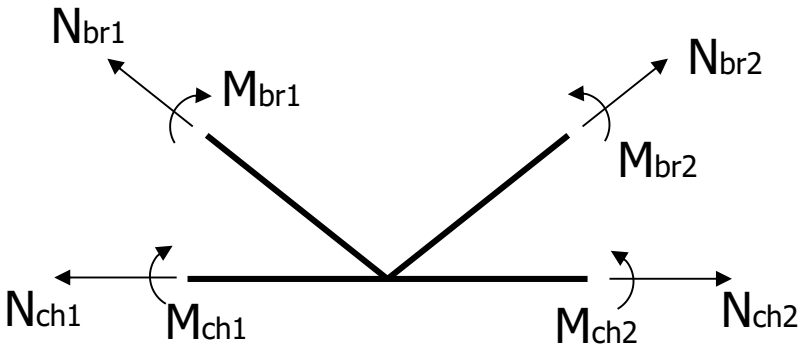

Figure 5-7 Load definition on joint

5.4.2 Shell element model

As for the bridge deck case study, regular quadratic curved shell elements are used for this finite element analysis. Through the thickness a 3-point Simpson integration scheme is applied.

The joint is modelled both with and without the weld profile. For both models, the location of the hot spot is to be defined at the intersection of the plate surfaces. This intersection line is to be determined for the entire circumference of the chord-brace connection.

The weld is also modelled using quadratic curved shell elements. The thickness is chosen to equal the wall thickness, i.e. 8 mm. This size approximates the protruding weld material from the base plates. Modelling the weld profile accurately for each spot of the weld is complex. The model is also subjected to limitations within the DIANA FEA GUI for building curved shapes. For this study a decent weld profile was achieved, though it should still be considered a rough approximation. Figure 5-8 shows the configuration of the weld profile for the shell element model at the three characteristic locations. The red points correspond to the hot spot location, from where the distances for read out points are measured. Note that at the crown location on the chord, this point would be behind the shell plate intersection. This is a typical discrepancy when adopting this method for shell elements. The hot spot location is here to be shifted to the plate intersection.

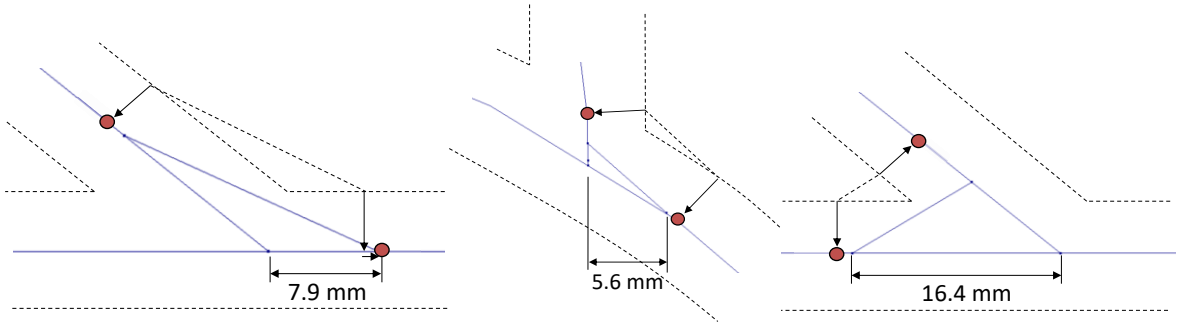

Figure 5-8 Shell weld profile representation for crown (left), saddle (middle) and heel (right)

Around the weld, a fine mesh is to be used (see Figure 5-9). For this analysis, an element size of t/4 (equals 2 mm) is applied. Note that with this length/thickness ratio, the plate element does not represent a shell anymore. It was found that the FEA results were not affected by element mesh-size.

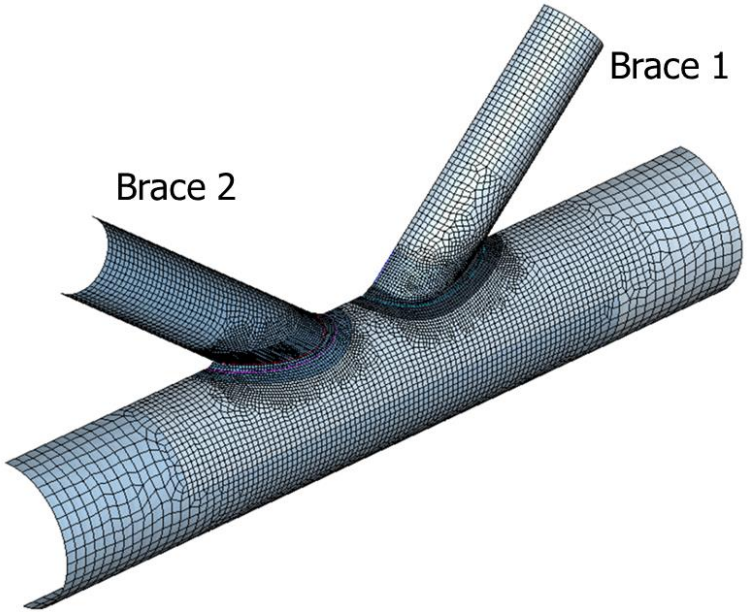

Figure 5-9 Shell element model including weld profile

5.4.3 Solid element model

Quadratic structural solid elements are used for this model. The joint is modelled both with and without the weld profile. A relatively accurate weld profile model according to the CIDECT recommendations shown in Figure 5-3 is achieved. For this recommendation, the best representation for the weld was found to be a circular shape, with a constant radius. The radius of the circle should be order of magnitude the weld throat thickness. For this model, the radius of the weld shape is 7 mm (~0.9t). See Figure 5-10 for the weld profile at the three characteristic locations. The chosen weld shape contains one inconsistency with regards to the CIDECT guide; at the heel the penetration of the weld is fairly limited (undercut of 4 mm). Overcoming this inconsistency resulted in issues during mesh generation. However, from sensitivity analyses it was found that the difference between this detail and full penetration at the heel location was marginal.

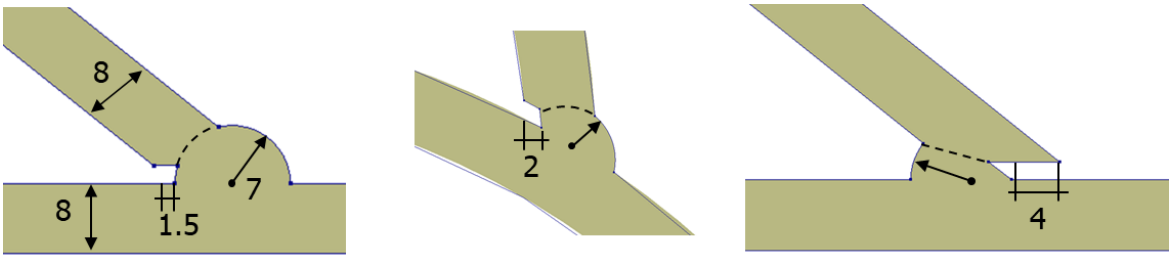

Figure 5-10 Solid weld profile representation for crown (left), saddle (middle) and heel (right)

Around the weld, a fine mesh is to be used (see Figure 5-11). As for the shell element model, an element size of t/4 (equals 2 mm) is applied. The hot spot stresses are found to be governing at Brace 1. Therefore the fine mesh is only applied at the weld around this brace.

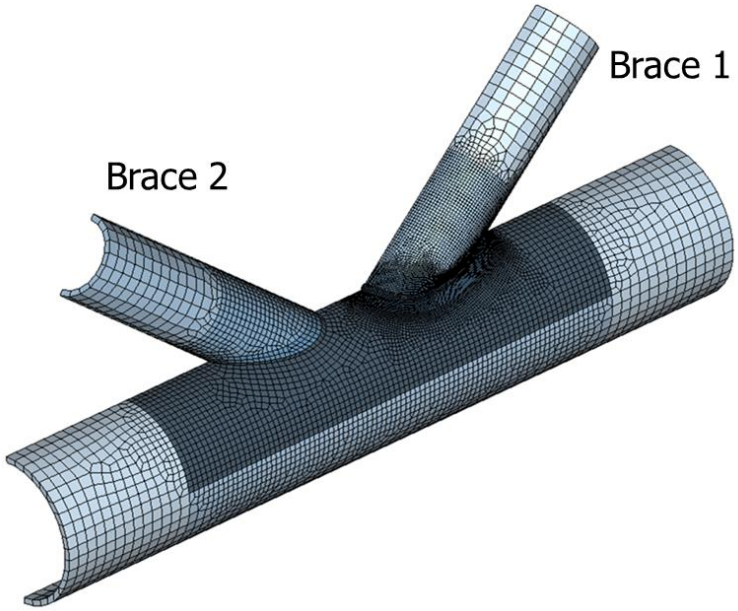

Figure 5-11 Solid element model including weld profile

5.4.4 Full truss model validation

According to Romeijn [17], the SCF calculations should be independent of the effects from the boundary conditions of the model. He found that the carry-over effects were particularly dependent on the boundaries. For his studies, he adopted a model by applying compensating moments at the boundaries to eliminate this influence. These compensating moments are not applied to this study; therefore some differences with the SCF calculation can be expected. To assess the severity of not applying these compensating moments, a validation analysis for the entire truss is performed. The loads are applied as shown in Figure 5-2. The simple case of the shell element model without weld profile is used as reference.

The same mesh-size is applied to the considered joint. A coarse mesh is applied to the rest of the truss, using an element size of 50 mm (see Figure 5-12). The symmetry of the sections is considered as well; therefore the truss is split in half length-wise.

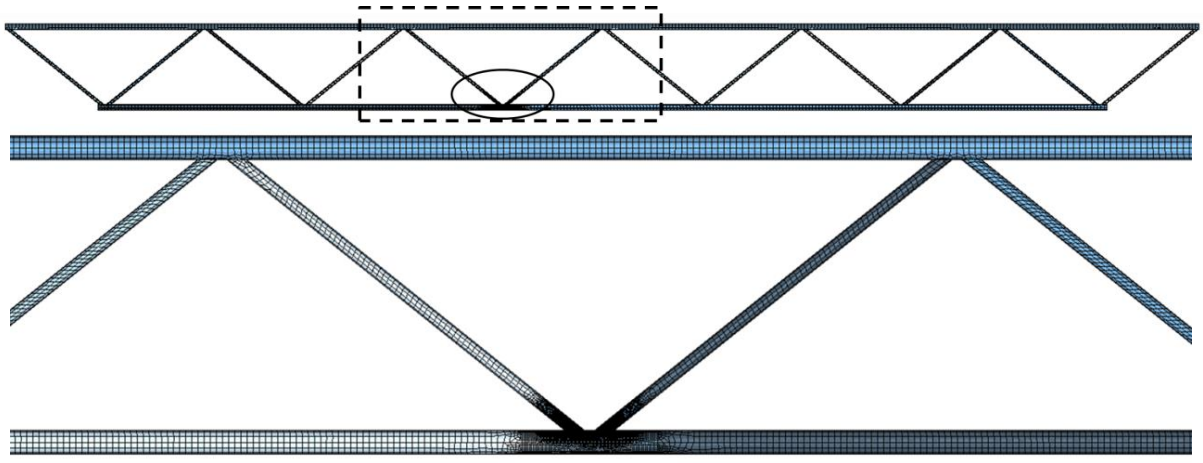

Figure 5-12 Entire truss shell model

5.5 FEA Results

The hot spot stresses are extrapolated from read out points at distances 0.4t and 1.0t. The hot spot stresses are plotted along the peripheral angle of the weld according to Figure 5-13. Focus will be only on Brace 1, as shown in Figure 5-9 and Figure 5-11. This brace was found

to be governing. First, the boundary and loading conditions are validated with the whole truss shell model. Next, the different FEA models are compared.

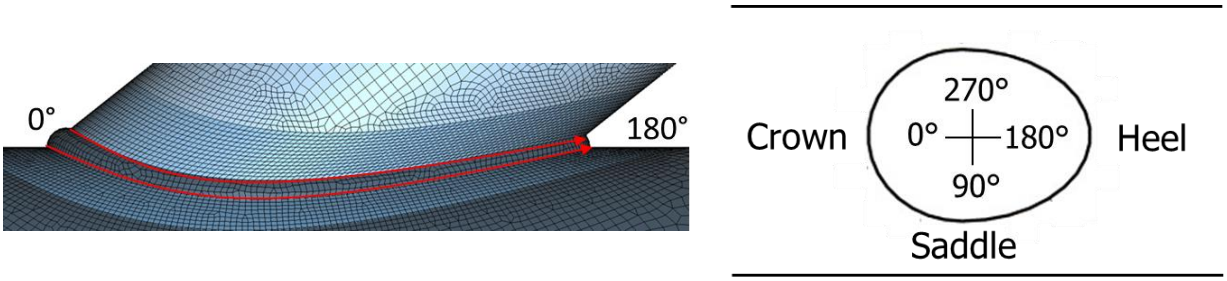

Figure 5-13 Weld line for hot spot stress plots

5.5.1 Boundary and loading conditions validation

Load case 3 (LC3) represents the sum of LC1 and LC2 and corresponds with the resultant internal force distribution at the joint. The results of LC3 should therefore correspond with the results from the whole truss analysis. The results for the shell joint model for LC3 along with the results from the whole truss model are presented in Figure 5-14.

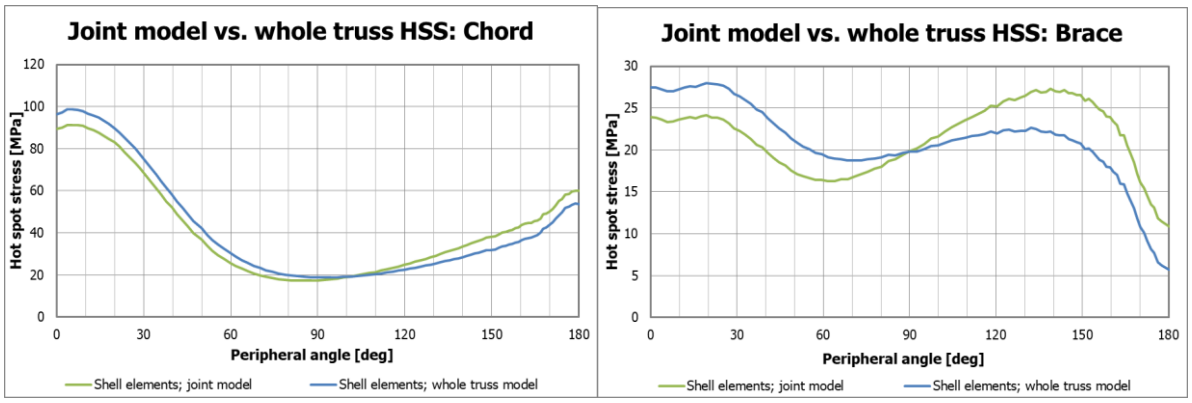

Figure 5-14 Joint model vs whole truss hot spot stresses LC3

It can be observed that the curves show good correspondence to each other. The curves have similar shapes. The stresses also are of the same order of magnitude. However, for both plots the stresses of the joint model are slightly lower at the crown, whereas the stresses are slightly higher at the heel. The curves intersect almost exactly halfway, at approx. 90 degrees. The difference in absolute sense between each model type is presented in Figure 5-15. These curves appear quite symmetric and give the appearance that a small additional bending moment is to be considered locally. It is observed that the calculated internal moments from a full-scale model are not fully accurate when applied as external loads to the small-scale joint model.

A correction function for the hot spot stresses is determined. This function is presented in Figure 5-16. The critical location is found at the crown toe, in both the chord and brace. For the subsequent models, the hot spot stresses can then be multiplied with this correction factor. This factor is found to be 1.07 for the chord and 1.14 for the brace at the crown toe. It is to be noted that for the brace this correction shifts the critical location to the crown toe. Otherwise, the critical location is found at the saddle.

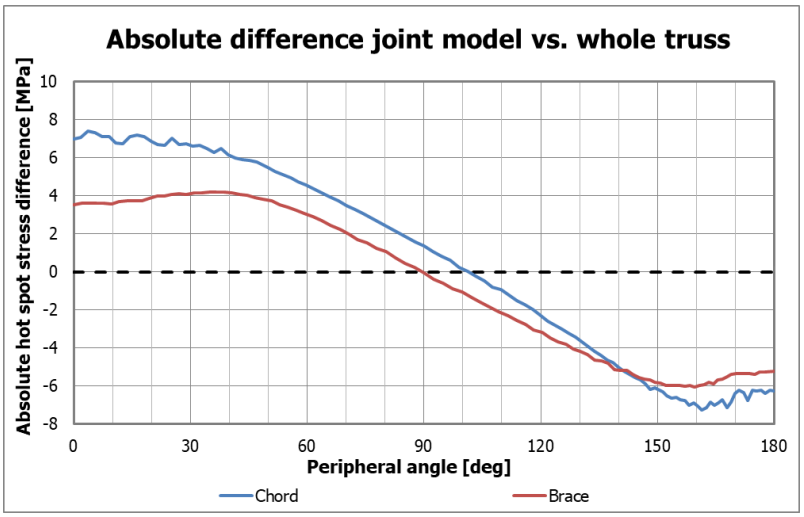

Figure 5-15 Absolute hot spot stress difference between joint and whole truss model

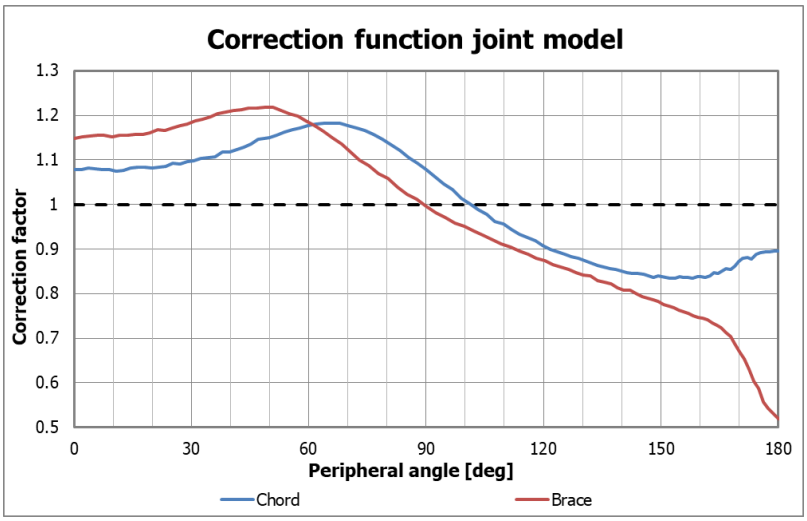

Figure 5-16 Correction function for joint model from whole truss model

5.5.2 FEA model comparison

The hot spot stresses for the four different models are plotted in Figure 5-18 for each load case. They are compared to the corresponding hot spot stress calculated from the CIDECT recommendations. The (hot spot) location for each case from where the read out points are measured is presented in Figure 5-17.

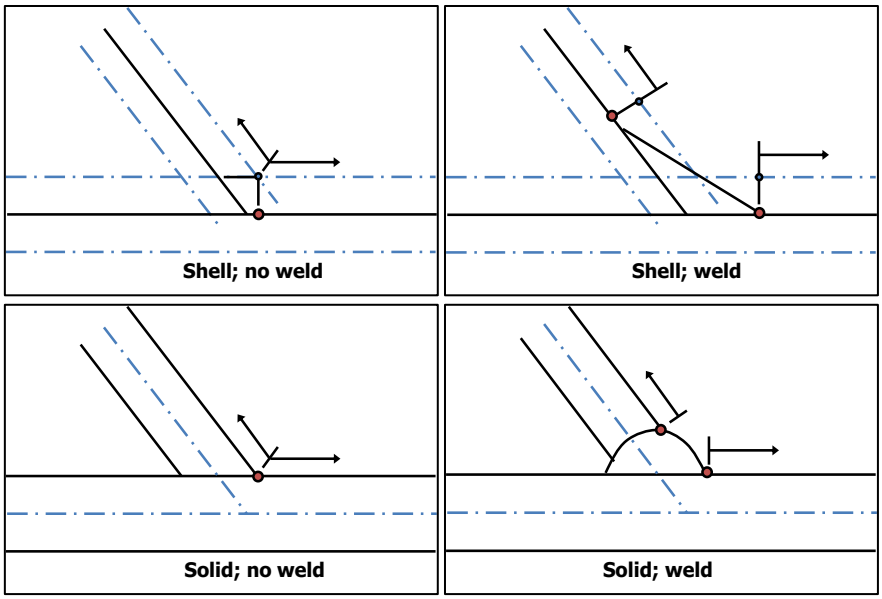

Figure 5-17 Solid and shell element read out distance points

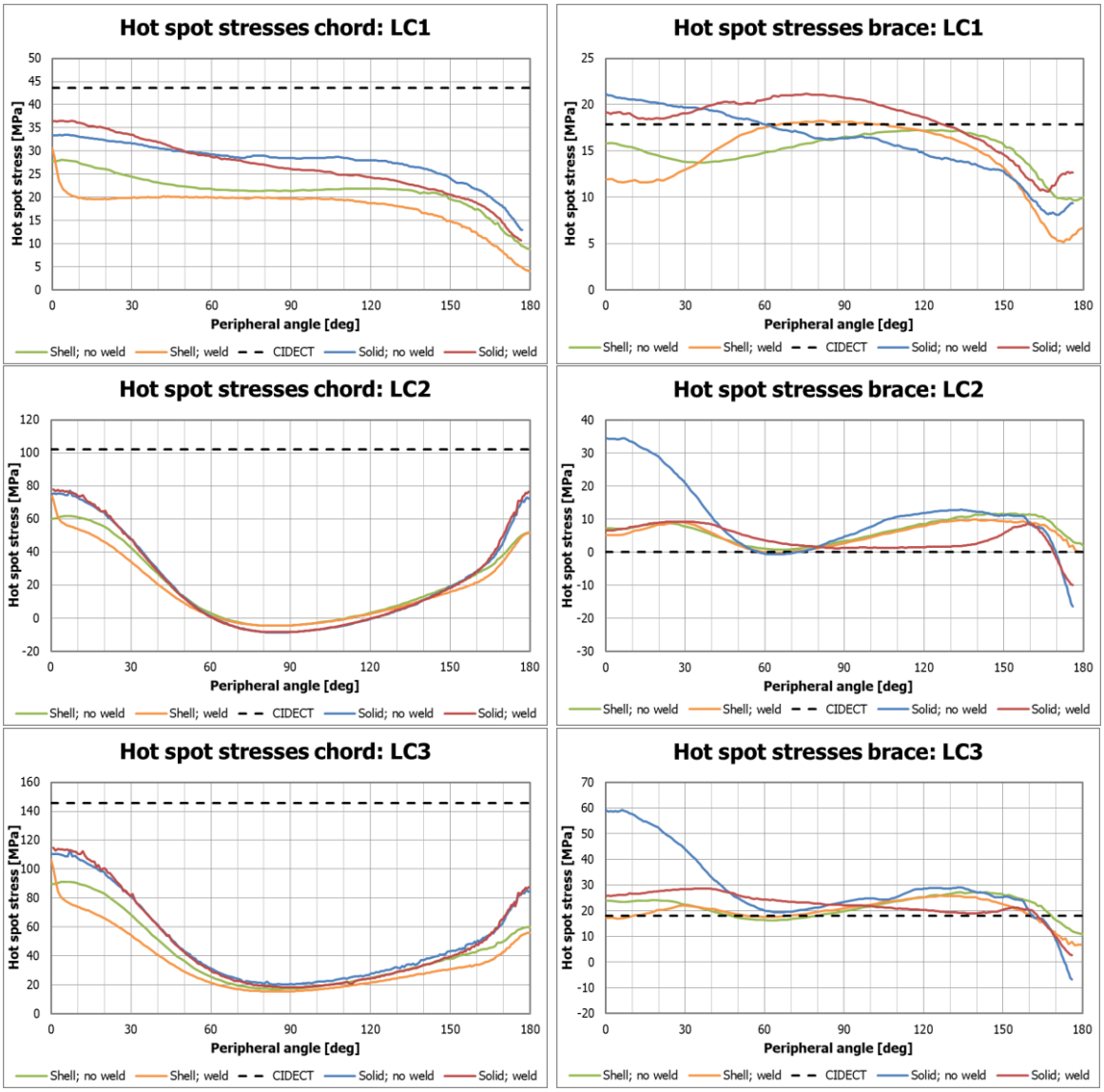

Figure 5-18 CHS hot spot stress results

From the results it can be seen that overall the graphs show good correspondence between each finite element model. Comparing the shell and solid element model, the curves show similar shapes to their respective with/without weld profile model. The shell element model generally shows lower stresses, with for the maximum hot spot stress at the chord crown a difference of 8%.

The influence of the weld profile can also be seen from the graphs, which is similar for the shell and solid element models. Including the weld profile gives generally lower stresses. The main reason is that without the weld profile the hot spot location is positioned at the plate intersection. If the hot spot is located at the weld toe, which is at a few millimetres from the plate intersection, lower stresses are expected here. Due to the large stress gradient in this region, this difference could be significant. This is best noticed at the brace crown. From 0° to 40°, the stresses are significantly higher. Compared to the CIDECT recommendation, it is clear that this HSS value deviates too much from what is expected. It shows the importance of considering the weld profile in the model, especially when using solid elements.

One final remark is to be made about the stress values in the brace for LC2. Only chord loading is considered for this loading condition. Therefore, the CIDECT recommendation assumes all nominal stresses in the brace to be zero. However, the presence of the brace affects the local chord stiffness. Redistribution of stresses in the brace is therefore to be considered. Stress magnitude is limited to only 10 MPa (solid element model with weld), but it increases the total brace stress with 50% as can be seen for LC3.

5.6 Conclusions

The maximum hot spot stresses from the solid weld model are summarised and compared with the CIDECT stresses in Table 5.5. Additionally, the hot spot stresses at the crown toe locations are multiplied with the correction factor discussed in Section 5.4.4. For the chord stress, this factor is only applied to LC3. For the brace stress, this factor is applied to both LC1 and LC3. The reason for this is that CIDECT disregards LC2 in the brace; it assumes no redistribution of stresses occurs as a result of the chord loading. The SCF in the brace from CIDECT is therefore best compared with the FEA results from LC1. For LC1 it is found that the FEA hot spot stress is 17% higher than from CIDECT.

It is found that the FEA results show lower hot spot stresses than the SCF calculations from CIDECT, though the same order of magnitude is achieved. The corrected stresses show better correspondence, with for the governing case (chord, LC3) being 16% lower than the CIDECT HSS.

The computed FEA hot spot stresses are calculated within an acceptable margin from the CIDECT formulae. It is to be noted that the CIDECT formulae are simplified equations based on the best curve-fit of a large amount of parametric numerical analyses. Scatter can be expected. Particularly for this case, with the thickness ratio τ is equal to one. In practice the brace thickness is usually smaller than the chord thickness. This τ-value represents the limit value of the range of applicability for the recommendation as well. Lower τ-values could therefore give FEA stresses closer than 16% from the CIDECT stresses.

Table 5.5 - FEA hot spot stresses for solid element model with weld profile

	LC1	**LC2**	**LC3**
	Brace member		
FEA[*)]	$\sigma_{hs,br} = 21.5\ MPa$	$\sigma_{hs,br} = 9.9\ MPa$	$\sigma_{hs,br} = 29.0\ MPa$
FEA[**)] (corrected)	$\sigma_{hs,br} = 21.6\ MPa$	-	$\sigma_{hs,br} = 28.9\ MPa$
CIDECT	$\sigma_{hs,br} = 17.9\ MPa$	$\sigma_{hs,br} = 0\ MPa$	$\sigma_{hs,br} = 17.9\ MPa$
	Chord member		
FEA[*)]	$\sigma_{hs,ch} = 36.5\ MPa$	$\sigma_{hs,ch} = 78.0\ MPa$	$\sigma_{hs,ch} = 114.8\ MPa$
FEA[**)] (corrected)	-	-	$\sigma_{hs,ch} = 123.8\ MPa$
CIDECT	$\sigma_{hs,ch} = 43.6\ MPa$	$\sigma_{hs,ch} = 102.2\ MPa$	$\sigma_{hs,ch} = 145.8\ MPa$

*) The FEA stresses present the maximum hot spot stress along the weld, which occurs in the braces at the saddle
**) The corrected FEA stresses present the hot spot stress at the crown toe for all cases

The studies by Romeijn [17] and Karamanos [11], who developed the parametric formulae for the SCFs, assumed the stress direction in the brace in the direction of the brace axis. This is done for simplicity, since the surface direction at the brace is complex to calculate. However, with use of the subroutine the stresses perpendicular to the weld can be calculated. At the crown toe and heel locations, this direction coincides with the brace axis. In general these locations are critical; therefore no serious consequences of this simplification are expected. If the critical location occurs at the brace saddle however, more care has to be taken when comparing to the CIDECT calculation.

It is recommended to use solid elements including the weld profile for the HSS calculation. This model gives the best representation of the actual structure. Using shell elements, the critical HSS for this case was underestimated by roughly 8%. However, the general tendency of this difference around the weld is quite higher than 8%. The shell element model does provide a good validation method for the boundary and loading conditions. The joint model can easily be expanded to the full truss structure. Not much computation time is required for such an analysis and is therefore more suitable than using solid elements. A correction function can be derived from this validation study which can improve the analyses involving solid elements.

6 Experiments on tubular joints in a marine environment

Fatigue experiments were conducted on large scale tubular joints in a marine environment. Strains were measured extensively on the test specimen. The experimental results are compared to results from finite element analysis.

6.1 Introduction

As part of the research program of the European Coal and Steel Community in corrosion fatigue, eleven welded tubular joints were tested on fatigue. The experiments were conducted in seawater, except for one which was tested in air. The joints were made of fine grain structural steel S355.

Furthermore, four high-strength steel welded tubular joints wit post-weld treatment and four cast nodes were tested.

Strain gauges were placed around the weld of each specimen from which the hot spot strains were derived. The joints were exposed to cyclic loading until fatigue failure (crack break-through) occurred.

For this case study, the eleven welded tubular joints are of particular interest for the fatigue assessment, because the benefits of using high strength steel, post-weld treatment and cast nodes are not included in the current hot spot stress recommendations. However, the hot spot strain measurements from the high-strength steel will be included for comparison with the computed strains from FEA.

6.2 State of the art

The tubular joint is loaded axially on the braces, through the actuator attached to one end of the chord. The loading condition represents balanced axial loading. On each end of the chord ovalisation of the pipe is restricted; at one end the pipe end is welded to a base plate, at the other end a thick ring is welded around the tube to achieve the same effect. The dimensions of the specimen are presented in Figure 6-1. A photo of the test rig is presented in Figure 6-2.

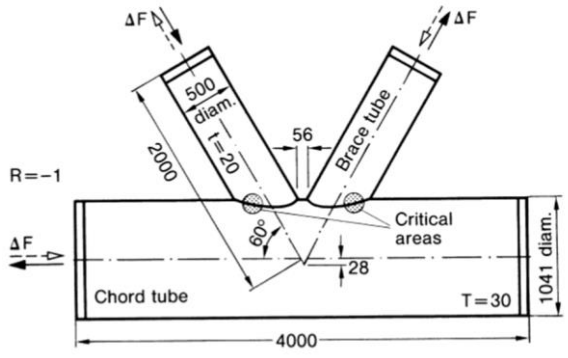

Figure 6-1 Specimen dimensions [21]

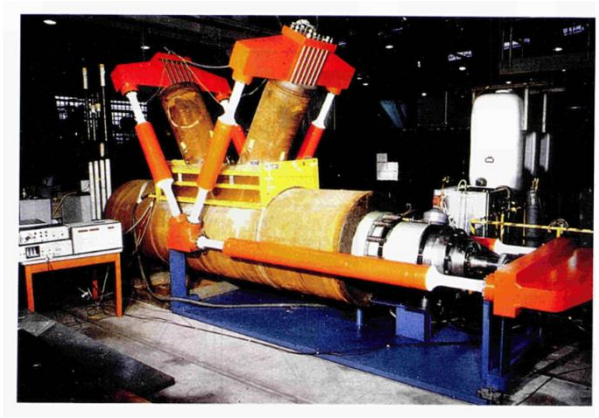

Figure 6-2 Test rig [23]

The steel grade of the specimen is StE 355, modified for offshore quality. The braces are butt welded to the chord, according to recommendations of the Germanischer Lloyd [7] for braces that are inaccessible from the inside (as shown in Figure 6-3). Mean stress of the loading condition is zero (R = -1). A variable amplitude loading was applied to most specimens, according to the so-called Common Load Sequence (COLOS) spectrum as presented in Figure 6-4. The load amplitudes of the spectrum are tabulated in Appendix D.

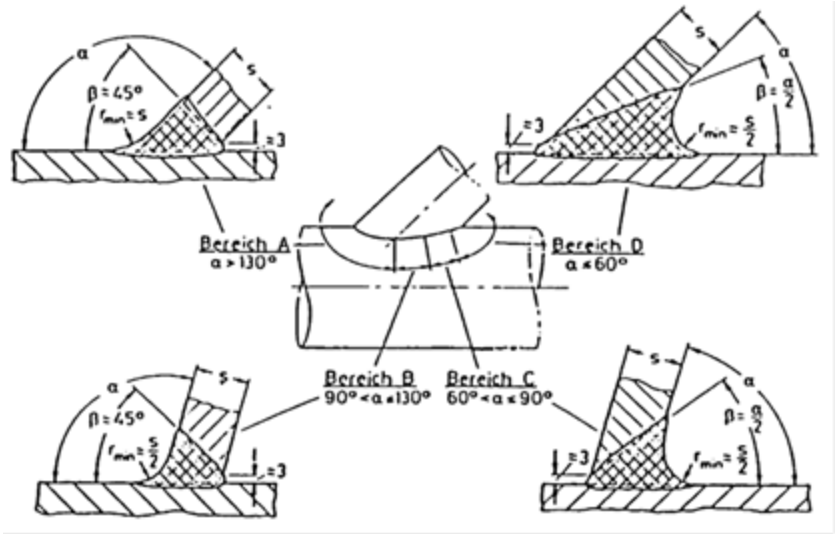

Figure 6-3 GL weld profile recommendations [7]

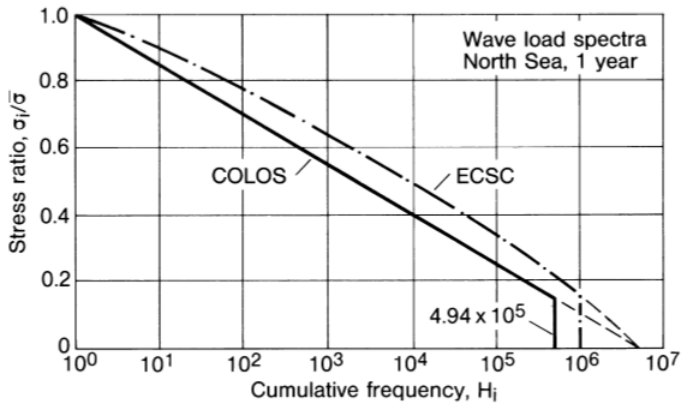

Figure 6-4 Standard load spectra [23]

Strain gauges are placed on the chord along the weld for each joint. The hot spot strains are extrapolated from the strains measured at 14 mm and 49 mm from the weld toe, see Figure 6-5.

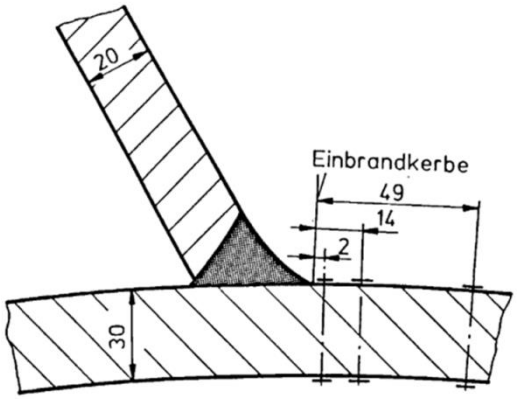

Figure 6-5 Strain gauges [23]

6.3 Finite element model

Finite element analyses are performed of the experiment set-up by using both shell and solid elements. For the shell element model, regular quadratic curved shell elements are used. Quadratic structural solid elements are used for the solid element model. A linear elastic analysis is performed.

The analysis will be load controlled. The load is applied normal to the braces. At one end the displacements are constrained in longitudinal direction. A horizontal chord reaction force equalling the brace force results from the brace loading (since $2\cos 60° = 1$).

In the experiments ovalisation of the chord ends was restricted. Therefore, for both ends the transverse and vertical (y and z) displacements are constrained. One end is also constrained in longitudinal (x) direction, while the other end is free to move longitudinally. The schematic of the model is presented in Figure 6-6.

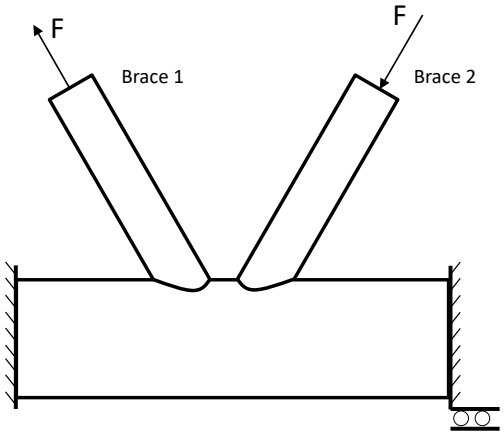

Figure 6-6 Model schematic

Focus is only on Brace 1 for this analysis, which was found to be the governing brace. To avoid memory issues for computation, the weld profile and a fine mesh is only applied to this brace. Because of symmetry, only one half of the joint can be considered.

6.3.1 Shell element model

Shell element connections are considered a decent representation of a butt weld, however modelling the weld size accurately according to Figure 6-3 is still complex. It is therefore decided to not include the weld profile in the shell element model. An element size of t/5 (equals 6 mm) is applied to the weld region. Outside this region, an element size equalling the chord thickness is applied.

A screenshot of the finite element model is presented in Figure 6-7.

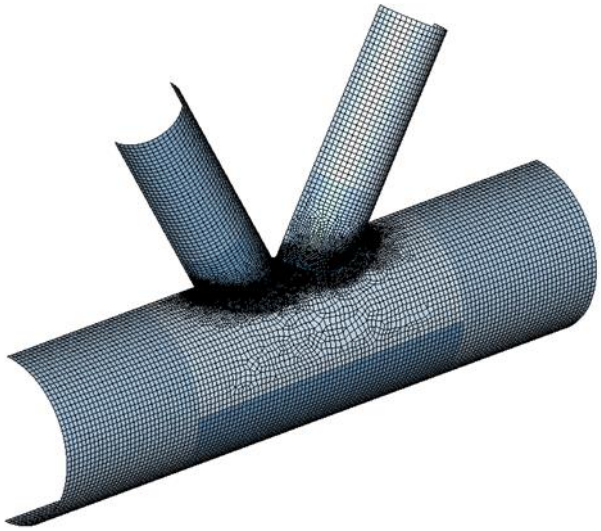

Figure 6-7 Shell element model

6.3.2 Solid element model

A representative weld profile according the GL specification from Figure 6-3 is included in the model. The shape differs from the specification considered in Section 5.2.2, therefore a different approach to model the weld is adopted. See Figure 6-8 for the weld profile at the three characteristic locations.

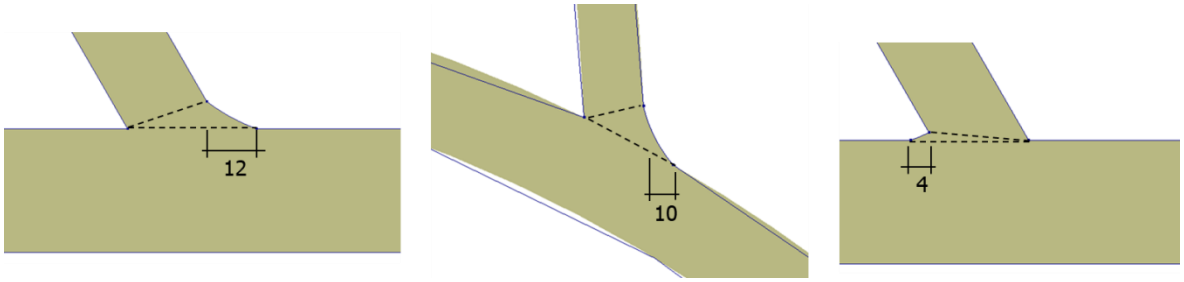

Figure 6-8 Solid weld profile representation for crown (left), saddle (middle) and heel (right)

Around the weld, a fine mesh is to be used (see Figure 6-9). An element size of t/10 (equals 3 mm) is applied in the weld region. To reduce the total amount of elements, a coarse mesh is applied at the ends. The element size equals three times the chord thickness in longitudinal direction. These elements are quadratic and bending contributions are only minor, therefore no issues are expected with this large element size.

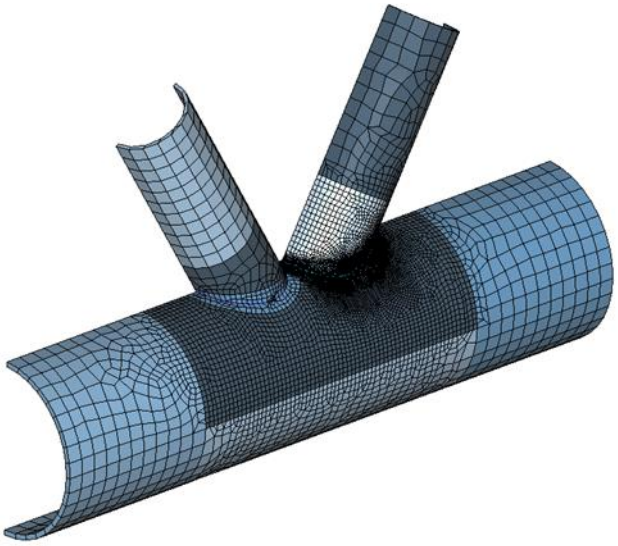

Figure 6-9 Solid element model

6.4 FEA results

For validating the numerical results to the experimental measurements, the normal strains at the read out points corresponding with the strain gauge locations are considered. All strains and stresses are plotted along the peripheral angle of the weld according to Figure 5-13, with the crown at 0° and the heel at 180°.

First, the different finite element models are compared to each other. The influence on the stress levels are assessed for the different modelling aspects. Next, the strains at the locations of the strain gauges are computed, and compared to the measurements. The hot spot calculations for the experiments were done in terms of strains rather than stresses.

6.4.1 Finite element model comparison

The influence of the element type and weld profile on the stresses is assessed. It is expected that the modelling method is of most influence closer to the weld region. For the comparison analysis, the peripheral stresses at the first read out point at 14 mm from the hot spot are computed. For convenience, the Von Mises equivalent stresses are used, since only the relative influence of each method is to be assessed.

Solid and shell element model

Firstly, the shell and solid element models are compared, see Figure 6-11. For a reliable comparison, the weld profile is not included in the solid element model. For the shell element model, the hot spot locations are chosen at both the surface intersection (which corresponds with the location of the solid element mode) and the shell plate intersection. The (hot spot) location for each case from which the 14 mm distance is measured is presented in Figure 6-10.

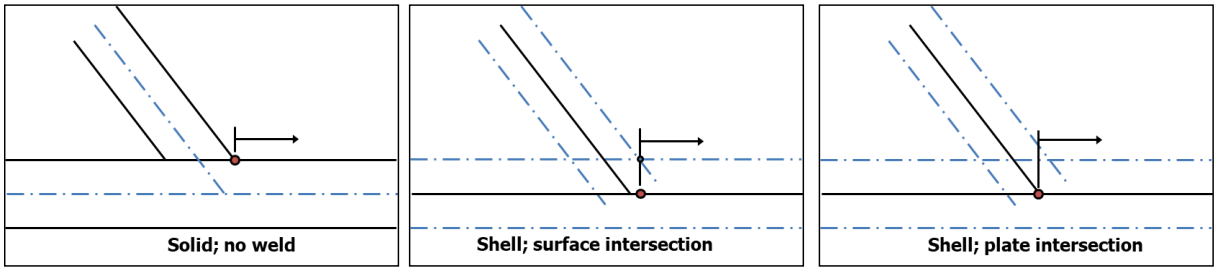

Figure 6-10 Solid and shell element read out distance points

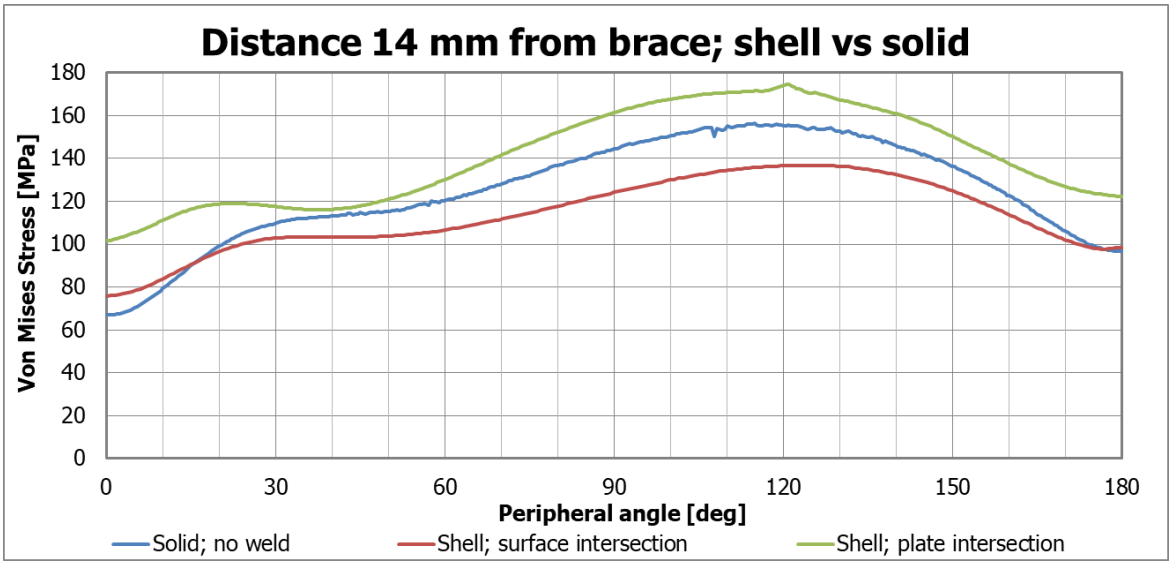

Figure 6-11 Shell vs. solid elements

As can be observed, choosing the shell plate intersection as the hot spot, the stresses are being overestimated. This is because the read out points are located closer to the weld location. The stresses at the crown and heel show good correspondence with the solid element model for the surface intersection hot spot. However, the stresses are underestimated at the saddle.

Weld profile for solid element model

Next, the influence of the weld profile is assessed, see Figure 6-13. The presence of the weld gives a hot spot location further away from the brace plate. The stresses are compared at this location, with and without the weld included in the model. The (hot spot) location for each case from which the 14 mm distance is measured is presented in Figure 6-12.

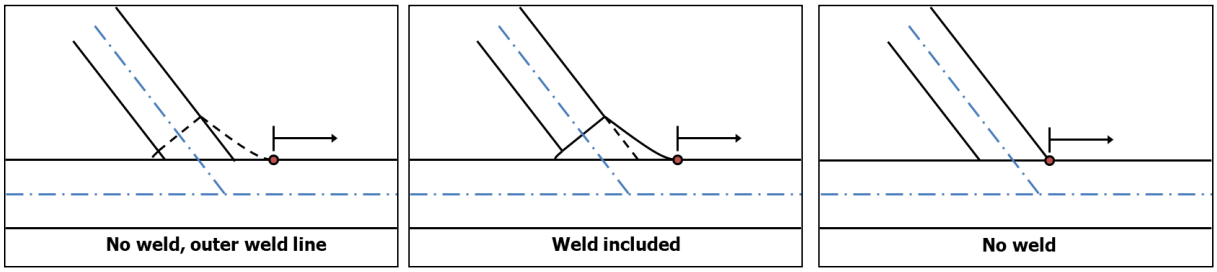

Figure 6-12 Weld profile read out distance points

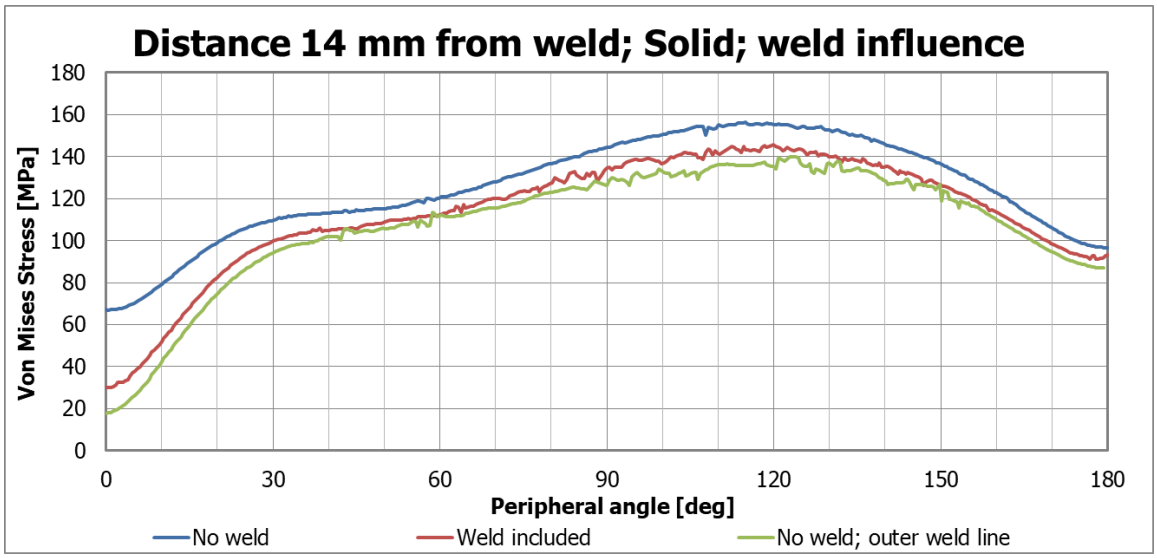

Figure 6-13 Weld profile influence

Even though the influence is small, it shows that the additional material added for the weld results in a stress increase. Additionally, the hot spot location at the brace plate intersection is shown, when no weld is included. It can be seen that the stresses increase when the hot spot is taken closer to the actual brace.

From the results it can be concluded that the location of the hot spot has to be chosen carefully. For shell elements, the surface intersection is to be considered. For solid elements, the weld toe is to be considered, regardless whether the weld profile is included in the model or not. It is recommended to include the weld, since this additional material would also be present in practice.

6.4.2 Comparison FEA to experiments

For validating the finite element models, the strain gauge measurements are compared to the normal strains computed by the fatigue subroutine. For test specimen #15, the strains at 14 mm from the weld toe are available for a range of positions around the brace. For the solid element model, the weld profile is included. For the shell element model, the hot spot is located at the surface intersection. The FEA strains are compared to the strain gauge measurements in Figure 6-14.

From the experiments it followed that the critical hot spots were located at the saddle between 90° and 120°, which also follows from the numerical analyses. The general shape of the curves shows good correspondence. However, at the crown position the shell and solid element model show a large difference, which can be explained by the presence of the opposite brace in this region.

Care has to be taken when interpreting the strain gauge measurements. A symmetric behaviour can be expected, however there is a significant difference observed between the left and right side of the experiment curves. It shows the level of scatter already present within a single specimen.

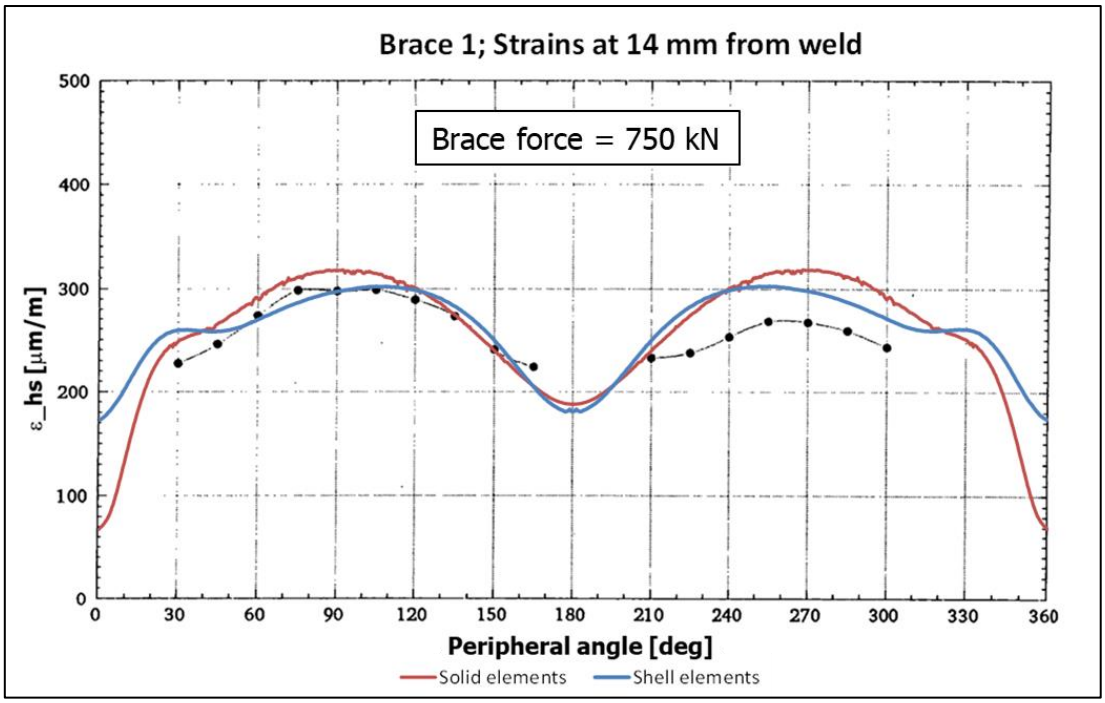

Figure 6-14 Strains at 14 mm from weld for test #15

A more detailed strain measurement is done for test #10 at the critical location at 105°, where the peak strains were found. Strains were measured at one millimetre intervals close to the weld region. The measured strains are compared to the computed strains from the solid element model, see Figure 6-15. It can be observed that the numerical results show particularly good correspondence with the measurements. It can therefore be concluded that reliable hot spot strains can be obtained with the chosen finite element models. This can be expanded by numerically calculating the hot spot stresses, which in turn provide the input for the fatigue assessment.

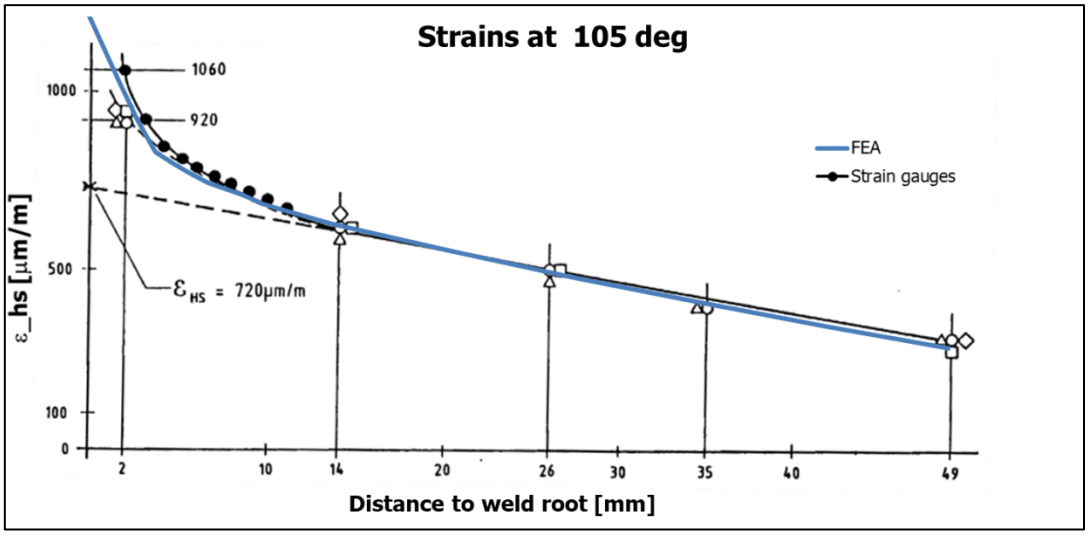

Figure 6-15 Strains at 105° for test #10

The hot spot strains of all experiments are plotted against the brace force amplitude, see Figure 6-16. A tabulated overview of the experiments, including the hot spot strains and cycles to failure, is presented in Appendix E. The green and red lines represent the hot spot strains obtained from the solid and shell element model respectively. A normal distribution of the hot spot strains from the measurements is applicable. This can be concluded from

comparing the cumulative distribution function with the characteristic shape of this curve in Figure 6-17.

The line representing the mean is also plotted in Figure 6-16. Additionally, the mean ± one time the standard deviation are plotted. A 68% confidence level of the hot spot strain being within this range corresponds to these lines.

The numerical results are close to the mean from the experiments, which shows further that the finite element results can be interpreted reliably. The solid element model strains are found to be 4% higher than the mean from the experiments. From Figure 6-15, for both numerical and experimental strains, it was found that strains decrease by approximately 3% each millimetre further away from the weld toe. Sensitivity analyses on the weld profile size also showed a 3-4% strain difference for each shift of one millimetre of the weld toe. Weld size recommendations usually only specify a minimum throat or leg size, therefore the maximum leg size can vary. For thick walled sections as used in these experiments, as-welded weld sizes could vary by several millimetres. E.g. an inaccuracy of 3 mm could already lead to an inaccuracy of the hot spot strains (or stresses) by 10%.

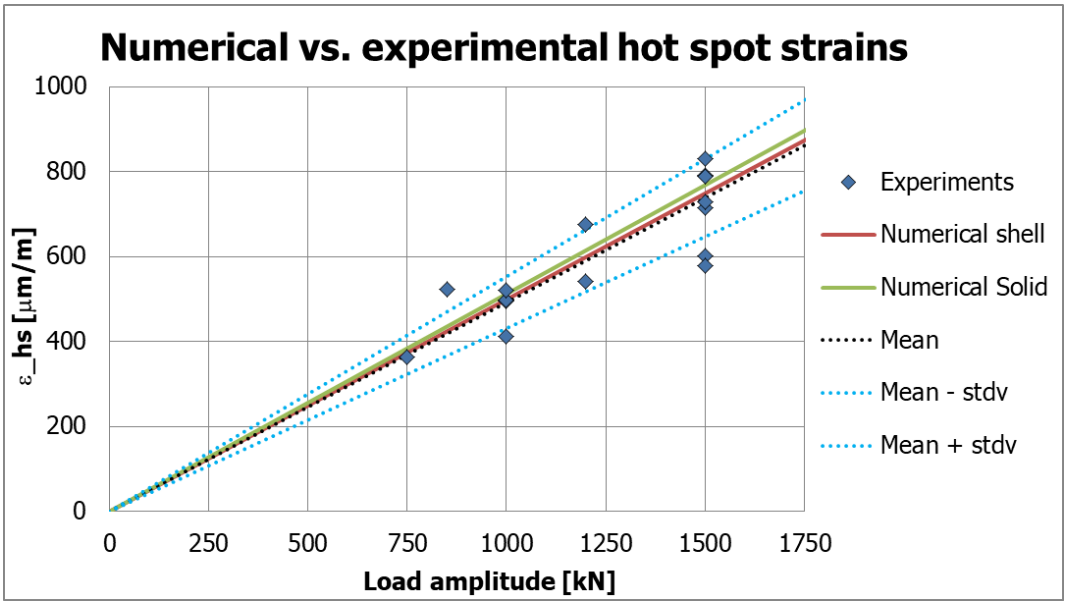

Figure 6-16 Hot spot strains from experiments

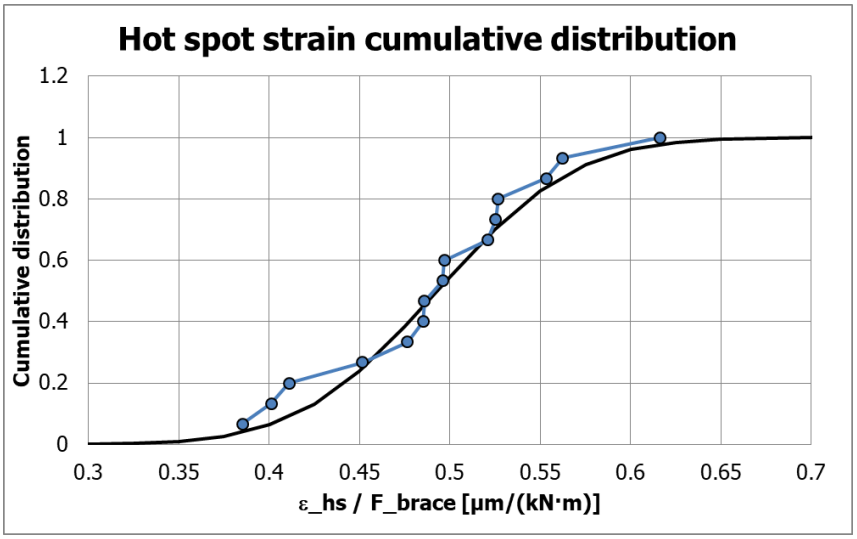

Figure 6-17 Cumulative distribution hot spot strains

6.5 Fatigue assessment

The hot spot strains obtained by numerical analysis are validated by the experimental results in the previous sections. Therefore the stresses can be calculated reliably. The following subsections discuss the calculated hot spot stresses and the subsequent fatigue assessment according to the SN-curves from DNV [3].

6.5.1 Hot spot stress

In accordance with the test report [23], stress concentration factors are calculated with respect to the nominal brace stress. A comparison with the stress concentration factors from parametric formulae described in the literature is made. SCFs from formulae developed by both Efthymiou [5] and Karamanos et al. [11] are used for this comparison. The formula from Karamanos corresponds to the recommendation described in CIDECT [2].

The boundary conditions for the constrained ovalisation, in accordance with the experimental set-up, are validated by the experiments. For the numerical derivation of the SCF parametric formulae, the boundaries at the chords ends were as such that ovalisation was allowed. For comparative purposes, an additional numerical analysis was performed according to these boundary conditions. The results are presented in Table 6.1 and Figure 6-18. Note that at the crown toe, from 0° to 10°, no hot spot stresses were calculated. This is a result from the limited gap size between the weld toes of the two braces; the read out point at 49 mm interferes with the opposite brace.

Table 6.1 - Stress concentration factors

	Constrained ovalisation	Free ovalisation	Efthymiou [5]	Karamanos [11]
SCF	3.74	4.24	4.48	5.25

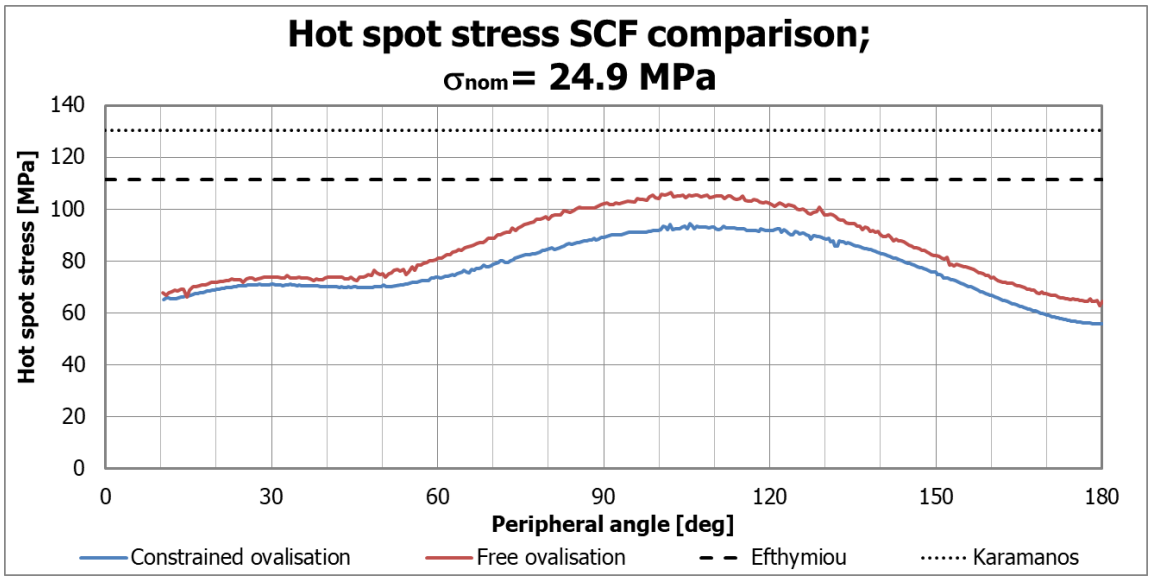

Figure 6-18 Hot spot stress SCF comparison with brace load 750 kN

The effect of the boundary conditions can be quite significant. The governing hot spot stress is increased by 13% for free ovalisation at the chord ends of the joint. Allowing free ovalisation, the numerically calculated hot spot stress corresponds well with the formula from Efthymiou. The formula from Karamanos (and subsequently CIDECT) is more conservative for this case; the governing hot spot stress is 24% higher than the numerically obtained stress.

6.5.2 SN-curve from DNV

Six experiments of the same joint type were performed in identical conditions, i.e. steel grade StE 355, variable amplitude loading in seawater and without kathodic protection (free corrosion). The fatigue assessment is performed according to the DNV T-curve for free corrosion [3], with the following constants:

$\log(C) = 11.687$
$t_{ref} = 32\ mm$
$n_{exp} = 0.25$

The Palmgren-Miner damage sum is applied to calculate the maximum number of cycles for the variable amplitude loading specified in Appendix D.

Due to the small amount of samples, a fixed value of m=3 for the slope of the SN-curve is taken. A statistical evaluation of the log constant is performed. For 6 samples, the characteristic SN-curve is obtained by reducing the mean curve by 3.293 times the standard deviation. The statistical calculation for this value is presented in Appendix B. The numerical fatigue assessment focusses on the failure at the weld itself, which is compared to the fatigue failure of the entire joint from the experiments. Only the FEA model with the boundary conditions corresponding to the experiments is presented, i.e. ovalisation of the pipe ends constrained. The results are presented in Figure 6-19. It can be concluded that the fatigue assessment from the numerical analyses in combination with DNV SN-curves satisfies the characteristic SN-curve from the experiments.

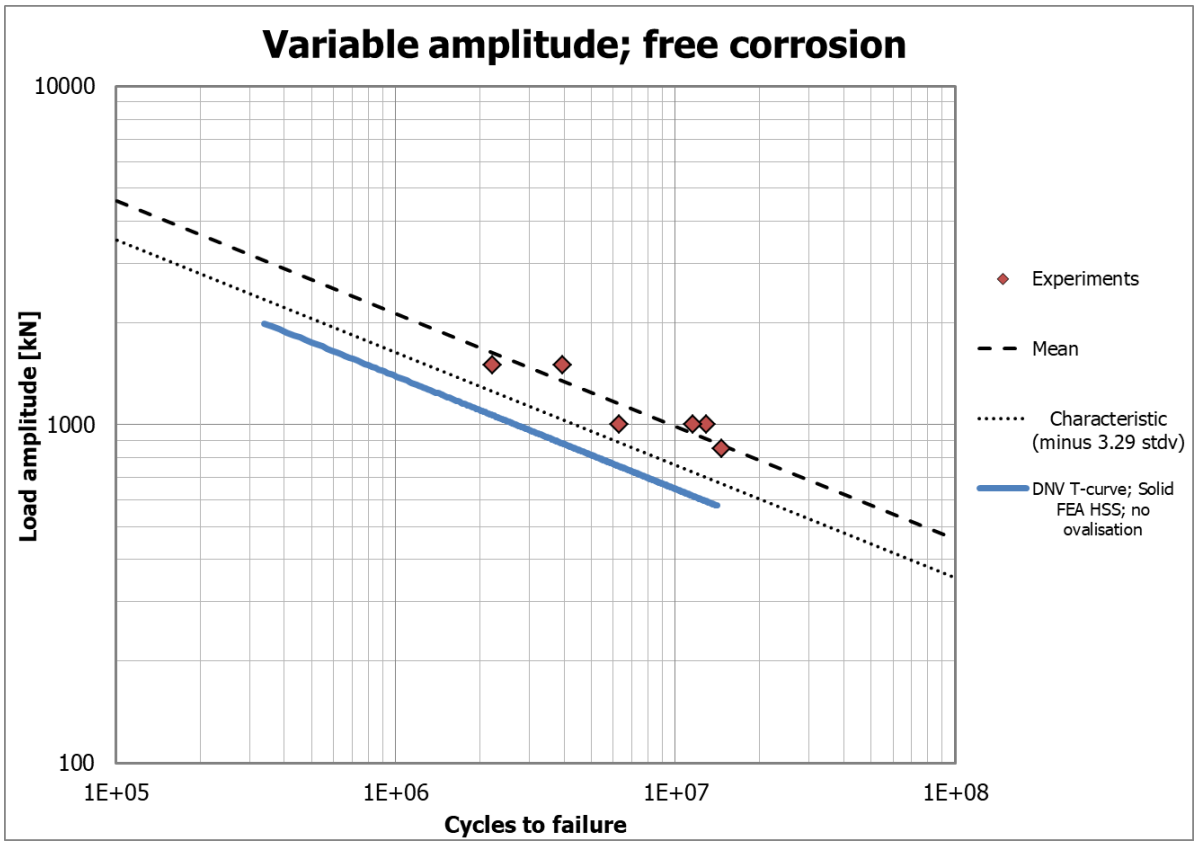

Figure 6-19 Fatigue assessment under free corrosion

6.6 Conclusions

The available data from the conducted experiments provided a good basis for assessing the different finite element modelling aspects. Strains were computed by FEA and the subroutine and compared to strain gauge measurements.

For the shell element model, no weld profile was included. The hot spot locations are to be at the plate surface intersection, from which the computed strains showed good correspondence with the experiments.

For the solid element model, the weld profile is recommended to be included. If not, too high strains (or stresses) were found with the hot spot at the plate intersection. If the weld profile is not included, it is more accurate to choose the hot spot location along a representative fictitious weld toe line. It would reduce the hot spot stresses by 5-6% with regards to the model including the weld profile. However, the critical hot spot strains from FEA were found to be 4% higher than the mean from measurements; therefore compensating for most of this underestimation. In addition, it was found that the distance of the weld toe to the plate intersection was of more importance on the stress levels than the amount of weld filler material. It can therefore be concluded that projecting a fictitious weld toe line for the hot spot location would give decent results for the hot spot stresses, in case the weld profile is not included.

Due to the sensitivity of the weld leg size to the hot spot strain levels, this property is to be determined accurately. Most welding recommendations only provide a minimum weld size, not a maximum; therefore varying tolerances can be expected. Each shift by one millimetre of the weld toe leads to a 3-4% hot spot strain reduction. For FEA, it is therefore better to be conservative and use the minimum specified weld size for modelling the weld profile.

From the validated FEA solid element model, the hot spot stresses are computed. The fatigue assessment according to DNV shows good compliance with the experiments.

7 FEA modelling issues CHS joints

The modelling of the tubular joint in FEA provided some challenges. The developed strategies to obtain a representative model are briefly discussed in this section.

7.1 CIDECT case study

For the CIDECT case study, modelling a representative weld profile in the DIANA FEA graphical user interphase (GUI) proved quite challenging. Also, applying a bending moment to a tubular cross-section required some special attention.

7.1.1 Weld profile

The main challenge was modelling a representative weld profile, for both the shell and solid element models. The 'sweep' and 'subtract' functions in DIANA FEA are used particularly for creating the weld model.

The shell element model uses a curved plate shape as weld representation. The steps are shown in Figure 7-1. For the three characteristic locations at the crown, saddle and heel, the intersection of the weld plate and plate surfaces with the chord and brace are to be determined (cf. Figure 5-8). First, a curved line is projected on the chord, representing the base of the weld shape on the chord (1). Next, a diagonal line is swept around the brace to create the weld (2). Last, the surface intersections for the hot spot locations are projected on both the chord and brace (3).

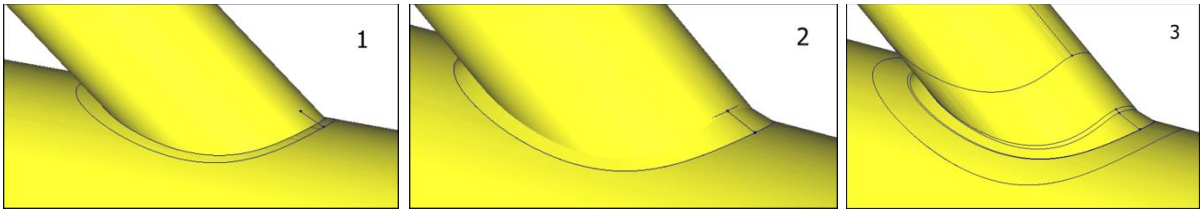

Figure 7-1 Steps for modelling weld profile with shell elements

The weld profile for the solid element model is achieved by creating a solid circular shape. The discussed steps are presented in Figure 7-2. Similar to the shell element model, a curved line is projected around the brace as the base for the weld shape. This base will be the centre point for the circular shape. It should be located within the wall thickness of the brace (1). The circle shape is swept around the base line to form the initial weld shape (2).

The undercut on the inside of the brace is created by extracting the inner brace wall as a sheet. The sheet is scaled in order to create the right intersection at the saddle and heel, and no intersection at the crown (Figure 5-10). The sheet is subtracted from the weld shape (3). Next, the brace is translated up by 2 mm to create the gap at the undercut (4). To finalise the weld profile, the brace is subtracted from the remaining weld shape (5).

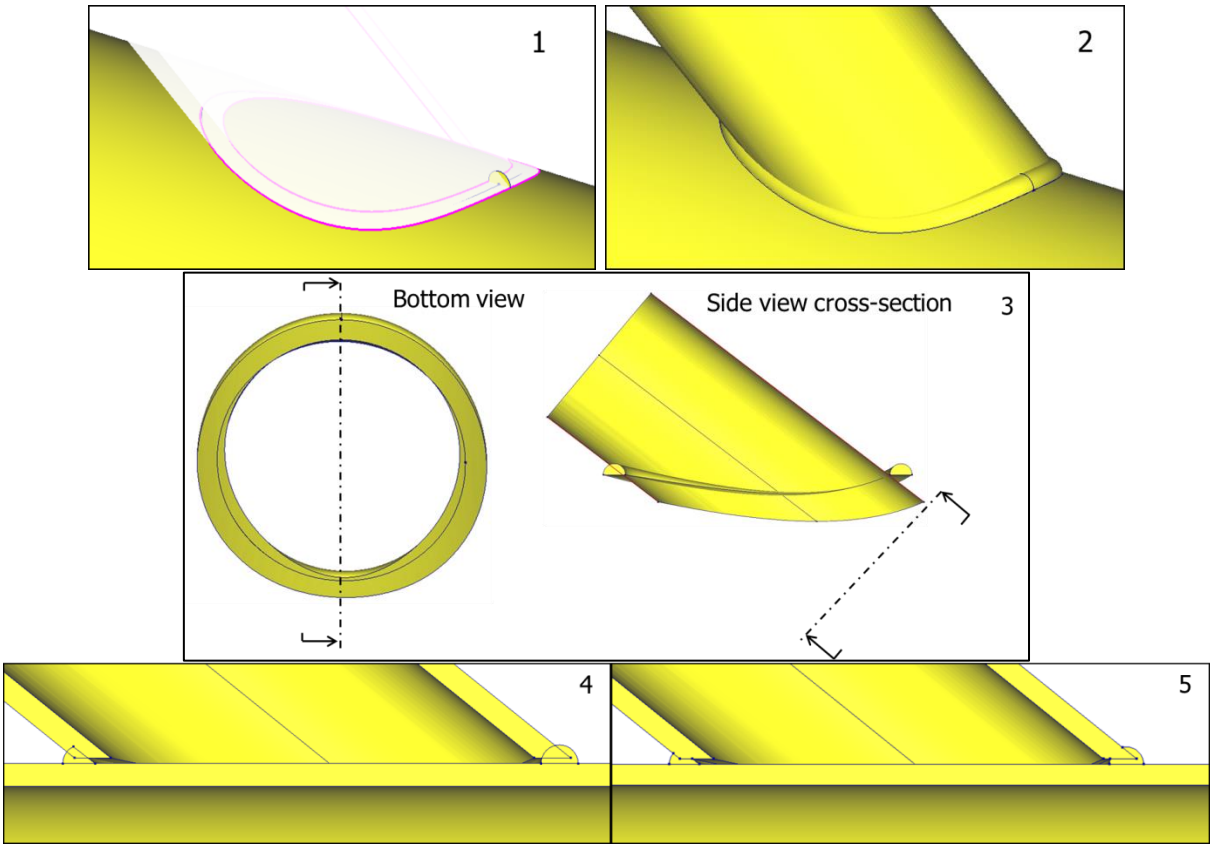

Figure 7-2 Steps for modelling weld profile with solid elements

7.1.2 Bending moment

As part of the load cases, bending moments are applied to the chord and brace ends. For tubular sections, this is not straightforward to apply. Solid elements do not have rotational degrees of freedom, so applying a bending moment directly has zero effect. Shell elements have rotational degrees of freedom, but the effect of the applied bending moment is dependent on the orientation of the shell with regards to the moment axis. For circular shapes, this orientation is different all around the section.
To overcome these issues, for both element types the bending moment is applied by means of a distributed force over the entire cross-section, as shown in Figure 7-3.

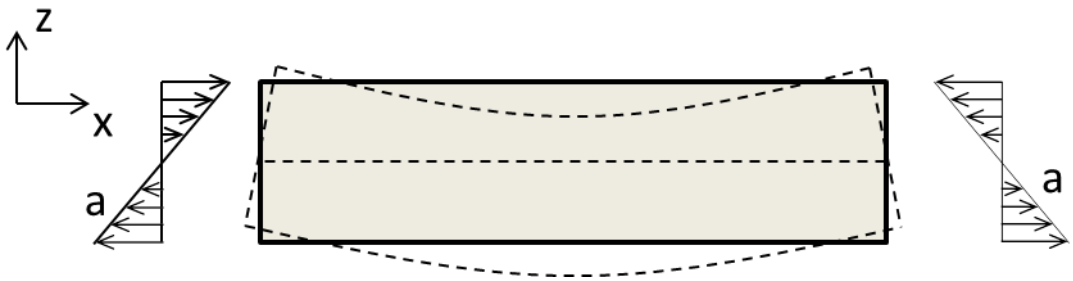

Figure 7-3 Bending moment by distributed force

A function in DIANA FEA is defined for the distributed load. A linear function with slope *a*, dependent on the z-coordinate, described the applies load. For solid elements, the load is distributed over the cross-section surface. For shell elements, the load is distributed over the cross-section edge. The value of slope *a* is calculated by means of integration of the distributed force over the cross-sectional area, multiplied by the distance to the neutral axis. An example calculation is provided in Appendix C.

7.2 CHS joint from experiments case study

As discussed in Section 7.1.1, modelling the weld profile is the main challenge for the tubular joints. For this study, the weld profile was only included for the solid element model. The weld profile is modelled as a hollow circular shape at the edge. As for the CHS joint of Section 5, the 'subtract' function in DIANA FEA is used. In addition, the 'fillet edges' function is used to create a curvature at shape intersections.

The steps are presented in Figure 7-4. Two circles are projected around the brace. The faces within these circles on the chord are extracted as sheet shapes (1). The inner sheet is extruded up vertically, whereas the sheet within the outer ring is extruded down into the chord wall (2). A curvature is applied to the intersection edge, creating the required weld shape (3). The shape is translated downward by approx. 2.5 mm, in order to submerge the weld curve into the chord wall (4). Finally, the brace and chord shapes are subtracted from the weld shape (5) to obtain the resulting weld profile (6).

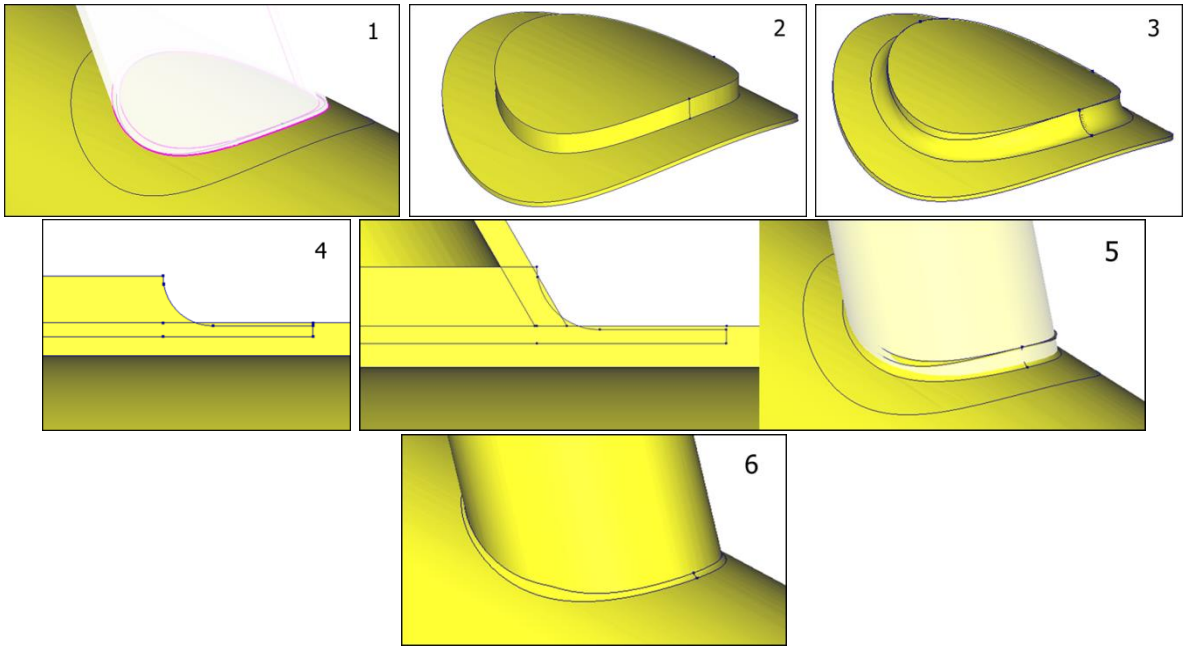

Figure 7-4 Steps for modelling weld profile with solid elements

8 Conclusions & recommendations

Several conclusions and recommendations can be made from the results presented in this report. Reference is made to Section 1.3 for the research questions, which formed the basis for this research.

8.1 Conclusions

During this research, a subroutine as post-processor for FEA output to calculate the hot spot stresses was successfully developed. It enables fatigue assessments at welded connections according to design recommendations from IIW, EC3, DNV and CIDECT. It is able to calculate the normal surface stress perpendicular to the weld, regardless of the weld's orientation. Its calculation is also independent of the mesh configuration; i.e. a method is developed to obtain representative stresses at locations not coinciding with the element nodes. Currently the subroutine is written in VBA as a separate program, however it is scheduled to be implemented into the DIANA FEA software.

The developed subroutine increases the possibilities of more advanced and detailed hot spot stress calculations for complex structures. An assessment of the full weld can be made, rather than making an assumption on the location of the critical spot to focus on. This study focussed on three cases, where the benefits of the subroutine were exploited. These case studies provided validation for the subroutine, as well as areas of further research. Of particular interest was the influence of several finite element modelling aspects on the hot spot stress. Main focus was the use of shell and solid elements, as well as including the weld profile in the FEA model. The conclusions that can be drawn from these studies are summarised below.

Bridge deck stiffener

- For cracks starting from the root through the weld, the weld also needs to be modelled when using shell elements. Defining its geometry and read out points is complex, however. If done correctly it shows good correspondence with the solid element models. There is a mesh-size dependency on the maximum stress at the weld, however the location of this peak shifts linearly along the same stress path.
- For solid elements, the stress distribution at the weld is highly dependent on the mesh-size. The minimum required mesh-size is t/3, refining the mesh further would give the same results. For shell elements, the optimal mesh-size was found also to be t/3. A smaller mesh-size gives a less representative stress distribution at the weld intersection.
- The fatigue classification in EC3 [12] assumes the maximum stress to occur at the weld root. However, it was found that the stresses reduce within the weld region. In order to extrapolate the stresses to correspond with the fatigue classification, stresses are extrapolated from points further away from the weld. At these locations, for both shell and solid elements, an element size equalling the plate thickness suffices (when using quadratic elements).
- Comparing the hot spot stresses according to the fatigue classification in [12] from shell and solid elements, only 4% lower stresses were observed for shell elements. Neglecting the weld profile in the solid element gives a 10% stress reduction. The weld profile is therefore not to be excluded. If the stresses within the weld region are of relevance, only solid elements should be used.
- The weld size was found to be of minor influence on the stress levels at the weld, provided that tolerances stay within a few millimetres. A total four millimetre height increase was considered, which increased the peak stress by less than 3% with regards to the actual weld height.

- The stress levels at the weld root for various levels of weld protrusion were compared. Stress levels at the surfaces reduced for reduced protrusion. However, the relative stresses at the root (crack initiation point) increased significantly. This would result in a shorter crack initiation period.

Tubular joint

- For butt weld connections, shell and solid element models correspond well. When shell elements are chosen, the surface intersection needs to be considered for the read out points, as well as which integration point represents the relevant surface. Overall, solid element models show slightly higher stresses.
- For more protruding welds, particularly where a gap is present between the connecting plates, more variation occurs between the shell and solid element models. It is recommended to use solid element models for a more realistic representation of obtaining the stress concentration factors.
- A method was found to include the weld profile for shell elements. It showed better correspondence to the solid element models, however for each change in geometry a cumbersome process follows to define a representative weld profile. This is because the build-up of the shapes could be different by changing a small parameter within the DIANA FEA GUI.
- The critical hot spot stress for the FEA model was found to be 16% lower than from calculations according to the CIDECT parametric formulae. A correction factor was applied to the FEA results, derived from a reference whole truss analysis. This correction corresponds with the loading and boundary condition inaccuracies for modelling a small-scale joint model from a full-scale truss model.
- Dimensions of the weld profile in FEA models are of importance for the hot spot stresses. Each millimetre of the weld leg size results in a 3% stress change. Neglecting the weld profile altogether for solid element models leads therefore to too conservative results. A (safe) conservative approach is to model the weld profile size according to the minimum weld size specified in the welding recommendations.
- Solid element model analyses generally show slightly higher strains/stresses than measured during experiments. However, due to the large amount of scatter in measurements the numerical results are relatively close to the mean values. This scatter is directly related to the scatter in the fatigue failure observations (i.e. larger measured strain/stress corresponds to a lower fatigue life). The characteristic SN-curve from the experiments takes this scatter into account. This provides the safe lower bound for the fatigue assessment.
- For solid elements models the weld profile is to be included. The hot spot is located at the weld toe location.
- For shell elements, including the weld profile is not required. The hot spot is to be location at the surface intersection point.

8.2 Recommendations

Based on the results of this study, several recommendations can be made:

General

- Only uniaxial stress states are considered in this study. An expansion of the subroutine would be to include multiaxial stress states. Further studies should consider the combination of normal and shear stresses.
- For the considered models, either only shell or only solid elements were used. No models where these element types are combined were used. Shell elements have low computational cost and are therefore good to model the general structure. Solid elements proved to provide more accurate results at the area around the weld.

Further research into sub-modelling the weld area with solid elements is therefore recommended. The correct transfer of forces and degrees of freedom at the connection requires high attention. For the orthotropic deck plate this combination model could be more feasible. For tubular joints, the curved shapes might prove more challenging to implement this combination.

Bridge deck stiffener

- The fatigue classification of 100 MPa for automatic welding is out-dated. For the analysed set of experiments, the classification could be increased to even 150 MPa. The benefits of automatic welding should be incorporated in the relevant design codes. More tests on this type of welding would be required, if insufficient data is still available.
- The current fatigue classification in EC3 for cracks through the weld is not representative of the actual observed stress distribution. A stress extrapolation method as shown in Figure 4-29 could be considered.
- Further study is required on the effect of residual stresses on the stress/strain distribution in the weld region.

Tubular joints

- More guidance should be given in the design codes on modelling weld profiles in solid FEA models. A conservative approach is recommended by using a minimum weld leg size.
- A simple reference shell element joint is to be assessed for the entire truss. It provides a good validation for the loading and boundary conditions. In addition, a correction function can be derived which in turn can be applied to the more representative solid element model.

APPENDIX A

Bridge deck stiffener stresses

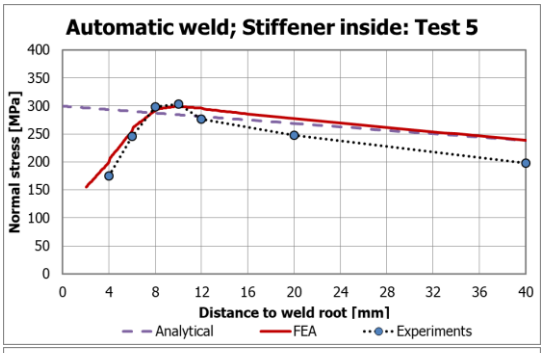

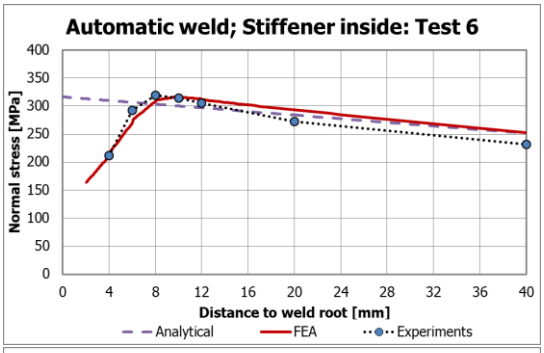

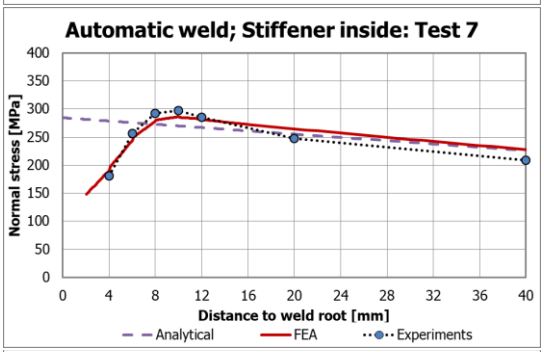

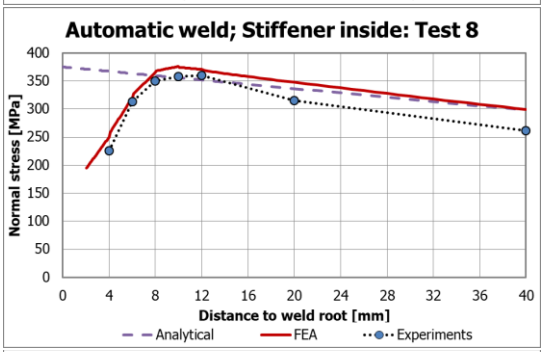

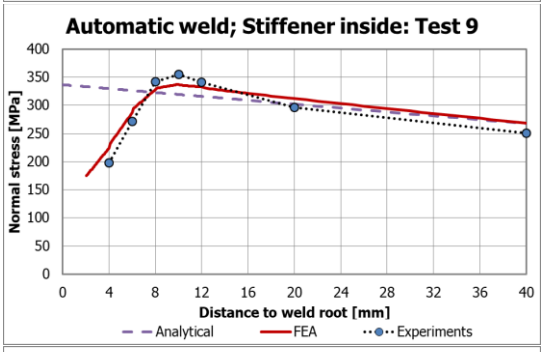

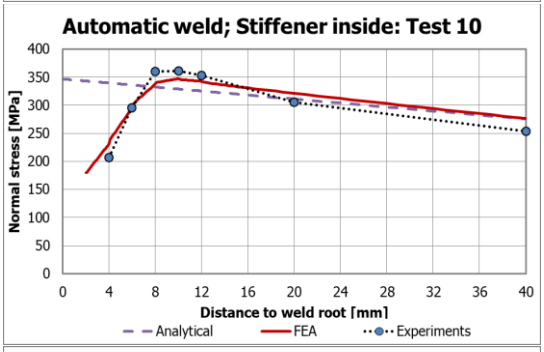

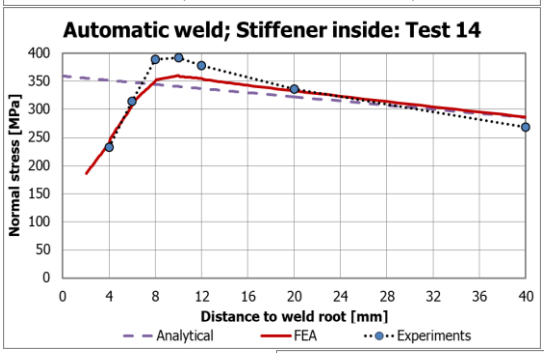

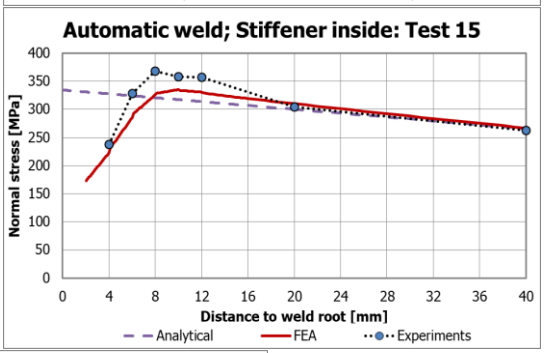

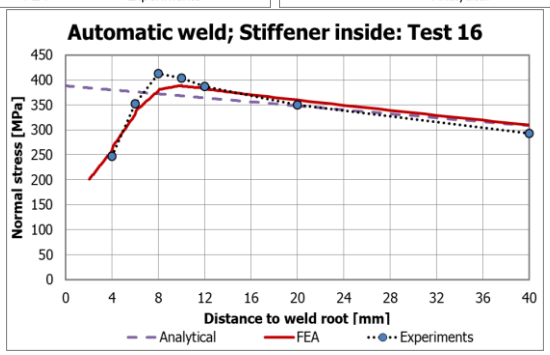

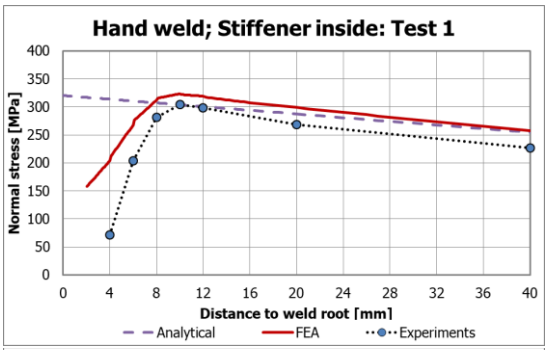
Hand weld; Stiffener inside: Test 1
Normal stress [MPa]
Distance to weld root [mm]
Analytical
FEA
Experiments

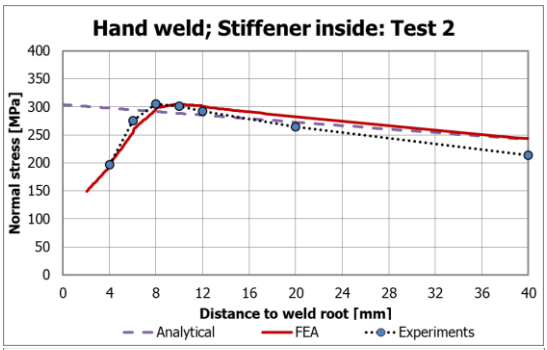
Hand weld; Stiffener inside: Test 2
Normal stress [MPa]
Distance to weld root [mm]
Analytical
FEA
Experiments

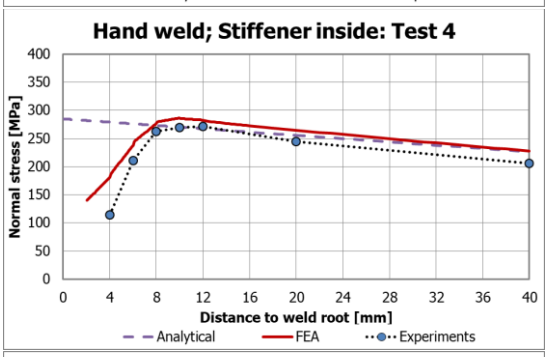
Hand weld; Stiffener inside: Test 4
Normal stress [MPa]
Distance to weld root [mm]
Analytical
FEA
Experiments

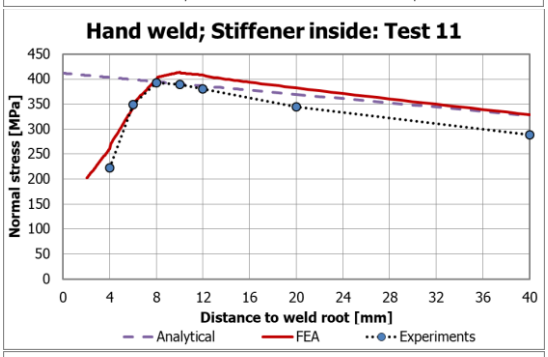
Hand weld; Stiffener inside: Test 11
Normal stress [MPa]
Distance to weld root [mm]
Analytical
FEA
Experiments

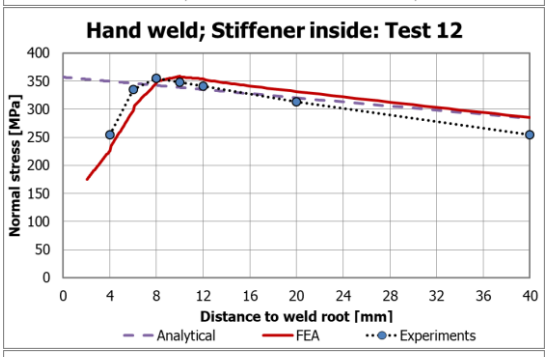
Hand weld; Stiffener inside: Test 12
Normal stress [MPa]
Distance to weld root [mm]
Analytical
FEA
Experiments

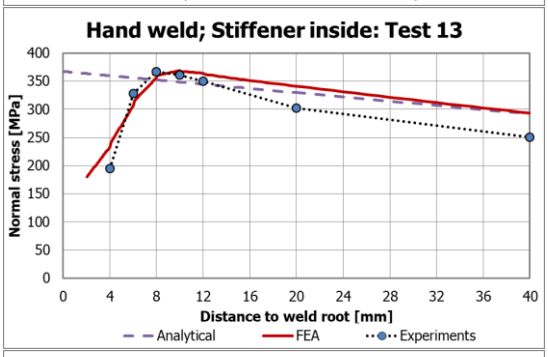
Hand weld; Stiffener inside: Test 13
Normal stress [MPa]
Distance to weld root [mm]
Analytical
FEA
Experiments

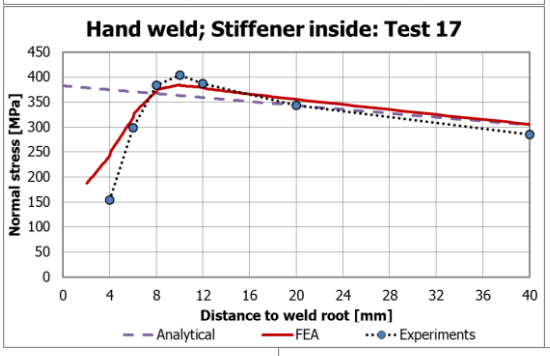
Hand weld; Stiffener inside: Test 17
Normal stress [MPa]
Distance to weld root [mm]
Analytical
FEA
Experiments

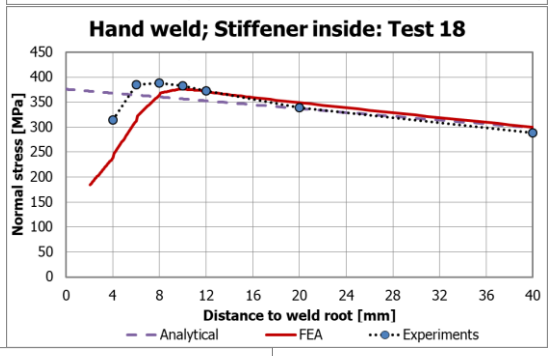
Hand weld; Stiffener inside: Test 18
Normal stress [MPa]
Distance to weld root [mm]
Analytical
FEA
Experiments

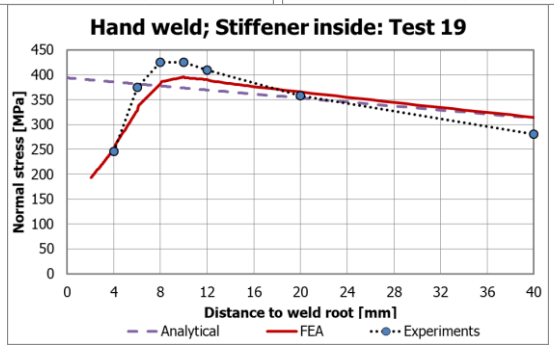
Hand weld; Stiffener inside: Test 19
Normal stress [MPa]
Distance to weld root [mm]
Analytical
FEA
Experiments

APPENDIX B

Characteristic SN-curve from experimental data

General

IIW [9] provides guidance on the statistical evaluation of fatigue test data. Described below is a summary of the provided recommendation.

The SN-curve is described by the following equation:

$$logN = logC - m \cdot log\Delta\sigma$$

Due to the small amount of samples (n<10) for the considered experiments, the fixed value of $m = 3$ is taken for the statistical evaluation. The log(C) constant is calculated by linear regression. Values x_i equal to log(C) are calculated from the experimental results, as a function of the applied load range and cycles to failure. The characteristic value is calculated from the mean with factor k as:

$$x_k = x_m - k \cdot Stdv$$

The mean and standard deviations are calculated as follows:

$$x_m = \frac{\Sigma x_i}{n}$$

$$Stdv = \sqrt{\frac{\Sigma(x_m - x_i)^2}{n-1}}$$

The general formula for factor k is:

$$k = \frac{t_{p,n-1}}{\sqrt{n}} + \phi_\alpha^{-1} \cdot \sqrt{\frac{n-1}{\chi^2_{\left(\frac{1+\beta}{2},n-1\right)}}}$$

With:

t = Value of the two sided t-distribution (Student's law) for p=β=0.75

n = Number of test results

ϕ = Distribution function of the Gaussian normal distribution probability of exceedance of α = 95% for a probability $\left(p = \frac{1+\beta}{2}\right)$ of 0.875 at n-1 degrees of freedom

χ^2 = Chi-squared for a probability of 0.875 at n-1 degrees of freedom

For several sample amounts the values of k_1 a table are provided in IIW. For an amount of samples not presented, the calculation breakdown is presented below.

Student's law t-distribution

The probability density function of the Student's t-distribution is given by:

$$f(t) = \frac{\Gamma\left(\frac{\nu+1}{2}\right)}{\sqrt{\nu\pi}\Gamma\left(\frac{\nu}{2}\right)}\left(1 + \frac{t^2}{\nu}\right)^{-\frac{\nu+1}{2}}$$

With:
$f(t)$ = Probability density function
= $2 \cdot (1 - 0.875) = 0.25$ for two-sided probability
ν = degrees of freedom (amount of samples minus 1)
$\Gamma()$ = Gamma function

The T.INV.2T function in MS Excel is used to calculate the two tailed t-distribution at probability 0.25. For 6 samples, $t = 1.301$ is found. For 9 samples, $t = 1.240$ is found.

Chi-squared distribution
The probability density function of the chi-squared distribution is given by:

$$f(\chi^2) = \frac{\chi^{2\left(\frac{\nu-2}{2}\right)} \cdot e^{-\frac{\chi^2}{2}}}{2^{\frac{\nu}{2}} \cdot \Gamma\left(\frac{\nu}{2}\right)}$$

The CHIINV function in MS Excel is used to calculate the chi-squared value for a probability of 0.875. For 6 samples, $\chi^2 = 1.808$ is found. For 9 samples, $\chi^2 = 3.797$ is found.

Gaussian normal distribution function
The probability density function of a Gaussian normal distribution is:

$$f(x) = \frac{1}{\sqrt{2\pi}\sigma} e^{-\frac{(x-\mu)^2}{2\sigma^2}}$$

For mean zero and standard deviation 1 this reduces to:

$$f(x) = \frac{1}{\sqrt{2\pi}} e^{-\frac{x^2}{2}}$$

The probability of exceedance of 95% is then found by:

$$\phi_{\alpha=95\%} = 1 - f(1 - 0.95) = 1 - \frac{1}{\sqrt{2\pi}} e^{-\frac{0.05^2}{2}} = 1 - 0.398 = 0.602$$

Characteristic factor k
According to the given equation by IIW, factor k can now be calculated:

$$k_{6\ samples} = \frac{1.301}{\sqrt{6}} + 0.602^{-1} \cdot \sqrt{\frac{6-1}{1.808}} = 3.293$$

$$k_{9\ samples} = \frac{1.240}{\sqrt{9}} + 0.602^{-1} \cdot \sqrt{\frac{9-1}{3.797}} = 2.825$$

SN-curve from test samples
As example, the characteristic curve for the CHS joint case study from Section 6 is calculated. The cycles to failure are plotted against the brace loading. The statistical evaluation is performed for constant log(C). On overview of the values for each sample is presented in Table B.1.

Table B.1 Statistical evaluation for fatigue experiments on CHS joint

Sample #	F_{amp} [kN]	Log(F)	Cycles to failure (*10^3)	Log(N)	Log(C)
1	1500	3.176	2220	6.346	15.875
2	1000	3.000	6300	6.799	15.799
3	1000	3.000	12900	7.111	16.111
4	1000	3.000	11600	7.064	16.064
5	1500	3.176	3960	6.598	16.126
6	850	2.929	14600	7.164	15.953

The mean and standard deviation for Log(C) are now:

$x_m = 15.988$
$Stdv = 0.1222$

The characteristic constant Log(C) follows:

$x_k = 15.988 - 3.293 \cdot 0.1222 = 15.585$

The characteristic SN-curve as function of the brace load is now given as:

$logN = logC - m \cdot log\mathrm{F} = 15.585 - 3 \cdot log\mathrm{F}$

APPENDIX C

Applying bending moments on tubular sections

Derivation

Bending moments are applied to tubular sections through an equivalent distributed load function. This method is applied to both shell and solid elements. The distributed load function f(z) is a linear function as shown in Figure C-1. As a function of the z-coordinate it is described by:

$$f(z) = a \cdot z$$

At z = z_1, for element height *dz* and thickness *t*, its contribution to the bending moment is:

$$dM = t \cdot f(z_1) \cdot z_1 \cdot dz = t \cdot a \cdot z_1^2 \cdot dz$$

Integration over the entire height of the cross-section gives the total bending moment:

$$M = \int_{-h/2}^{h/2} az^2 \cdot t \, dz$$

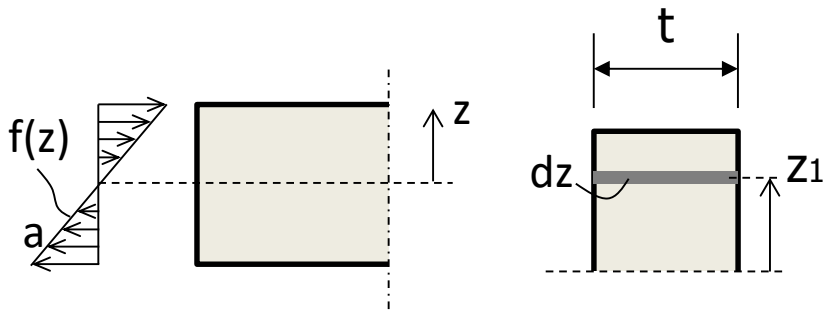

Figure C-1 Contribution bending moment on cross-section

Considered is a quarter of the CHS cross-section, see Figure C-2. The thickness of the cross-section is dependent on the z-coordinate. To avoid using two separate equations for defining the thickness, thus avoiding two separate integrals, the forces are only integrated up to the inner radius. The integral for the bending moment now becomes:

$$M = \int_{0}^{r_1} az^2 \cdot t(z) \, dz$$

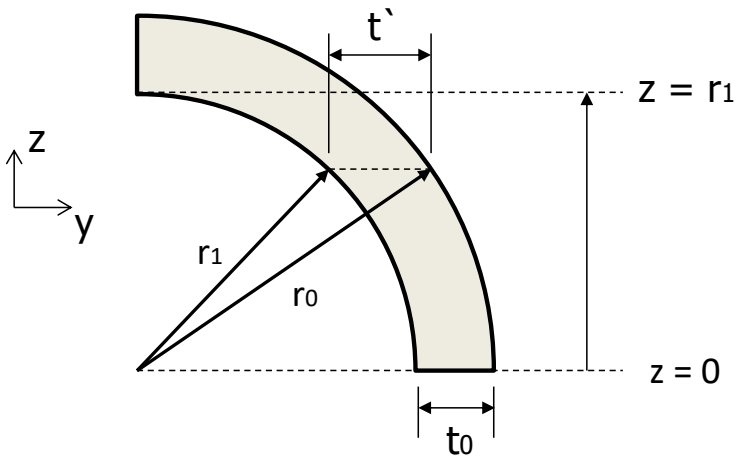

Figure C-2 Quarter cross-section CHS

The general circle equation is:

$r^2 = y^2 + z^2$

From which follows:

$y = \sqrt{r^2 - z^2}$

The thickness, as function of the z-coordinate, can then be expressed as:

$t'(z) = y_0 - y_1 = \sqrt{{r_0}^2 - z^2} - \sqrt{{r_1}^2 - z^2}$

Since only a quarter circle is considered, the contribution of this part for the total bending moment is to be multiplied by four. Substitution in the bending moment equation gives (taking constant *a* out of the integral):

$$M = 4a \int_0^{r_1} z^2 \cdot \sqrt{{r_0}^2 - z^2} - \sqrt{{r_1}^2 - z^2}\, dz$$

Numerical integration is used to solve the integral. With bending moment *M* known, the constant *a* can be found to define the equivalent distributed force function. The maximum force value for solid elements is:

$f_{solid}(z = r_1) = a \cdot r_1$

For shell elements, a distributed line load is applied. Therefore the loads need to be multiplied by the plate thickness:

$f_{shell}(z = r_1) = a \cdot t \cdot r_1$

APPENDIX D

Test spectrum steps COLOS

i	$\sigma_i/\bar{\sigma}$	*H(i)*
1	1.000	1
2	0.975	1
3	0.925	3
4	0.875	5
5	0.825	12
6	0.775	25
7	0.725	55
8	0.675	120
9	0.625	257
10	0.575	555
11	0.525	1203
12	0.475	2598
13	0.425	5621
14	0.375	12156
15	0.325	26284
16	0.275	63754
17	0.225	92675
18	0.175	289127
		Σ = 494452

APPENDIX E

Tubular joint fatigue experimental data

Test #	*Yield strength [MPa]*	*Post-weld treatment*	*Loading*	*Environment*	*Load amplitude [MN]*	*Hot spot strain* $*10^{-6}$	*First crack (N2)* $*10^{3}$	*Cycles to failure (N3)* $*10^{3}$
1	355	No PWT	Variable	Free corrosion	3.0	830	593	2220
2					2.0	496	1200	6300
3					2.0	497	2820	12850
4					2.0	411	3979	11605
5					-	-	-	-
6			Constant		1.5	364	-	395
7			Variable to constant	Cathodic protection	2.0	521	600	1921
8			Variable	Air	3.0	602	1174	3710
9				Cathodic protection	3.0	790	2972	6178
10				Free corrosion	3.0	715	-	3960
11				Cathodic protection	3.0	729	-	7084
12				Free corrosion	-	-	-	-
13					1.7	524	9210	14640
14	690	Shot-peening	Variable	Free corrosion	3.0	788	-	3430
15		TIG dressing			3.0	578	4200	11018
16		Shot-peening			2.4	675	-	7650
17		TIG dressing			2.4	542	3324	12070

APPENDIX F

Subroutine interface

The fatigue subroutine consists of two main interfaces, as presented in Figure F-3 and Figure F-4. Four design codes on fatigue are included in the subroutine, i.e. IIW, DNV, EC3 and CIDECT for tubular joints. Depending on the applicable code, the next interface automatically assigns the applicable SN-curve definition. Additionally, from the CSV input file it reads which welds were defined in the FEA model.

The user can choose whether a stress or strain calculation is to be made. This is of relevance for the tensor matrix transformation, where tensorial shear strain equals half the engineering shear strain ($\varepsilon_{xy} = \frac{1}{2}\gamma_{xy}$). Also, strain based SN-curves are not included in the subroutine, so a fatigue assessment is omitted for the obtained hot spot strains.

Finally, the extrapolation method and read out points can be defined. Either absolute or relative to thickness read out points can be selected. Also, quadratic extrapolation or simply a single read out point can be chosen by the user.

During calculation, a log screen appears that tracks the progress (see Figure F-5). In case of any errors occurring, they are reported here.

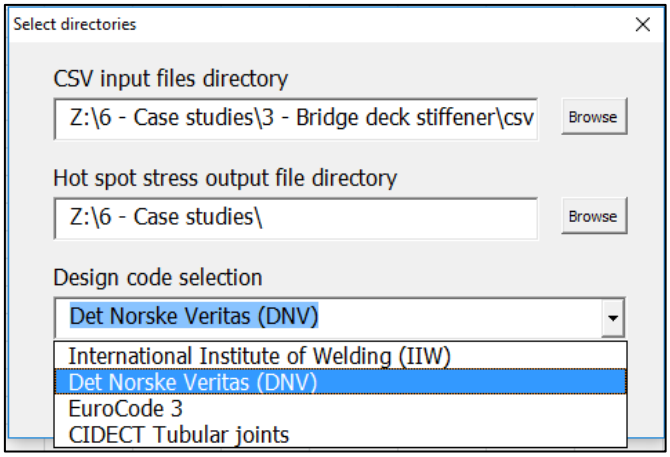

Figure F-3 Input file subroutine

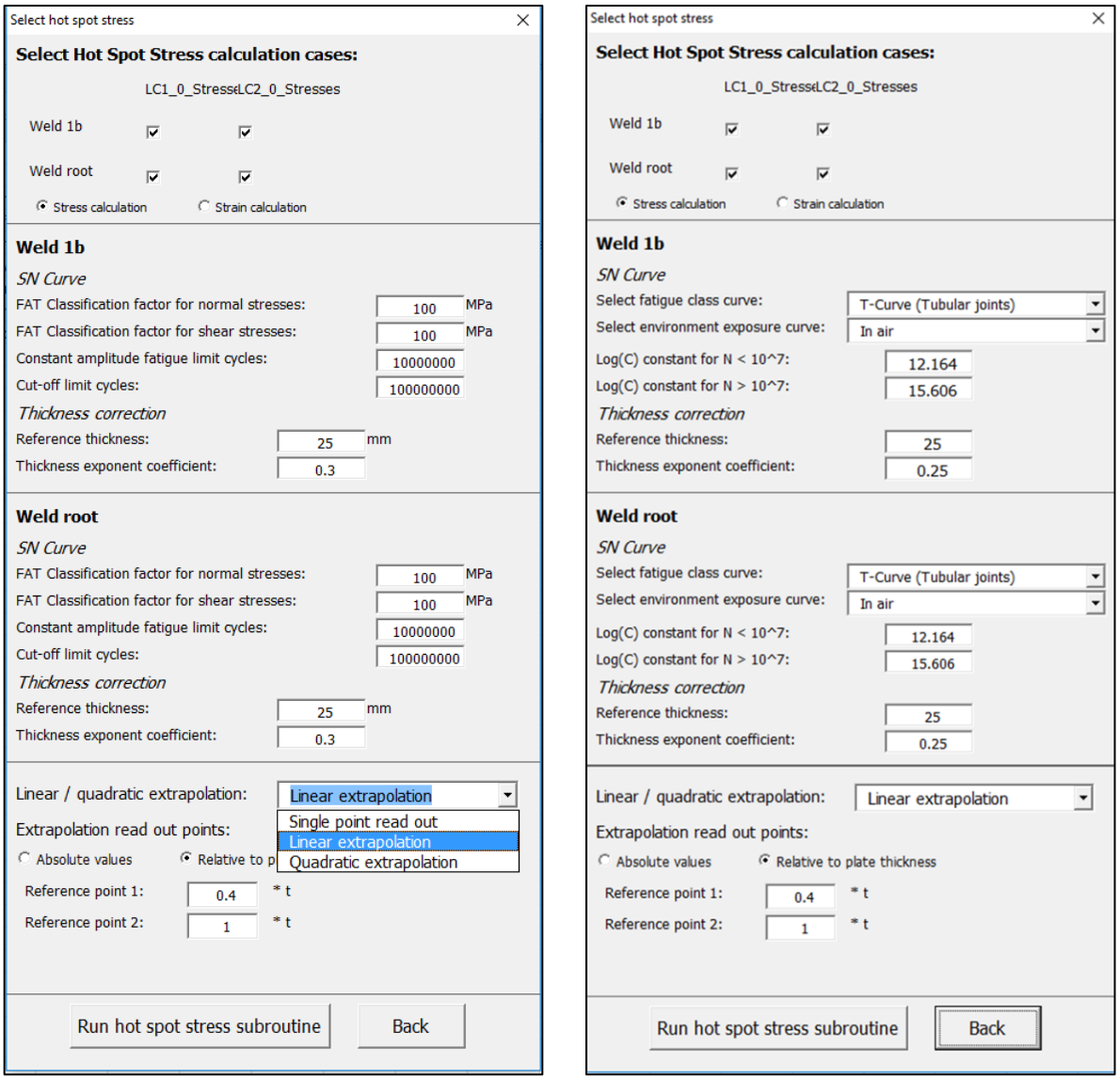

Figure F-4 User interfaces for fatigue subroutine for IIW (left) and DNV (right)

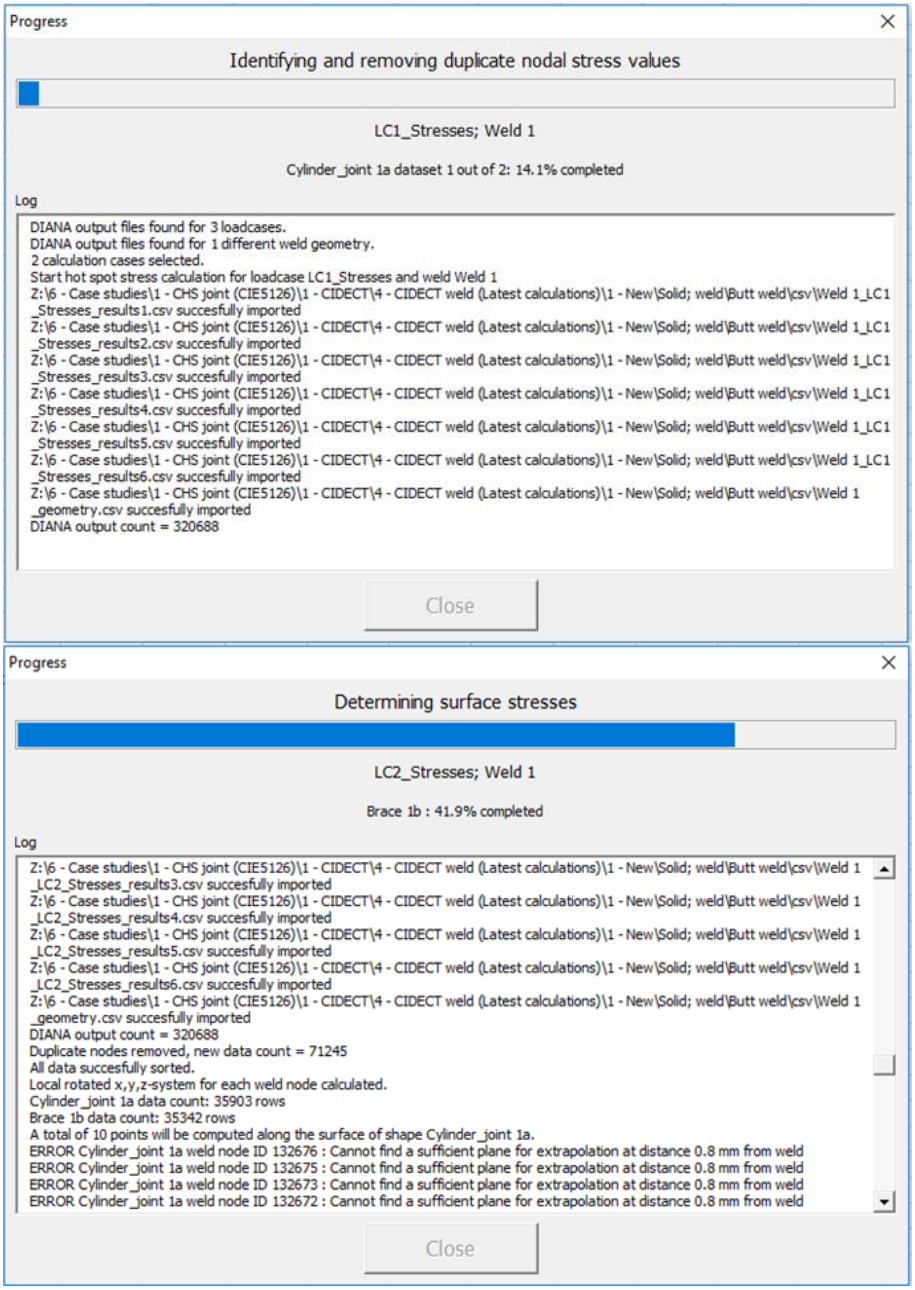

Figure F-5 Calculation log interface

Bibliography

[1] CIDECT (1998). Design Guide 6: For structural hollow sections in mechanical applications. Köln: TUV Verlag

[2] CIDECT (2001). Design Guide 8: For CHS and RHS welded joints under fatigue loading. Köln: TUV Verlag

[3] DNV RP-C203 (2010) "Fatigue design of offshore steel structures". Det Norkse Veritas

[4] Dong, P. (2001) A structural stress definition and numerical implementation for fatigue analysis of welded joints

[5] Efthymiou M. (1988). Development of SCF formulae and generalized functions for use in fatigue analysis. OTJ88, Surrey, U.K.

[6] EN 1993-1-9: Eurocode 3: Design of Steel Structures. Part 1.9: Fatigue

[7] Germanischer Lloyd (1976). Vorschriften für Konstruktion und Prüfung von meerestechnischen Einrichtungen. Hamburg.

[8] Haagensen P.J., Maddox S.J. (2013). IIW Recommendations on methods for improving the fatigue strength of welded joints. Woodhead Publishing Ltd., Cambridge.

[9] Hobbacher A.F. (2008). Recommendations for fatigue design of welded joints and components, Doc. IIW-1823-07 (ex-doc. XIII-2151r4-07/XV-1254r4-07), WRC Bulletin 520, Welding Research Council, Inc., New York.

[10] Hobbacher A.F. (2010). New developments at the recent update of the IIW recommendations for fatigue of welded joints and components. Steel Construction, 3: 231-242.

[11] Karamanos S.A., Romeijn A., Wardenier J. (2000). Stress concentrations in tubular gap K-joints: Mechanics and fatigue design. Engineering Structures, Vol. 22: pp. 4-14.

[12] NEN-EN 1993-2+C1:2011/NB:2011, Eurocode 3: Design of Steel Structures - Part 2: Steel bridges

[13] Osawa N., Yamamoto N., et al. (2011). Study on the preciseness of hot spot stress of web-stiffended cruciform welded joints derived from shell finite element analyses. Marine Structures, vol. 24, Issue 3: pp. 207-238.

[14] Pijpers R., Abspoel L., Kolstein M.H. (2014). Vermoeiingsclassificatie langslasscheur, Infraquest - Competence centre for roads and structures, Delft.

[15] Poutiainen I., Tanskanen P. & Marquis G. (2004). Finite element methods for structural hot spot stress determination - a comparison of procedures. International Journal Fatigue, vol. 26: pp. 1147–1157.

[16] Radaj D. (1990), Design and analysis of fatigue resistant welded structures. Cambridge: Abington Publishing.

[17] Romeijn A. (1994), Stress and strain concentration factors of welded multiplanar tubular joints. Doctoral Thesis, Delft University of Technology.

[18] Schijve J., (2012). Fatigue predictions of welded joints and the effective notch stress concept. International Journal Fatigue, vol. 45: pp. 31-38

[19] Schumacher A. & Nussbaumer A., (2006). Experimental study on the fatigue behavior of welded tubular K-joints for bridges. Engineering Structures, vol. 28, issue 5: pp. 745-755.

[20] Sonsino C.M., Fricke W., de Bruyne F., Hoppe A., Ahmid A. & Zhang G. (2012). Recent developments in local concepts of fatigue assessment of welded joints - background and applications. International Journal Fatigue, vol. 34: pp. 2-16.

[21] Sonsino C.M. (2012), Comparison of different local design concepts for the structural durability assessment of welded offshore K-nodes. International Journal Fatigue vol. 34: pp. 24-34

[22] Transport en Logistiek Nederland (2016). Afsluiting Merwedebrug heeft grote logistieke gevolgen. Retrieved from https://www.tln.nl

[23] Umbach R., Sonsino C.M., et al. (1993). Korrosionsschwingfestigkeit von geschweißten Rohrknoten und Stahlguß-Verbundkonstruktionen in bauteilähnlichem Maßstab. Report EUR14316DE, Kommission der europäischen Gemeinschaften, EGKS-EWG-EAG, Brussels and Luxemburg.

[24] Ummenhofer T. & Weidner P. (2013). Improvement factors for the design of welded joints subjected to high frequency mechanical impact treatment. Steel Construction, vol. 6: pp. 191-199.